Mr L G Pocock 3323

ELECTRICAL COMMUNICATION

Technical Journal of the
International Telephone and Telegraph Corporation
and Associate Companies

•

INTERNATIONAL TELEPHONE AND TELEGRAPH

Volume 31 **SEPTEMBER, 1954** **Number 3**

ELECTRICAL COMMUNICATION

Technical Journal of the
International Telephone and Telegraph Corporation
and Associate Companies

H. P. WESTMAN, Editor
J. E. SCHLAIKJER, Assistant Editor

Published Quarterly by the
INTERNATIONAL TELEPHONE AND TELEGRAPH CORPORATION
67 BROAD STREET, NEW YORK 4, NEW YORK, U.S.A.
Sosthenes Behn, Chairman William H. Harrison, President
Geoffrey A. Ogilvie, Vice President and Secretary

Subscription, $2.00 per year; single copies, 50 cents

Volume 31 SEPTEMBER, 1954 Number 3

CONTENTS

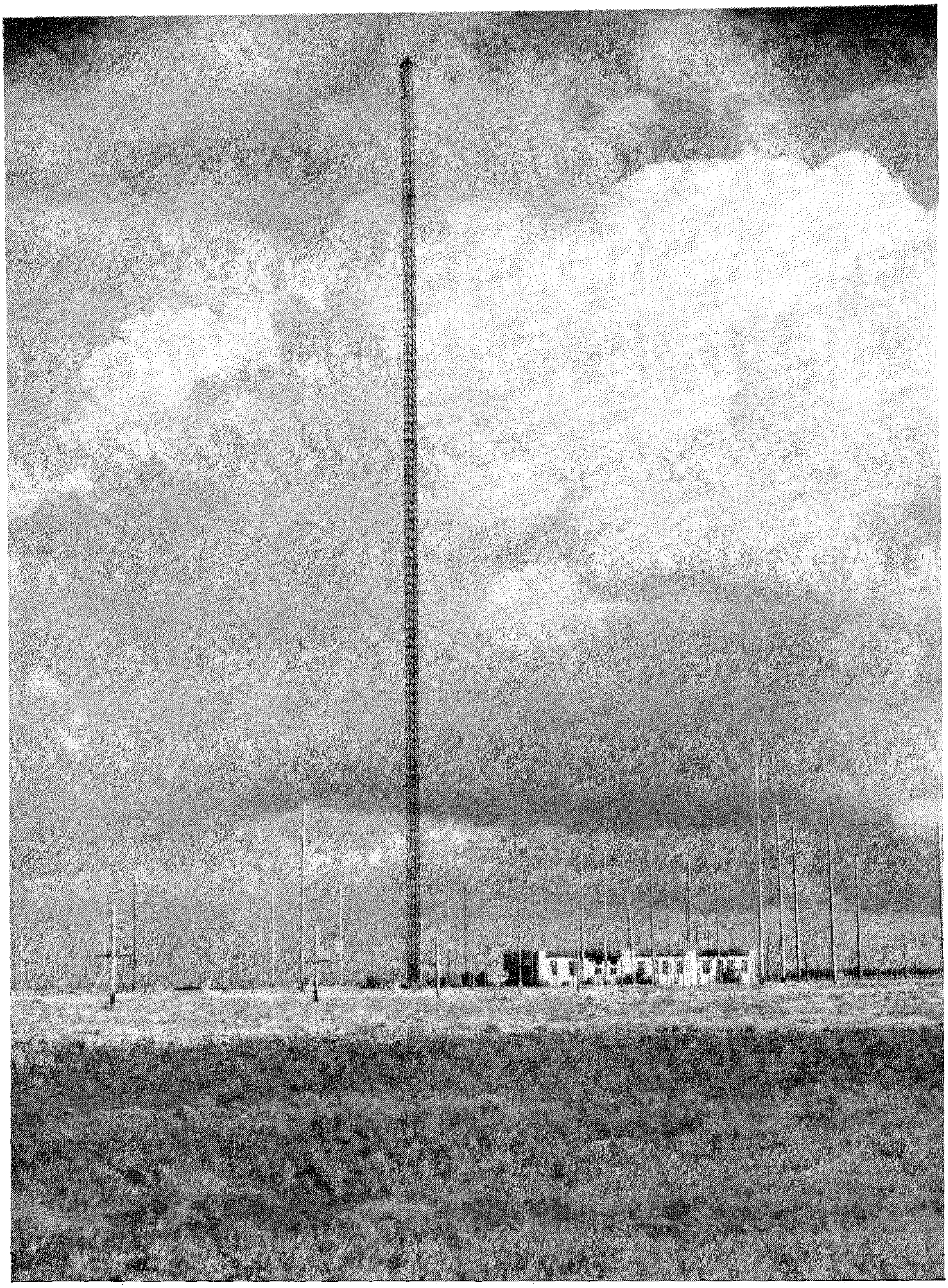

Palo Alto, California, station of Mackay Radio and Telegraph Company, which is part of the American Cable and Radio Corporation system. The tall mast was originally for low-frequency transmission but is now a support for numerous intermediate- and high-frequency antennas. The station handles both international and marine traffic.

Navaglobe—Navarho Long-Range Radio Navigational System*

By C. T. CLARK, R. I. COLIN, MILTON DISHAL,

Federal Telecommunication Laboratories, a division of International Telephone and Telegraph Corporation; Nutley, New Jersey

IRVING GORDY,

Rome Air Development Center; Griffiss Air Force Base, New York

and MORTIMER ROGOFF

Now With the McDermott Company; Trenton, New Jersey

NAVAGLOBE is a long-distance radio navigational system under development by Federal Telecommunication Laboratories for the United States Air Force. For obtaining reliable long-range service, it operates in the low-frequency band and with a very-narrow bandwidth. Service is omnidirectional and the airborne bearing indications are automatic. The principles of the transmitting and receiving equipment are described, including features designed for minimizing the effects of atmospheric noise. Views of actual equipment are shown, and the various stages through which the developmental program has progressed are discussed. Performance of the experimental equipment is described, including the results of transcontinental and transatlantic flight tests. Work and future plans for the incorporation of distance measurment by means of phase comparison of the Navaglobe signals with reference to an airborne crystal-controlled frequency generator, forming the complete Navaglobe—Navarho system, are discussed.

• • •

The Navaglobe project has been carried on for the United States Air Force by Federal Telecommunication Laboratories, with the goal of providing a radio navigational system that is truly long-range and reliable, and that gives automatic readings. Construction of experimental transmitting and receiving equipment has progressed to a stage that has made possible extensive laboratory, field, and flight tests. Performance in these tests, indicating that the system will fulfill its goals, makes it timely to present a review of this project, which may result in a valuable new facility for this age of global air operations.

Long-range air navigation today is done essentially by dead reckoning, as it was 10 and 20 years ago.[1] Because of the cumulative effect of inaccuracies in estimates of distance and direction, dead reckoning on long flights should be checked as frequently as possible by positive position determinations; the goal, of course, is a supplanting system that could provide reliable position determination at will or continuously. To obtain position determinations by celestial methods requires complicated time-consuming calculations based on observations by trained navigators in clear weather at certain times of day and on a well-stabilized aircraft. These conditions are unduly restrictive in air operations, whether civil or military. As regards position determination by radio methods, there are certain facilities available for this purpose from time to time and place to place, but there is no single radio aid in use that does give or could consistently give navigational guidance during the entire distance of transoceanic or transpolar flights.

For air traffic over populated land areas, where there is no problem in locating a sufficient number of ground stations, short- and medium-range radio aids of various types successfully provide continuous navigational guidance to contribute to the safety, efficiency, and economy of air operations.[2] In other regions that constitute

* Reprinted from *Convention Record of the 1954 IRE National Convention*, volume 2, part 5—Aeronautical Electronics and Telemetry, pages 88–97. Presented at the National Convention of the Institute of Radio Engineers in New York, New York, on March 23, 1954.

[1] L. S. Kuter, "Military Air Transport Service," *Journal of the Institute of Navigation*, volume 2, pages 159–161; June, 1950.

[2] R. I. Colin, "Survey of Radio Navigational Aids," *Electrical Communication*, volume 24, pages 219–261; June, 1947.

the larger part of the earth's area, the basic problems involve geography (availability of land sites suitable for the location of navigational transmitters) and radio propagation (the range required of the transmissions if they are to reach aircraft flying anywhere over oceanic, polar, and other nonpopulated regions with the reliability that is vital for a navigational system). Some existing radio navigational systems approach a satisfactory range, but only under certain limited propagation conditions; at other times their range falls quite short of the needs, so that they are really quasi-long-distance systems. None of these automatically give a direct reading and so are unsuitable for cockpit use by the pilot, nor are they omnidirectional in coverage.

1. Basic Reliability Considerations

The Navaglobe project started with a study of the basic problem mentioned above.[3] Examination of the globe showed that there are geographically available sufficient and suitably related land sites for navigational transmitters to cover, ultimately, all oceanic and polar regions with radio position-fixing service, provided that the reliable day-in-and-day-out range of the transmitters is around 1500 nautical miles (2780 kilometers). The next step was to determine the general parameters of a radio system to fulfill that requirement. A detailed survey of data on radio transmission in all portions of the radio spectrum was undertaken, considering also the related practical factors of atmospheric-noise intensities and antenna radiation efficiencies. Statistical studies were made on all these points of data accumulated over many years by governmental agencies and commercial communication companies.

The conclusion, since supported by independent studies, was that the practical hope for reliable long-range radio navigation lay in low-frequency operation, in the vicinity of 70 to 100 kilocycles per second. The International Telecommunications Convention has since reserved the band between 90 and 110 kilocycles for this type of service.[4] At the same time, very-narrow bandwidths of the order of 20 to 100 cycles per second should be used. This is not only to conserve channel space, always a critical practical problem at low frequencies, but also to produce

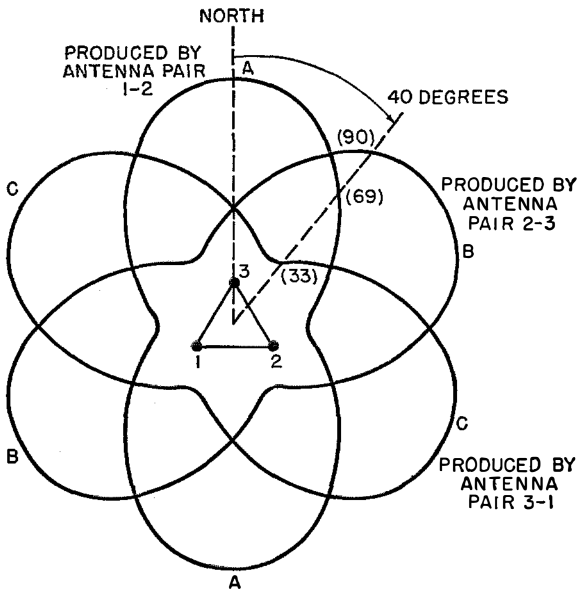

Figure 1—Navaglobe transmitter radiation patterns. The numbers in parentheses indicate the relative strengths of the *A*, *B*, and *C* signals at the 40-degree bearing. Antennas are at the apexes of the central triangle.

useable signal-to-noise ratios at long distances without requiring prohibitively expensive transmitter powers and antenna sizes.

The original Navaglobe proposal,[5,6] and the equipment since developed and tested, conforms to the conclusions of the basic study, for it was recognized that propagational reliability is the critical element of a long-distance radio navigational system, to which must be added the usual requirements of equipment reliability. The Navaglobe transmission rate of 4 continuous-wave signals per second is compatible with very-narrow-bandwidth low-frequency opera-

[3] P. R. Adams and R. I. Colin, "Frequency, Power, and Modulation for a Long-Range Radio Navigational System," *Electrical Communication*, volume 23, pages 144–158; June, 1946.

[4] "Final Acts of the International Telecommunication and Radio Conferences, Atlantic City; 1947," chapter 3, article 5, paragraph 112.

[5] H. Busignies, P. R. Adams, and R. I. Colin, "Aerial Navigation and Traffic Control with Navaglobe, Navar, Navaglide, and Navascreen," *Electrical Communication*, volume 23, pages 113–143; June, 1946.

[6] P. R. Adams and R. I. Colin, "Navaglobe Long-Range Radio Navigational System," *Proceedings of the National Electronics Conference*, volume 2, pages 288–298; October, 1946.

tion, and yet is a fast-enough information rate for long-range navigational purposes. A major effort went into designing the system and equipment so as to minimize the effects of atmospheric noise generated by local thunderstorms, which is particularly serious in midsummer and near the tropics. Such noise is generally the limiting factor in obtaining consistent long-distance operation of low-frequency radio circuits. As a further measure to insure reliability and to instill confidence in the pilot, the system provides automatic fail-safe indications and automatic calibration-checking indications. A description of these features and of the general principles of operation of the Navaglobe system follows.

2. *Principles of Operation*

The Navaglobe ground installation consists of three antennas situated at the corners of an equilateral triangle, as indicated in Figure 1. The antennas are spaced 0.4 wavelength apart, which amounts to approximately 3600 feet (1100 meters) when transmitting at 100 kilocycles. Radio-frequency power is supplied to the antennas according to this schedule: currents of equal strength and phase go to antenna pair *1–2*; then similarly to antenna pair *2–3*; and finally to antenna pair *3–1*. This cycle is constantly repeated at a rate of 1 per second. The timing and switching apparatus for controlling this cycle is

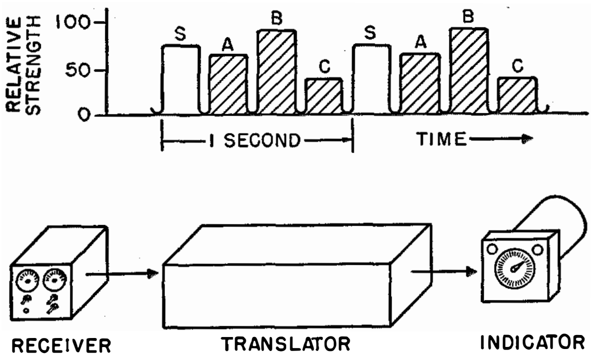

Figure 2—Operation of Navaglobe receiving system. At the top is shown the detected signals at the 40-degree bearing. The synchronizing signal is at *S*. In the lower drawing, the receiver detects signals from the selected ground station and applies them to the translator, which in turn identifies them, examines their relative amplitudes, and positions the indicator to the 40-degree bearing.

located in a central hut, which also houses equipment for monitoring the phase and amplitude of the currents in the three antennas.

Antenna pair *1–2* produces a radio signal with a strength greatest in the directions perpendicular to the line joining the antennas and weakest in directions parallel to that line. The systematic variation in strength along different directions is indicated graphically to scale by radiation pattern *AA* in Figure 1, which resembles the figure 8. Patterns *BB* and *CC*, produced by antenna pairs *2–3* and *3–1*, respectively, are identical in shape but their axes are shifted 120 and 240 degrees from that of pattern *AA*.

The net result is that 3 signals, *A*, *B*, and *C*, are radiated over and over again, and that the relative strengths of the 3 signals are different along each direction. At bearing 40 degrees, for example, the relative strengths of the 3 signals received in time sequence are as shown to scale in the upper part of Figure 2. At the receiving end, the 3 signals are isolated and applied to a bearing-translator circuit that automatically rotates a shaft to a position that depends on the relative strength of these signals. Thus a pointer attached to this shaft indicates the bearing of the receiver from the transmitter. From the nature of the overlapping radiation patterns and the method in which the information in the resulting signals is utilized, it is evident that the Navaglobe station provides omnidirectional bearing-indication service.

The signal denoted *S* in Figure 2 is the synchronizing signal. It is radiated once each cycle from a single antenna and hence is received with equal strength in all directions. It is radiated on a slightly different frequency from that used for the *A*, *B*, and *C* signals, and thus is separately identifiable in the airborne receiver. The *S* signal marks the start of each transmission cycle and enables the receiving equipment to isolate and identify the *A*, *B*, and *C* signals for proper application to the bearing-translator circuits.

The elementary principle of the bearing translator is explained in the upper half of Figure 3. The *A*, *B*, and *C* signals from the receiver are fed to the designated stator inductors through gating and switching circuits controlled by the synchronizing signal. Coming from the receiver in direct-current form, these signal currents produce successive individual direct-current magnetic-field components aligned with the respective inductors. The angle ϕ of the resultant magnetic field is assumed by the magnetic needle and depends on the relative strengths of the A, B, and C signals, and hence on the bearing from the transmitter array.

Elementary indicators of the above-described "ratiometer" type were used in the initial experimental demonstrations of the Navaglobe principle. For this purpose, a 3-antenna transmitting installation was erected and placed in operation near Adamston on the New Jersey coast. This station, however, was built for operation at 150 kilocycles since a channel in the preferred 100-kilocycle band was not obtainable at the time. Exploratory field tests of system operation with this transmitter were performed in 1951, the receiving equipment being installed in a motor vehicle that travelled to points at various distances and directions. While reception was effected at times as far as Colorado Springs, Colorado, and the indications were in close accord with the theoretical calculations, the need for certain improvements was indicated, particularly in regard to the system behavior under heavy local-thunderstorm atmospheric-noise conditions. Improvements were accordingly made in the bearing translator, receiver, and synchronizing system.

The principle of the mathematically equivalent but practically superior "resolver" form of bearing translator now used is also shown in Figure 3. Here the A, B, and C signal voltages from the receiver's intermediate-frequency output pass in alternating-current form to the designated stator inductors under control of the synchronizing system. In the rotor or pickup coil, individual voltages are successively induced that depend on the strengths of the A, B, and C signals and also on the angular position of the rotor coil. An integrating-type square-law detector (essentially a watthour-meter device) measures the algebraic sum of these induced voltages over an integral number of transmission cycles, and its output serves as an error signal to control a servomechanism. The servo automatically positions the rotor coil to an angle ϕ at which there is a null output from the integrating detector. This angle ϕ, as before, depends on the strength ratio of the original A, B, and C signals and hence on the bearing of the transmitter array.

To insure that the signals going to the bearing translator and detector are at the optimum level for distortionless operation of these devices, an automatic-gain-control circuit is provided. Although this circuit acts relatively quickly in correcting the gain of the receiver as required, it is so devised as to do this without changing the A, B, and C signal strengths relative to each other. A flag alarm warns against reading the bearing indicator before the automatic-gain-control system and the automatic synchronizing system have had time to bring about proper operating conditions, or when they are prevented from doing so because of extremely weak, noisy, or otherwise unsatisfactory signals.

As remarked earlier, atmospheric noise is generally the limiting factor in obtaining consistent operation of long-distance low-frequency radio circuits. In Navaglobe operation, such

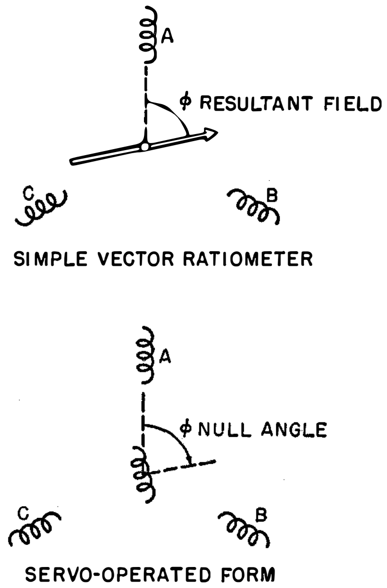

Figure 3—Principles of Navaglobe bearing translator. In the upper drawing is shown the simple vector ratiometer, in which the field resulting from application of the A, B, and C signals to the respective inductors gives a resultant field direction ϕ that determines the position of the magnetic needle. The servo-operated form of indicator shown in the lower drawing uses a moving-coil indicator instead of a magnetic needle. It is equivalent to the upper form but operationally superior.

noise piled on top of the signal could mask the proper strength ratios of the *A*, *B*, and *C* signals and so result in erratic bearing readings. Noise effects are minimized by use of square-law detection, very-narrow-bandwidth operation, and by signal-amplitude limiting in the initial wider-band stages of the receiver. The effectiveness of these measures in laboratory tests is demonstrated graphically by the oscillograms shown in Figure 4. Flight tests through actual thunderstorm areas have equally demonstrated the antinoise effectiveness of the improved receiver. Under the most severe conditions, useable bearing indications are still obtainable by increasing the reading time. For this purpose, the bearing translator is switched to a mode of operation wherein, in effect, it examines a large number of cycles of *A*, *B*, and *C* signals before it gives its answer; this tends to average out the disturbances caused by noise in one or a small number of cycles.

A second possible effect of atmospheric noise is to obliterate the synchronizing signal and hence incapacitate the bearing translator even though there may still be useful information in the *A*, *B*, and *C* signals. To minimize this effect, the airborne equipment contains a tuning-fork oscillator that is automatically kept locked in step with the recurring synchronizing signals received from the ground station. Should the latter signals be interfered with because of noise, the inherent frequency stability of the tuning-fork oscillator prevents the airborne timing cycle from being driven very far out of phase with the ground transmission cycle. Ordinarily, the ground synchronizing signal may be disturbed seriously for only a few seconds at a time; the airborne fork has proved to be stable enough to maintain adequate synchronization for lapses up to nearly a half-hour.

The automatic behavior of the receiver–indicator circuits with respect to noise may be likened to the mental action of a person viewing a noisy signal on an oscilloscope; by recourse to averaging and memory processes, the maximum information available from such a signal is extracted. In the extreme, should the signals be so bad as to contain no trustworthy bearing information, the automatic flag alarm warns the pilot, as it does in cases of equipment malfunctioning.

As a further safeguard and reassurance to the pilot, it is proposed that each Navaglobe transmitter will send out on the hour a special signal pattern that is identical in all directions. This pattern will correspond to a special check bearing, say 55 degrees, known in advance to all pilots. Regardless of where he is, every pilot should observe a 55-degree reading on his Navaglobe indicator during this checking period. Thus the pilot is periodically given simple and effective assurance that the airborne equipment is properly operative and calibrated.

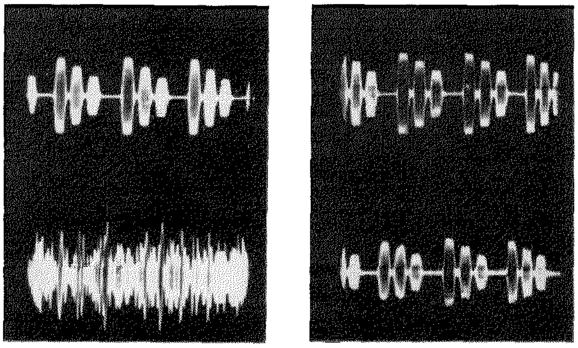

Figure 4—Oscillograms showing antinoise behavior of conventional receiver (left) and Navaglobe receiver (right). The upper waveform in each case shows the output when the signal only is applied to the receiver inputs, and the lower waveforms show the outputs when the signal with noise is applied.

3. Test-Flight Performance

Equipment operating according to the principles described above was used in a program of flight tests performed during the summer of 1952. A view of the experimental type of airborne equipment used in these tests is given in Figure 5. This equipment is bulky; the large indicators were specially designed for testing, calibrating, and recording purposes. (Descriptions of the type of equipment operating with the same basic circuits but packaged more compactly for operational use aboard aircraft are given in the next section; see also Figure 10.)

Consistent service out to very-long distances being the indispensable requirement for a long-range navigational aid, experimental determination of the performance of Navaglobe in this respect was the primary objective of the flights. The summer season was chosen because mid-summer daytime conditions provide the severest test for long-distance operation of low-frequency radio circuits, and low-frequency operation is conceded to offer the best hope for reliable long-distance radio *navigation*. The Navaglobe equipment was installed in an Air Force type *C-54* aircraft, accompanied by engineers and observers from the Federal Telecommunication Laboratories and from the Rome and Wright Air Development Centers of the United States Air Force.

For these tests, it was decided to use 100-kilocycle transmissions rather than 150-kilocycle transmissions, since all indications are that 100-kilocycle propagation is substantially better at 1500-mile (2780-kilometer) ranges. This precluded using the Navaglobe station at Adamston, which is restricted to 150-kilocycle operation by the physical spacing of its three antenna towers. A 100-kilocycle transmitter and efficient single-tower radiator were available at Forestport in central New York State. This nondirectional station was used to radiate a selection of signal patterns simulating the cycle of signals that would be produced along certain specific directions by a Navaglobe 3-antenna array. The particular pattern was changed every hour in a random sequence not known in advance on board the aircraft. During a 10-minute interval of every hour, a steady continuous-wave signal was radiated to permit field-strength measurements to be made.

The flight program included an overland phase from New York to California and return and an oversea phase, via Bermuda, the Azores, England, and Iceland. In addition to the round-the-clock visual inspection of the bearing indicators, oscillographic monitoring of the incoming signals, and periodic field-strength measurements, continuous pen recordings of the bearing indications were also made over some 12 days of testing, partly aloft and partly on the ground.

Figure 5—Experimental Navaglobe equipment used in flight tests.

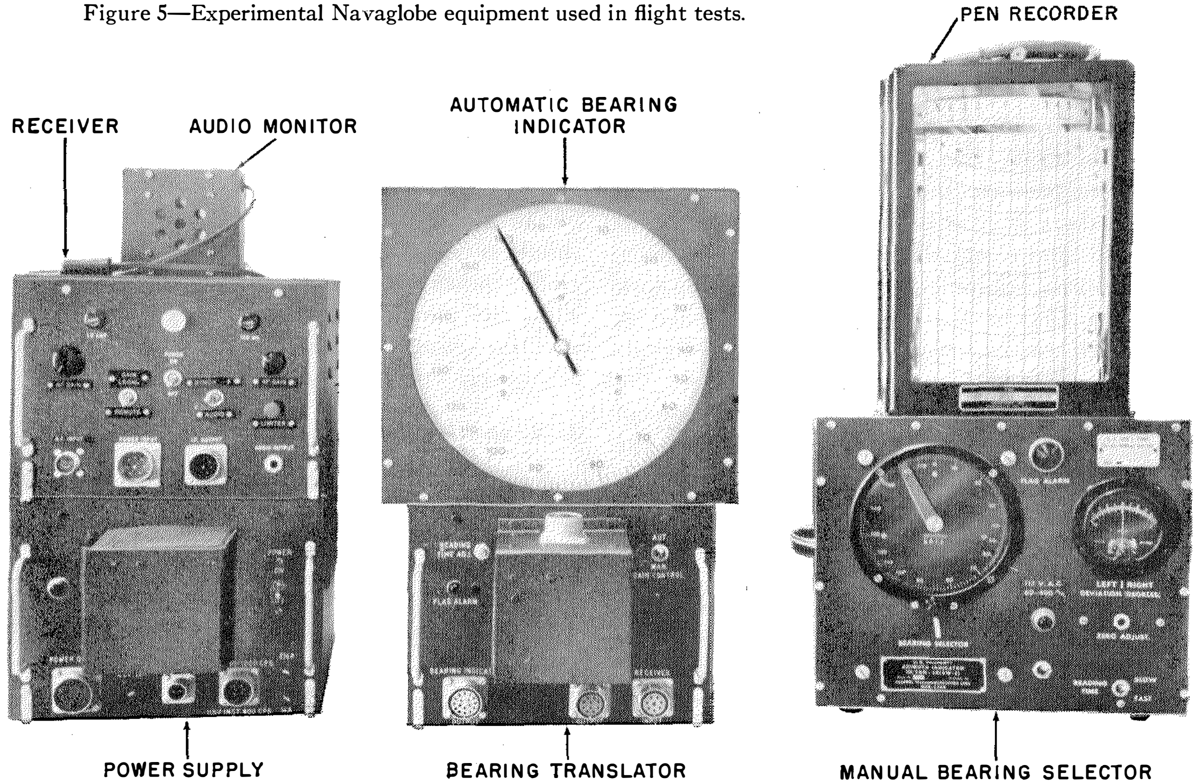

A chart summary of the flights is shown in Figures 6 and 7. Satisfactory reception of signals and operation of the bearing indicators was maintained *in the daytime* out to beyond Prescott, Arizona, and out to a point halfway between the

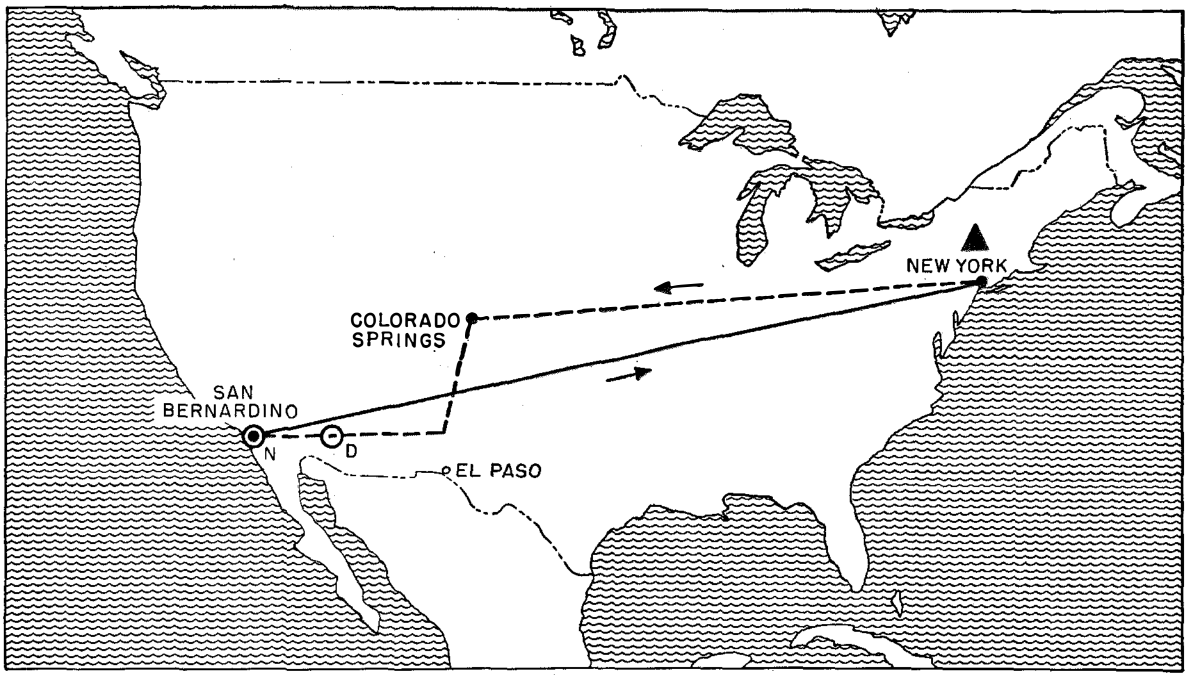

Figure 6—Map of transcontinental Navaglobe flight-test route. The black triangle marks the location of the transmitter. The dashed line shows the daytime portion of the flights and the solid line the nighttime portion. The maximum range obtained during the day was 1800 nautical miles (3330 kilometers) as shown by point *D*. The maximum range during the night, shown at point *N*, was 2000 nautical miles (3700 kilometers); but this was the limit of the flight.

southern tips of Iceland and Greenland. These points are approximately 1800 nautical miles (3330 kilometers) distant from the transmitter in New York State. *Nighttime operation* was observed out to San Bernardino, California, the limit of the transcontinental route, some 2000 nautical miles (3700 kilometers); and on the oversea flight to a point a few hundred miles southwest of England at which time daybreak occurred. The latter case represents a range of approximately 2600 nautical miles (4820 kilometers).

On one portion of the overland flight, north of El Paso, Texas, a violent summer-thunderstorm area with its high atmospheric-noise level was passed; the incoming signal deteriorated and the bearing indication fluctuated somewhat, but useable indications were still produced. Near Greenland on the transoceanic flight, the aircraft flew through a precipitation-static area. All other radio facilities aboard were inoperative for over a half hour, but the Navaglobe signals produced useable bearing indications except for about 7 minutes.

The true nighttime limit is not known, for although the European flight continued farther, signals from some powerful European low-frequency transmitters caused interference while the aircraft was near the European mainland. Also, it was discovered in flight that some conducted noise from a local power source on the airplane had been deteriorating performance. These facts indicate that the maximum day and night ranges observed might be bettered.

Undoubtedly winter performance and ranges would be considerably better, both day and night, since atmospheric noise levels are substantially lower in that season. However, the practical gauge of a radio navigational system is its performance under the least-favorable conditions, in this case midsummer daytime. A range of 1800 nautical miles (approximately 2100 land miles or 3330 kilometers) under such circumstances, overland as well as oversea, is unparalleled for radio navigational systems, even those of the nonautomatic-reading type. Even discounting the probability that still better ranges may be achieved with higher transmitter powers and with equipment improvements suggested by experience during the flight tests, the demonstration of 1800-nautical-mile (3330-kilometer) midsummer daytime operation by the experimental Navaglobe equipment indicates that the system will fulfill with comfortable safety margin the prime requirement for a truly long-distance radio navigational facility, that is, sufficient range to make possible reliable position-fixing service over all oceanic and polar regions.

4. *Airborne Presentation and Installation*

This section describes prototype airborne equipment that operates with the basic circuits and designs proved in the flight tests, but which is packaged more compactly and built to conform to standard Air Force specifications for airborne electronic equipment. While reliability is the primary consideration for a navigational aid, the size of the installation, and especially the simplicity of its use by the pilot, are important in determining the usefulness of any airborne equipment.

In Navaglobe, the numerical indications required for position fixing or for following a straight course to or from a selected ground station are presented in the simple terms familiar to pilots who navigate overland by conventional short-distance radio aids, such as the radio compass (ADF) or the omnirange beacon (VOR). That is, the automatic Navaglobe meter directly indicates in degrees the bearing of the observer from the selected ground station.

In the interest of standardization and economy of cockpit installation, Navaglobe bearings may be presented on the standard meters used for

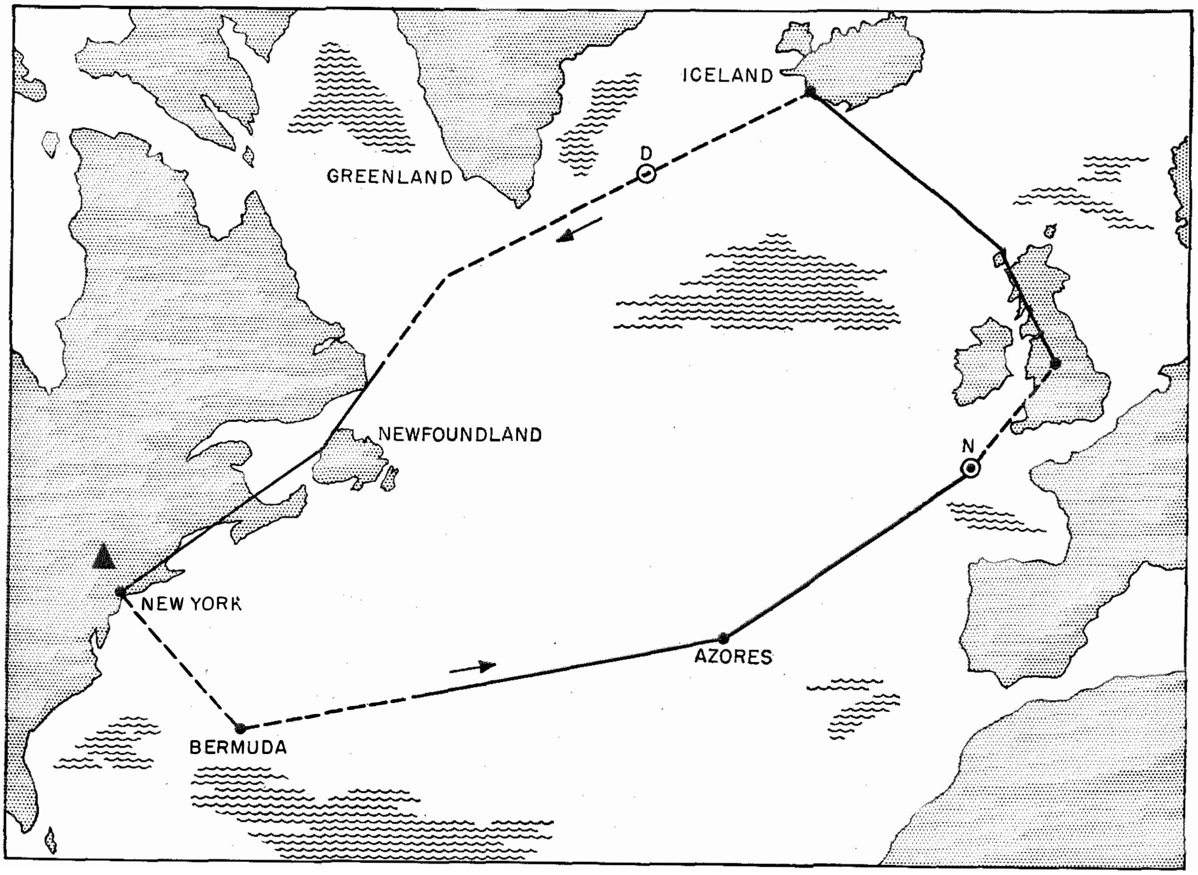

Figure 7—Map of transatlantic Navaglobe flight-test route. The black triangle marks the transmitter site. Dashed line indicates daytime and solid line nighttime portions of flights. The maximum range obtained during the day was 1800 nautical miles (3330 kilometers), at point *D*. Point *N*, 2600 nautical miles (4820 kilometers) from the transmitter, shows the maximum range measured during the night, but this was at the onset of daybreak during the flight.

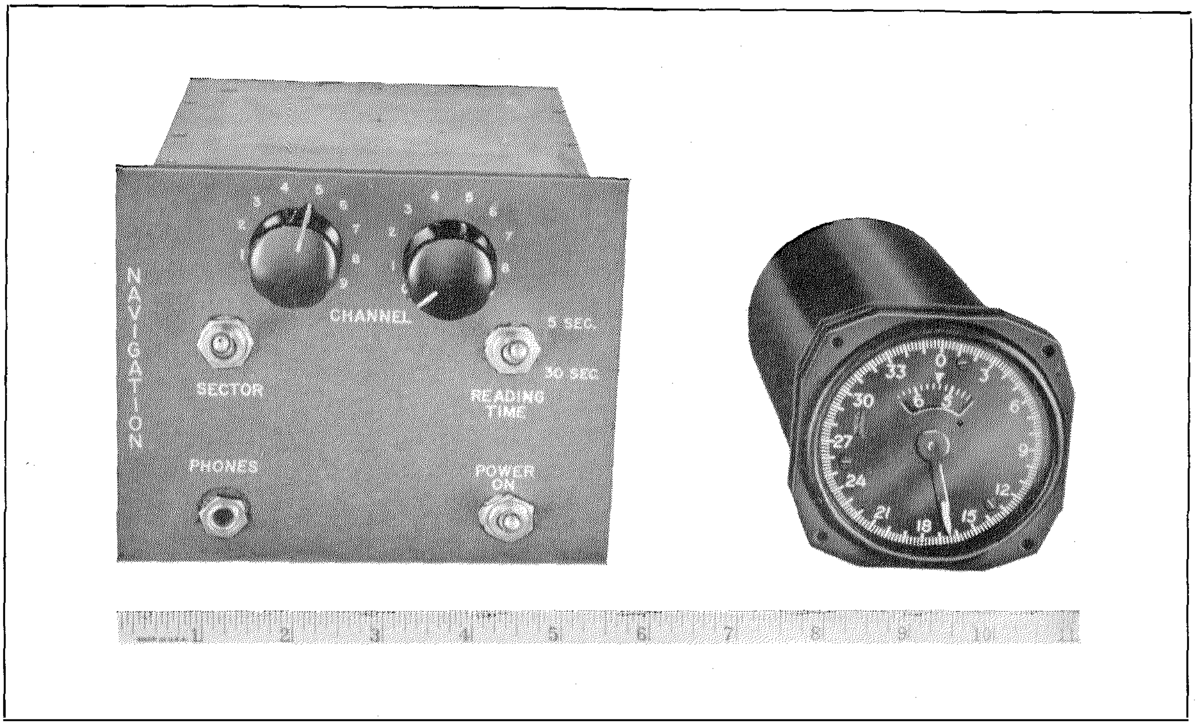

Figure 8—The miniature airborne Navaglobe control box and receiver is shown at the left and the vernier bearing indicator is at the right.

radio-compass, omnirange-beacon, or instrument-approach (ILS) services; namely the *ID-249* and *ID-250* meters. The Navaglobe airborne equipment has outputs provided to operate either or both of these standard indicators; but these instruments cannot be read closer than within 1 or 2 degrees.

Figure 8 shows the special Navaglobe indicator developed for cockpit or navigator's-compartment use. It is of standard panel-mounting size with a 360-degree dial and automatic pointer but includes an automatic 10-minute ($\frac{1}{6}$th-degree) vernier indicator. It also contains a built-in flag alarm indicator to warn against trusting the bearing indications when the signals or the equipment operation are unsatisfactory.

The only other item that the pilot need operate is the channel selector switch that tunes the receiver to any of 100 crystal-controlled channels to select a desired ground station. This switch is on the front panel of the receiver, which is miniaturized to the size of a standard control box and is installed in the cockpit. In this manner, the complexities and dangers of a remote-channel-switching system are avoided. A photographic view of this receiver, approximately 5 by 6 by 7 inches (13 by 15 by 18 centimeters), is shown in Figure 8.

If the standard *ID-250* meter is used to display Navaglobe information combined with magnetic-compass information (radio–magnetic-indicator operation), the indicating needle has the property of "pointing to the station" in the manner of an automatic direction finder, specially useful for homing toward the selected ground station. If the standard *ID-249* meter is used to display Navaglobe information, the pilot rotates a knob to select a given course, as appearing on the numerical indicator, and uses the vertical bar (deviation indicator) as a left–right meter, as in omnirange-beacon or instrument-approach-localizer practice. The deviation-indicator output could also be used to control an automatic pilot. It is possible that the *ID-250* or *ID-249* would be used by the pilot, and the special Navaglobe meter with its built-in $\frac{1}{6}$-degree vernier would be used for its greater reading accuracy if a radio operator or navigator were aboard.

On observing the Navaglobe bearing indication, the pilot immediately knows his direction from the selected ground station. He can fly to or from the station along this direction by maintaining a corresponding heading, correcting for wind drift so as to keep the Navaglobe bearing indication constant. In the absence of the complementary distance-measuring facility that

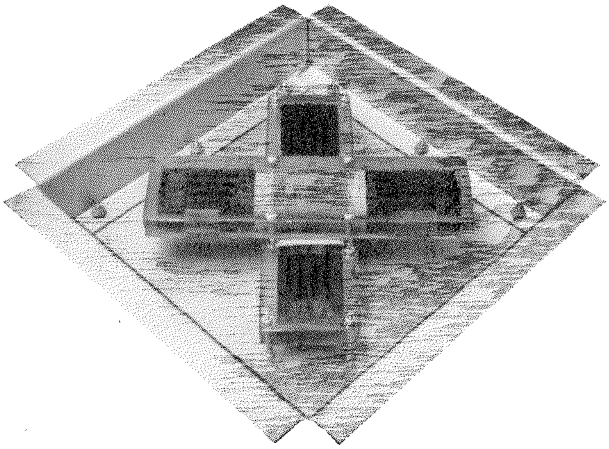

Figure 9—Flush-mounted airborne omnidirectional loop antenna for Navaglobe.

is intended to be added to the Navaglobe bearing-indication service (see discussion of Navarho in section 5), the pilot may use the Navaglobe bearing indications to fix his position in the same manner as with a radio-compass or short-range omnirange-beacon system. The outstanding advantages of Navaglobe over airborne direction finders are that Navaglobe has an over-all instrumental accuracy of the order of $\pm \frac{1}{2}$ degree, and will work reliably through severe noise at ranges approaching several thousands of miles regardless of time of day or season of the year.

The simplicity of the cockpit instrumentation and of the navigational interpretation of the automatic Navaglobe readings makes the system particularly suitable for use in a single- or two-place aircraft, for direct use by the pilot or co-pilot. This feature has a military significance, for certain types of missions may be carried out by long-range aircraft that carry no special radio operator or navigator.

The remaining portion of the airborne installation consists of the antenna, bearing translator, and power supply. In order that rapid changes in aircraft attitude will not modify the amplitude ratio of the A, B, and C signals, the omnidirectional antenna shown in Figure 9 has been developed. To minimize electrostatic noise pickup, a balanced double-loop system is used. The translator and power supply are each housed in a standard *A1-D*-size assembly. A photograph of the complete airborne Navaglobe installation (less antenna), designated *AN/ARN-27 (XA-1)*, is given in Figure 10. Also being supplied is a special Navaglobe signal generator and simulator for rapid testing and calibrating of the complete airborne installation in the laboratory or in the field. At present writing, the construction of prototype models of the *AN/ARN-27 (XA-1)* and associated test equipment is completed; after type testing and approval, which is in progress, a moderate quantity of these equipments is to be furnished to the Air Force.

5. Navarho

An ideal system for automatic position fixing would be one in which combined distance and bearing indications are provided for each ground station, preferably on a single radio-frequency channel. This is the type of service provided by certain very- or ultra-high-frequency medium-range systems operating over land. Distance indications by themselves also offer certain navigational advantages. In recognition of this fact, work is currently being done towards adding distance measurement to the long-range bearing system described in the preceding sections; the complete system has been named Navarho (pronounced Nava·rho).

The presently constructed Navaglobe equipment, ground and airborne, has been designed for the easy addition of automatic distance measurement at such time as airborne frequency sources are sufficiently perfected. The distance measurement involves comparison of the phase of the received Navaglobe signal with a locally produced signal from a highly stable airborne frequency generator. The phase comparison would be performed during reception of the non-directional synchronizing signal from the ground transmitter.

Such proposals were made a number of years ago by Federal Telecommunication Laboratories, where some research work has since been done along these lines. A high-precision oscillator with counter circuits was developed during 1951, utilizing a commercially available crystal. This work indicated the practicality of distance measurement through the use of a very-high-precision crystal clock. Certain long-distance flight tests made by the Rome Air Development Center of the United States Air Force in 1953 have further substantiated such expectations.

The problem of adding distance measurement to Navaglobe, resulting in Navarho, is essentially one of manufacturing in quantity relatively small-sized crystal units of the required high stability, which can maintain the requisite stability under the adverse conditions of temperature, shock, vibration, and power-supply variations encountered in aircraft. Oscillators with such stability have been in laboratory use since the second world war. The Rome Air Development Center now has a contractor working on the development of such a crystal oscillator with a specified frequency stability of one part per billion over an eight-hour period; preliminary results presage the successful completion of this development. The expected distance-measurement accuracy is a function of time and for fast aircraft is approximately 1 percent of range.

Plans call for a "building-block" arrangement whereby aircraft may be equipped for bearing measurement, distance measurement, or both. With combined indications, a computer for presenting fix and course information in the most direct terms is practical. As regards the airborne installation, the addition of a special translator unit, constructed along the lines of known techniques, is all that would be necessary to enable the present *AN/ARN-27* to provide distance indications. Present procurement plans of the Air Force for Navaglobe ground equipment operating in the preferred and allocated 90-to-110-kilocycle band include arrangements for permitting the future addition of the distance-measuring facility to make a complete Navarho system.

These planned ground stations will also be of higher power than the original 150-kilocycle Navaglobe transmitter at Adamston, which was rated at 10 kilowatts and had relatively small antennas. The experimental 100-kilocycle transmitter at Forestport radiated some 6 kilowatts and with this gave midsummer daytime ranges of 1800 nautical miles (3330 kilometers) and nighttime ranges up to 2600 nautical miles (4820 kilometers) or more. With the planned increase in radiated power, it is expected that still greater ranges and reliability will be achieved. With even the range demonstrated by the Forestport transmitter, the entire North Atlantic Ocean area could be provided with position-fixing service by means of 3 or 4 ground stations. All the oceanic and polar regions of the earth could be similarly serviced by some 30 stations, and as the Navaglobe—Navarho system is particularly

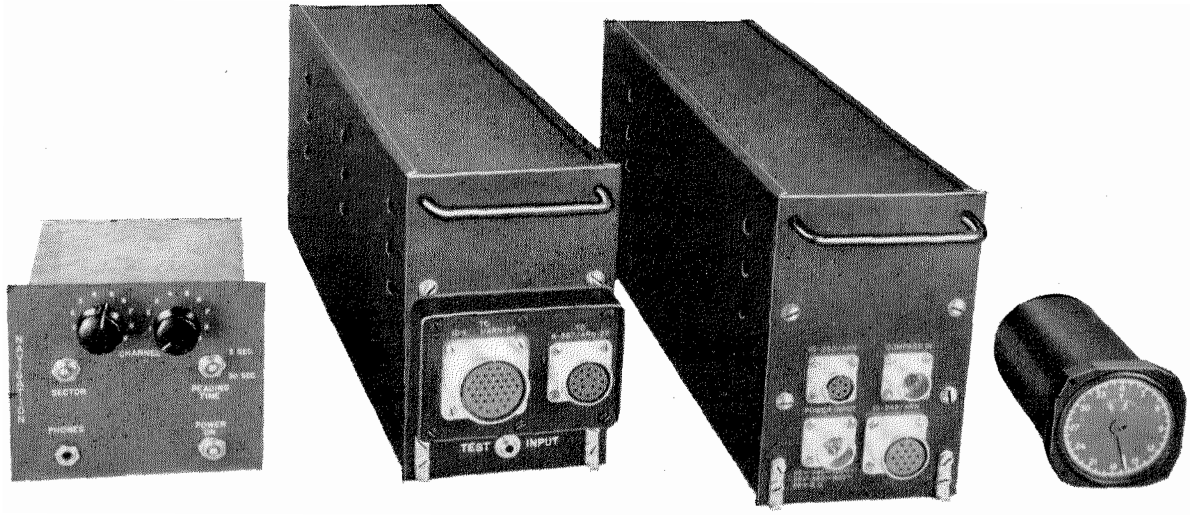

Figure 10—Photograph of complete airborne Navaglobe installation except antenna. From left to right are the control box and receiver, bearing translator, power supply, and bearing indicator.

characterized by extremely narrow-bandwidth operation, there is sufficient spectrum space for such ground stations within the allocated 90-to-110 kilocycle band.

These points, coupled with the fact that the present Navaglobe equipment is entirely compatible with the complete Navaglobe—Navarho system, indicate that such a system may well fulfill the need for a truly long-range complete radio navigational aid.

The Air Coordinating Committee (ACC) of the United States has recognized the above conclusion through its recently published announcement that the "USAF-developed 'Navarho' System appears to offer the greatest promise" for meeting the operational requirements for long-distance flight operations.[7] The committee proposes that the United States complete the development of this system and perform extensive evaluations both on the Pacific and Atlantic coasts of the United States. It further states that it will invite participation in this program by air and marine carriers, both domestic and international. The committee is currently informing other nations of its position through the International Civil Aviation Organization (ICAO) to promote future standardization of this system should results of its evaluation program of Navarho prove to meet the essential operational requirements. In this connection, the United States Air Force has been conducting preliminary demonstrations of Navaglobe—Navarho equipment for the benefit of the Permanent Council and of the international members of the 5th Session of the Communications Division of the International Civil Aviation Organization.

[7] R. B. Murray, "Press Release of the Department of Commerce," Washington, District of Columbia; March 16, 1954.

Recent Telecommunication Development

Techniques de L'Ingénieur

AMONG 8 VOLUMES that have been published in a series known as "Techniques de L'Ingénieur" are 2 on electronics and telecommunications that are the work of 120 authors. Of 100 articles that make up these 2 books, 11 were written by engineers and scientists associated with the following companies of the International System: Laboratoire Central de Télécommunications, Federal Telecommunication Laboratories, Compagnie Générale de Constructions Téléphoniques, and Le Matériel Téléphonique.

Gérard Lehmann, director of research of Laboratoire Central de Télécommunications, served jointly with P. Besson, director of Ecole Supérieure d'Electricité of Paris, as editor of the 2 volumes. Louis de Broglie, Nobel prize winner and member of the board of directors of Laboratoire Central de Télécommunications, prepared a paper on the electron in contemporary physics. Other contributors and their subjects are: J. Becquemont on gaseous and metallic-vapor rectifier tubes, M. Berger on carrier transmission on high-voltage lines and jointly with R. LeQueau on private telephone exchanges, A. G. Clavier on the theory of linear networks, M. François on tropicalization, J. Girard on metallic rectifiers, G. J. Lehmann on servomechanisms, I. Podliasky on waveguides, P. M. Prache on transmission lines, and A. Violet on radio navigation.

Collected into 2 loose-leaf binders are 2000 pages, $9\frac{7}{8}$ by $11\frac{3}{4}$ inches (25 by 30 centimeters), that include 2700 illustrations. Copies may be obtained at 108 dollars for the 2 volumes plus 8 dollars for the first 2 sets of replacement sheets from Techniques de L'Ingénieur, 26, Place Dauphine, Paris 1, France.

Training Course on Crossbar Equipment

By T. DEWITT TALMAGE

Kellogg Switchboard and Supply Company, a division of International Telephone and Telegraph Corporation; Chicago, Illinois

KNOWLEDGE of the operating principles and design characteristics of any mechanism permits the user to secure the best possible service that the device is capable of providing. Telephone dial switching equipment is no exception to this rule. The more thoroughly the maintenance technician understands the central-office equipment, the greater will be his effectiveness in maintaining it to operate at peak efficiency at all times.

The Kellogg crossbar dial switching system is inherently reliable and trouble-free but, like all telephone switching systems, its continuing satisfactory performance depends on proper maintenance. To provide practical knowledge and a basic understanding of the apparatus and system, an accelerated training program for maintenance personnel of telephone operating companies has been set up by the equipment manufacturer. Telephone technicians of average educational background have no difficulty in acquiring the knowledge and skills needed for adequate servicing of the equipment.

Applications for the course are made by the telephone operating company in behalf of its employees. Their educational and employment records, particularly in the telephone field, are carefully evaluated before the students are enrolled.

Practical knowledge of crossbar-switching-system fundamentals is taught each afternoon in a shop-type classroom in the factory.

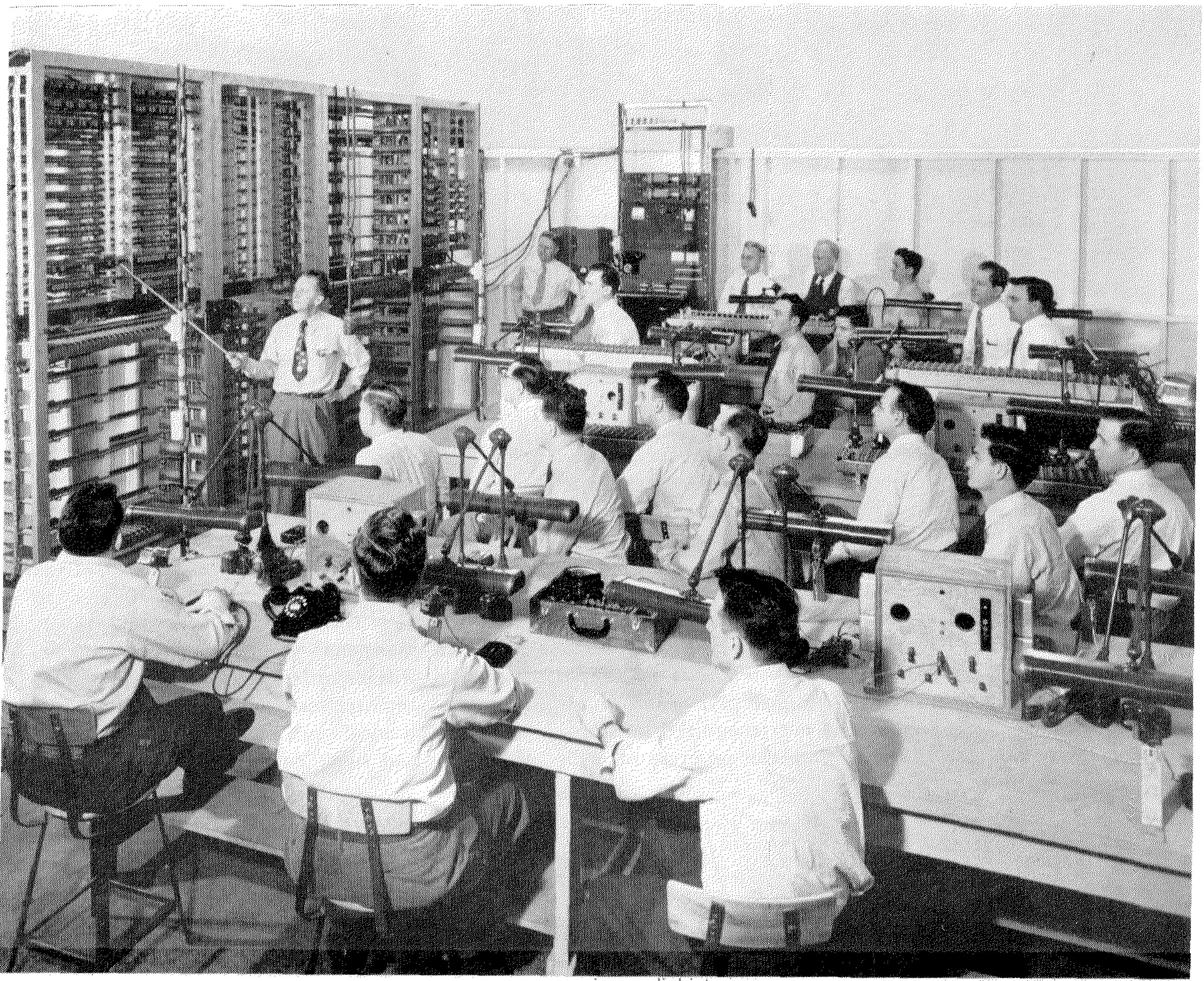

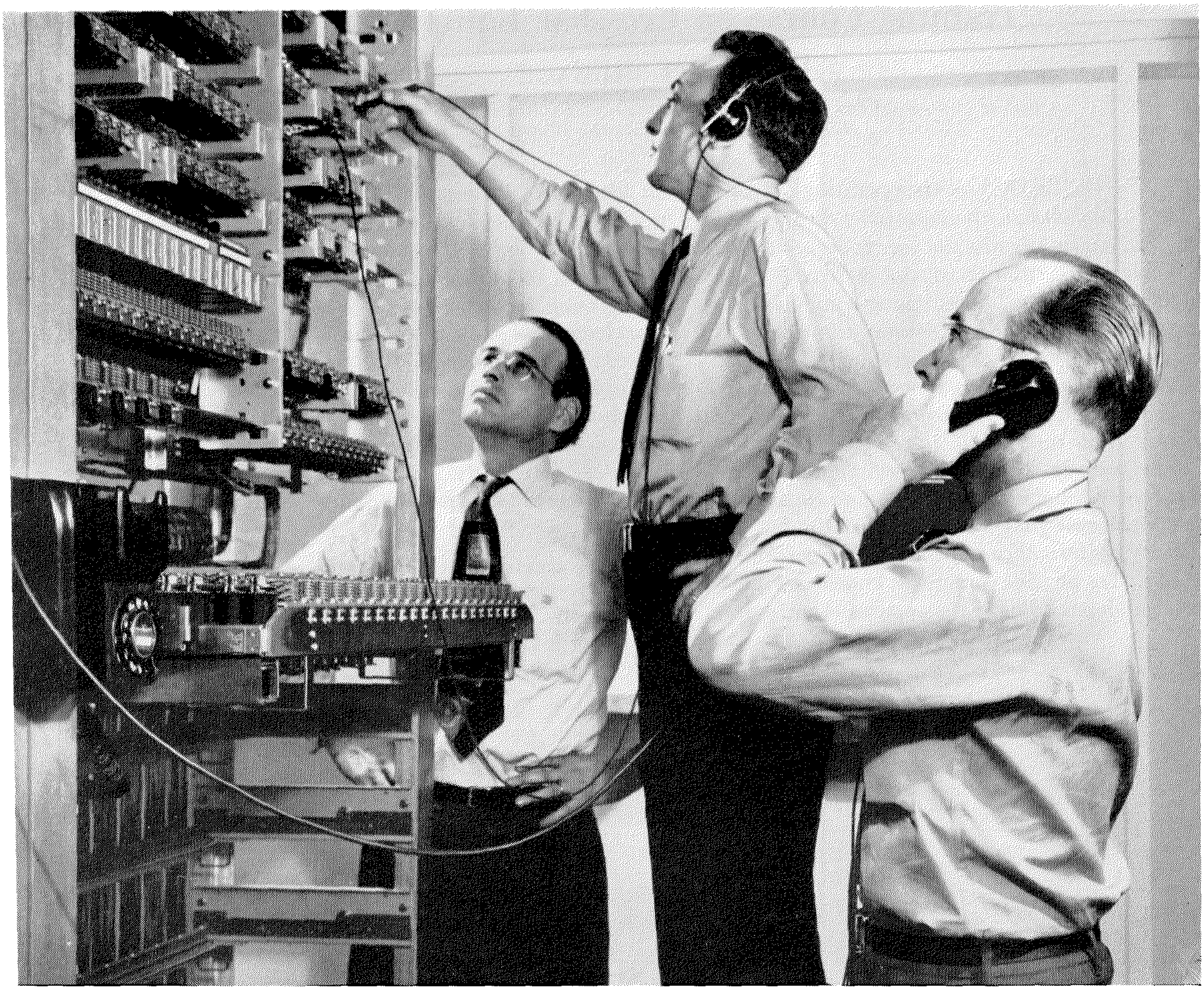

Checking operation of central-office dial equipment designed for, among other things, easy access by a maintenance technician. A crossbar switch has been pulled out from its normal position so that its performance can be readily inspected.

It has been found that students having less than a high-school education are sometimes so slow in learning that the progress of the entire class may be affected. Lack of such an education may be excused if the student has unusual aptitude or considerable practical experience with other types of switching equipment. Curiously enough, students with even a year or two of high-school training are quite often slow at simple arithmetic processes like multiplying and dividing. These possibilities are recognized and provisions are made so that the progress of each class can be kept reasonably close to its scheduled objectives.

The course starts with a thorough review of the essential electrical fundamentals and their application to dial telephony. Presentation of the basic principles of dial switching leads logically to a description of the crossbar system and its circuits and maintenance. Power equipment, attendant's switchboards, testing procedures, and preventive-maintenance practices are included.

The mechanical and electrical adjustment of the relays and switches used in the system are covered thoroughly, and a substantial amount of time is devoted to working with these devices to develop the manual dexterity and judgment needed to keep the apparatus in prime operating condition.

The course is taught by means of lectures, demonstrations, and conference-type discussions in the mornings with practical work in a well-equipped shop-type classroom each afternoon. Generous use is made of visual training aids such as motion pictures, projected slides, and Vu-Graph presentations. Greatest stress, however,

Using a kit of proper tools and gages augmented by simple test equipment, the student learns to adjust a magnetic impulse counter.

The type-*4000* relay being adjusted here, the crossbar switch, and the magnetic impulse counter are crossbar dial-switching-system elements whose design is based on the simple movement of a relay armature. A Kellogg current-flow test set is being used in this operation.

is placed on demonstration and actual experience in handling the switching apparatus. Each course takes from 5 to 8 weeks on a 5-day-week basis, depending on the objectives and other variable factors.

Checking and evaluating the progress of the students throughout the course is done at periodic intervals by oral and written examinations and by reviews. The examinations are based on essay-type questions, true-or-false statements, and multiple-choice answers to queries. In addition, the course terminates in a comprehensive examination that requires half a day.

The evaluation of each student's competency in the practical phases of the course is of equal importance to his progress in basic theory. The acid test is his ability to perform preventive-maintenance work correctly and to locate and clear promptly emergency troubles that may develop in switching equipment. Because the student is repeatedly drilled a step at a time to find and correct troubles in an operating crossbar switchboard included in the school's demonstrational apparatus, this part of the work becomes second nature to him.

A certificate attesting to the successful completion of the prescribed course is issued to each graduate, who then returns to his telephone operating company and shares his newly acquired knowledge and skills with his co-workers to assist in providing the best possible telephone service to his community.

The crossbar switch is the heart of the system and much time is devoted to studying its functions and adjustments.

Developments in Trustworthy-Valve Techniques*

By E. G. ROWE and PETER WELCH

Standard Telephones and Cables Limited; Footscray, Kent, England

IT HAS NOT been uncommon for designers of radio and radar equipment to state categorically that valves are inherently unreliable. Such criticism has been regarded with some scepticism by valve engineers, who have ample evidence of trouble-free operation of certain valves, such as those used in long-distance telephone repeater and carrier systems, and therefore were able to visualise suitably designed valves that could be manufactured by mass-production methods and yet give reliable operation under certain special mechanical conditions.

Valve-manufacturing methods are determined simply by the economics of supply and demand, and the valve maker must be sure that the many complicated piece parts that are used to build a modern receiving valve and the special finishing processes that are employed are all devised to secure ease of assembly and rapid exhaust so that the valves manufactured shall be salable. The standard of reliability possible is therefore commensurate with the price, and a delicate balance between these two has been maintained in a highly competitive market over the past twenty years. From the point of view of the engineer then, practical reliability is a flexible term that involves compatibility between the requirement and the price that the user is prepared to pay.

The acceptance of the fact that there were many usages where the low-price limitation imposed by the commercial radio and television market does not apply has permitted the valve engineer to embark on this quest for the better valve. It would appear that the urgency of the need has stampeded certain sections of the industry into crash action, which has often been based on questionable hypotheses—it has been argued that a valve is necessarily more reliable if it is a robust version of its commercial equivalent. This approach is crude and wasteful, and a scientific attack should be regarded as being the right one. Such an approach was made by establishing laboratory equipment that would simulate field conditions wherever possible. Then, having created a standard of testing by well-defined and repeatable methods, a comprehensive study was made of the electrical and mechanical performance of the valves for which special requirements existed.

1. *Special Testing for Reliability*

1.1 Field Failures

To establish suitable tests by which reliability can be measured it is necessary to get a proper understanding of the causes of valve failure. This may be done by analysing valves returned from various fields of usage.

The predominant failures are:—

A. Short circuits.

B. Disconnections.

C. Glass faults resulting in poor vacuum.

D. Heater faults.

E. Emission faults.

F. Noisy valves.

1.2 Manufacturing Failures

Examination of the methods of valve manufacture shows that failures may be attributed to two main causes, which we describe as "manufacturing variations" and "manufacturing errors."

The various possibilities that can occur in production may be illustrated in histogram form. In Figure 1, *A* shows the normal distribution of a particular parameter for a batch of valves when production is held in strict control, and *B* is the shift in distribution resulting from the uniform variation of any factor that influences a particular parameter. Such uniform variations occur when parts of the valve are manufactured either to the extremes of a tolerance or when processes are carried out for too short or too long a time.

* Reprinted from *Transactions of the IRE Professional Group on Quality Control.* Section 3 did not appear in the original publication of the paper.

Figure 1C indicates an enlarged distribution caused by the relaxation of production control such as the use of components outside limits. The results characterized in *B* and *C* are attributed to manufacturing variations.

Figure 1D illustrates a condition where the bulk of the manufacture is satisfactorily controlled

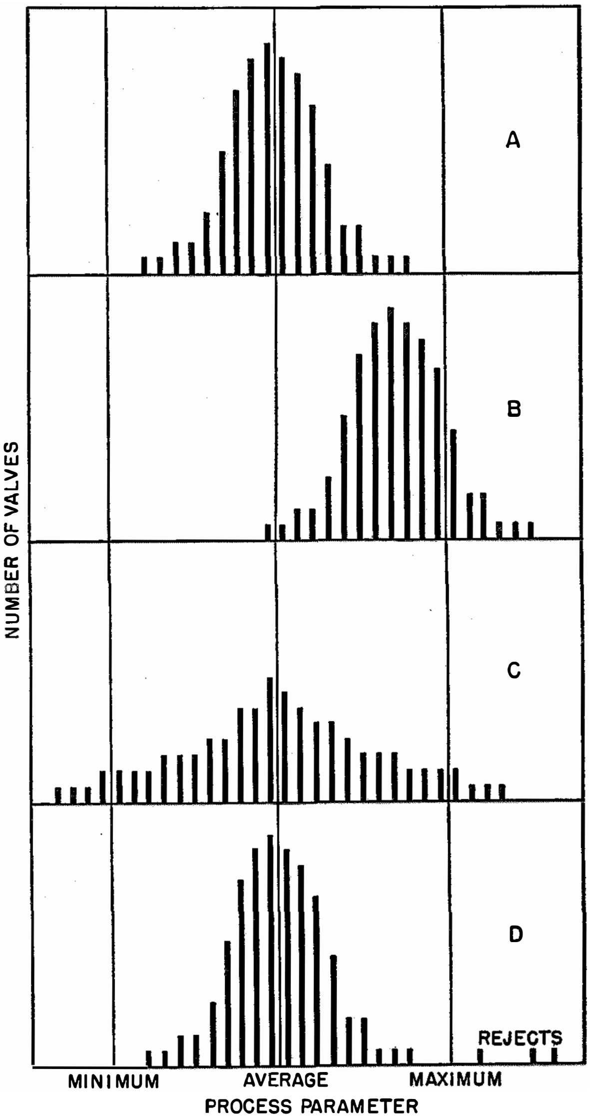

Figure 1—Histograms showing the distribution of a particular parameter in batches of valves as follows:

A—Normal condition with product in control.
B—The effect of a manufacturing variation with the product in control.
C—The effect of a manufacturing variation when the product is out of control.
D—Normal condition but with the inclusion of manufacturing errors.

but a small number is out of limits. Such a case is caused by faults in production defined as manufacturing errors. These will vary with the efficiency of the plant and personnel and an example of such is the random accidental distortion of grids during assembly, resulting in high anode current at cut-off.

It is obvious that to achieve reliability it is essential that all these causes be minimised and it is therefore important that methods of testing be devised to reveal and highlight them.

In this respect the manufacturing error is the more difficult to deal with because, unless the whole process of manufacture is suspect, faults attributable to a particular error rarely exceed 3 per cent. Nevertheless, this small order of faulty valves will contribute to the probability of catastrophic failure and therefore such valves must be removed and this can be done only by testing every valve.

In the case of manufacturing variations, it is possible sometimes to employ statistical methods of testing but in general the sample size required to ensure an adequately small customers' risk is so big a proportion of the batch that it is not worthwhile to attempt sample testing. To ensure that every valve lies in the required distribution it is desirable that each shall be tested individually. The batch quality is assessed from the number of rejections and a figure of 5 per cent has been set as the maximum permissible number to achieve the standard required. By careful planning it is usually possible to do this by the same tests that are used to check manufacturing errors.

1.3 Testing Procedure

A general testing procedure can be built up on the basis of the analysis of failures and the method of dealing with each fault will be discussed individually because the special tests necessary to improve the quality of the product by the elimination of errors and the control of variations depend on the nature of the particular fault. The tests required are given in Table 1.

1.3.1 Short Circuits

As a rule, short circuits are due to manufacturing errors, but cases do arise when they can be attributed to manufacturing variations.

They are either complete short circuits or transient short circuits that occur when the valve is struck or vibrated. All valves are therefore checked for both types of short circuit. The complete short circuit is usually rejected by tests

TABLE 1
BASIC TESTS REQUIRED

Test	Purpose	Extent
Manufacturing Errors	To eliminate random faults in production	100 per cent
Manufacturing Variations	To control and eliminate faults caused by trends in production	100 per cent or statistical
Design	To ensure that the basic valve materials and the basic design remain unchanged	Sample

prior to electrical characteristic testing, whilst the transient short circuit is revealed later on in the sequence of testing by excessive noise output developed across a suitable anode load resistor under 50-cycle-per-second vibration conditions.

1.3.2 Disconnections

Disconnections are either permanent or intermittent and are dealt with at the same time as short circuits.

1.3.3 Glass Faults Involving Insertion Losses With Miniature Bases

Except where severe mishandling occurs, insertion loss during installation of the valve in its socket is caused by inadequate compressive strain in the base or by hard or misaligned pins.

Since glass bases are machine-made, any fault will be uniform within the batch and therefore design tests for pin position, pin hardness, and strain are sufficient. It is usual to inspect a sample from each batch for pin position and then to check for hard pins and poor strain by means of a standardized test that consists of a thermal shock to the valve base whilst it is stressed by a tapered metallic plug placed so that it distorts all of the pins outwards.

1.3.4 Other Glass Faults

Glass cracks are due to excessive strain in the glasswork or to internal or external fissures formed during manufacture and which develop at later stages. These glass faults include cracked bases, bulbs, and pips or "tip-offs." Since the product will contain both manufacturing variations and manufacturing errors, a test is designed to cover both types of fault; each valve in the batch is tested. This test consists of a double thermal shock; the valve is immersed in boiling water and allowed to warm for 10 seconds and is then thrust into water at 20 degrees centigrade. By this means, the internal and external fissures may be developed into cracks and usually the severely strained envelopes break as well. Typical of the results found with this test are the rejections shown in Table 2 on commercial-type valves produced by various manufacturers.

TABLE 2
GLASS FAULTS DISCOVERED BY THERMAL TEST

Type	Per Cent Loss	Cause
6AL5	52	Cracked bases
6AM6	24	Cracked bases
1S5	21 27	Cracked bases Cracked tip-off
1R5	10 42	Cracked bases Cracked tip-off
6AM6	3	Miscellaneous
9D6	0·3	Miscellaneous

1.3.5 Heater Failures

The nature of a heater makes it liable to random manufacturing errors and therefore each valve must be checked. The test chosen consists of a sudden electrical overload applied in the cold state. The open-circuit voltage used is adjusted so that about twice the normal surge current flows and the time of testing is limited to about 7 seconds. This test will destroy all mechanically weak heaters that have been damaged during assembly and yet will not harm good valves. Typical results on valves of several types are given in Table 3.

In addition to this test, all valves are checked for heater–cathode insulation, which reveals both errors and variations, whilst a sample is taken from each batch for special switching life test. This switching test is arranged so that the heater is run for one minute and switched off for three minutes and is a design test that will reveal the quality of the materials used in the manufacture of the heater.

TABLE 3

HEATER FAULTS FOUND BY TEST

Type	Per Cent Loss	Cause
9D6	0·5	Miscellaneous
9D6	1·0	Miscellaneous
12AT7	10·0	Uncoated leg too long

1.3.6 Emission Failures—Catastrophic Nature

Emission failure in early life may be due to a manufacturing variation or to manufacturing errors. As it is not usually possible to detect the probable failure by emission checks at the normal test point, a more sensitive means of indicating cathode activity is needed.

One method of testing includes a 48-hour stabilizing period during which the valve is operated under approximately class-*A* conditions. After this treatment, each valve is re-tested for electrical characteristics including emission at the test point. Not only are the space requirements for 48-hour life tests embarrassing when the production of thousands of valves is needed, but it is doubtful whether all catastrophic failures can be eliminated in this way unless the characteristics of each valve are measured before and after the life test and the results compared.

Tests on early life performance of valves have shown that the main variations of contact potential and emission occur in the first few hours. With most valve types, we have established that a life test of 3 hours is sufficient to give reasonable stability and if used in conjunction with a sensitive emission test on each valve it will reveal the potential failure. The method of assessing cathode activity is to adjust the heater voltage to give 1·5 watts per square centimetre of total cathode area and, with the grid of the valve at a low negative potential, to draw a space current of about 20 milliamperes per square centimetre of cathode area. Figure 2 shows the grid-voltage–heater-voltage relation for a radio-frequency pentode as being typical of the testing theory. Tests on valves show that where grid voltage is adjusted to maintain a steady space current then both manufacturing errors and variations are obvious after a 3-hour run. This is illustrated in Figures 3 and 4. In both of these cases, the reject valves were satisfactory at the normal test point and yet began to fail after about 100 hours of life.

1.3.7 Noisy Valves

Both manufacturing variations and manufacturing errors can be checked by measuring the noise output produced across an anode load with

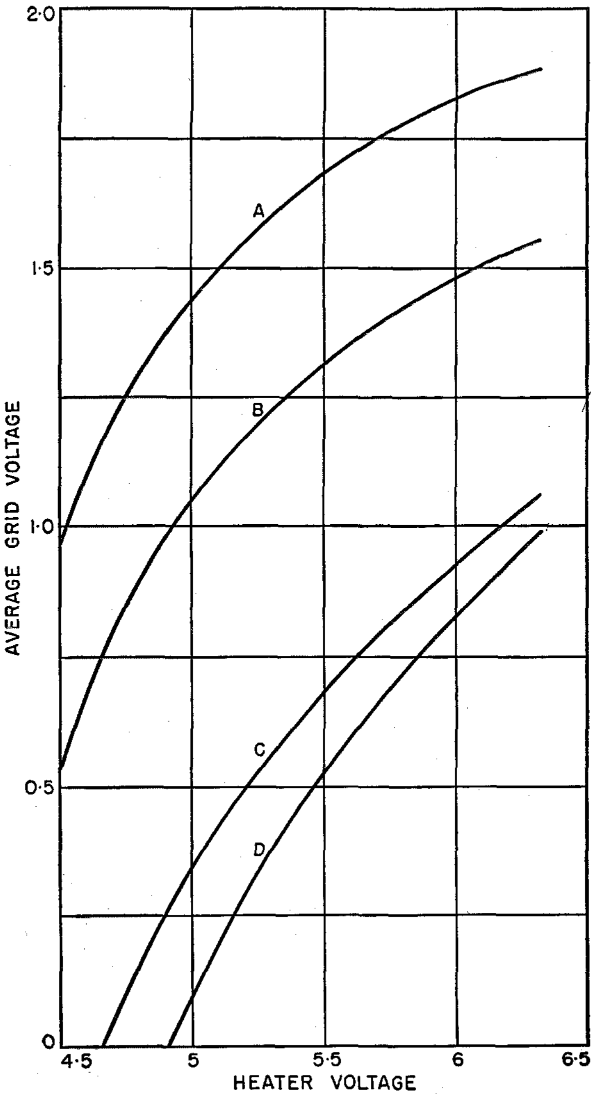

Figure 2—Curves of V_g against V_h for a constant I_a of 10 milliamperes in a *6AM6* valve. Curve *A* is initially, curve *B* after 20 minutes, curve *C* after 3 hours and 13 minutes, and curve *D* after 10 hours.

the valve operated under approximately class-A conditions whilst being vibrated at 50 cycles per second. Figure 5 shows the distribution within a batch of valves and illustrates how the

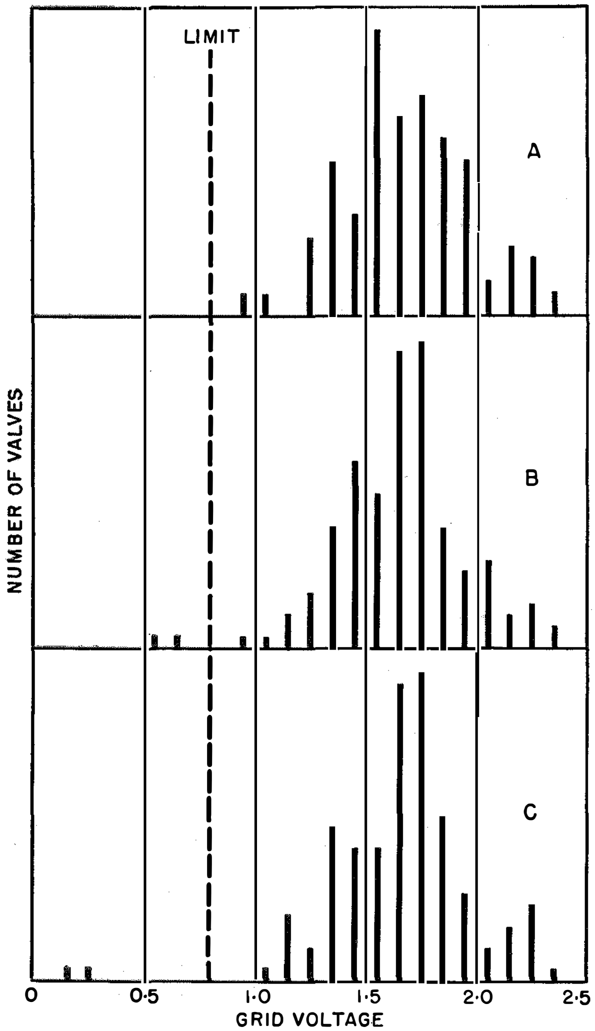

Figure 3—Histograms showing the grid voltage at constant anode current for a batch of *6AM6* valves operated at $V_h = 5{\cdot}1$ volts. Curve A is initially, B is after 3 hours, and C is after 10 hours. The valves suffering from manufacturing errors are revealed after 3 hours.

manufacturing error is eliminated. When manufacturing variations affect the result the distribution becomes skew as in Figure 6.

Test results show this method to be best for finding intermittent short circuits and disconnections, lint, et cetera.

1.4 Selective Tests Applied to Commercial Valves

The tests that have been described and the methods of analysis apply to the common faults that are met in normal usage. By employing these tests in addition to the electrical characteristic tests required to maintain a strict control over the product it is possible to select from normal commercial production a proportion of valves that have an improved reliability over normal manufacture. This is not at variance with the essential idea of valve reliability but rather supports it. For usage in equipments not liable to excessive mechanical vibration or shock,

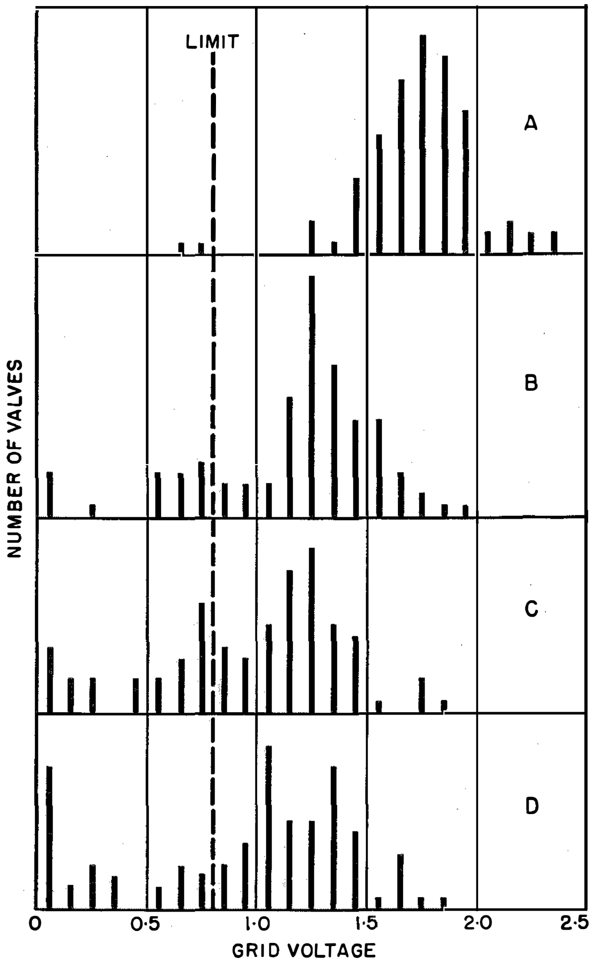

Figure 4—Histograms of grid voltage under conditions as in Figure 3 for a batch of *6AM6* valves suffering from a severe manufacturing variation. Curve A is initially, B is at 1 hour and 2 minutes, C at 3 hours and 13 minutes, and D is at 10 hours of life.

valves selected in this way give a high standard of performance that may be termed reliable. Even where mechanical movement is an essential requirement such valves show an improvement over the rejection rate of valves of unselected manufacture.

Experience with the selection of commercial radio valves by special tests has shown that in England it has formed a satisfactory interim measure before the fully reliable valves are freely available and from the engineer's point of view it has proved that the basis of reliable-valve production is controlled uniformity of the product. In this respect the use of statistical methods to determine the order of spread of

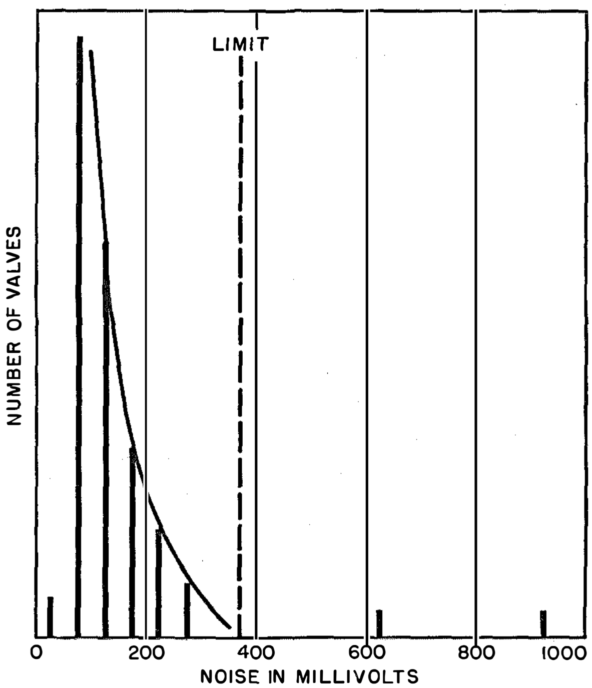

Figure 5—Histogram showing how manufacturing errors causing excessive noise may be detected by measuring the noise output developed across a 2000-ohm anode load with the valve vibrated at 50 cycles per second at an acceleration of 4*g*.

characteristics and of histograms to show the effects of manufacturing errors have been found invaluable. Such an approach has led to the inevitable minor changes in commercial-valve design that have benefited the normal user and has permitted the specification of certain assembly criteria for the design of the fully reliable valve.

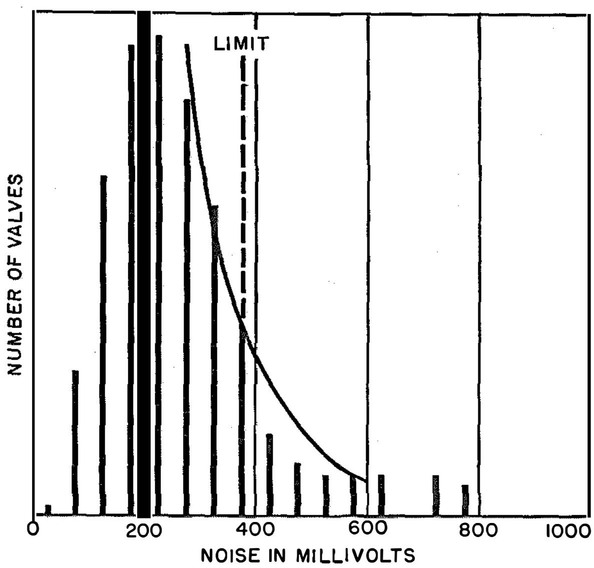

Figure 6—Histogram derived under the same conditions as Figure 5 but showing how manufacturing variations cause a larger spread of noise within a batch of valves.

2. *Special Tests for Trustworthy Valves*

2.1 General

If the only mechanical requirement for valves was that they should withstand a vibration of fixed amplitude, frequency, and wave shape, or a known repetitive shock, the design of valves to operate satisfactorily under such a particular condition would be relatively easy and the mechanical tests to check the initial engineering design and the quality of the product in mass production could all be conducted in a copy of the actual apparatus. The user would generally favour such a procedure, but valve engineers distrust such tests from bitter experience because, as the field of application of a valve increases, its behaviour must be known under many separate conditions, and such a method would result in a multiplicity of test equipments, each catering for a particular requirement. Unfortunately there has been a tendency for the earlier work on reliability to progress in this way and certain manufacturers have been cluttered up with mechanical test apparatus that gives an undefinable disturbance to the valve. Notable among such equipments are the many variations of mechanical bumper.

The principal mechanical requirements of the reliable valve are that it shall give noise-free operation under conditions of vibration, shall continue to operate satisfactorily after shock or high accelerations, and shall have a reasonable life under such conditions. In both the United States and Britain these requirements have been covered by a testing procedure consisting of a sinusoidal-vibration test and a resonance test for noise, a mechanical test for shock, and a continuous sinusoidal-vibration test for fatigue. It is necessary however to interpret the results of such tests similarly to the earlier analysis of field failures in order that the fullest use can be made of the information obtained during testing.

2.2 Noise Testing

A high noise output produced under vibration may be due to transient short circuits or disconnections, lint, loose electrodes, or to the fundamental vibration of the electrodes themselves.

Mechanical faults and lint constitute manufacturing errors that are minimized by close control over the valve-assembly procedure but as they represent a cause of valve failure they must be eliminated by testing.

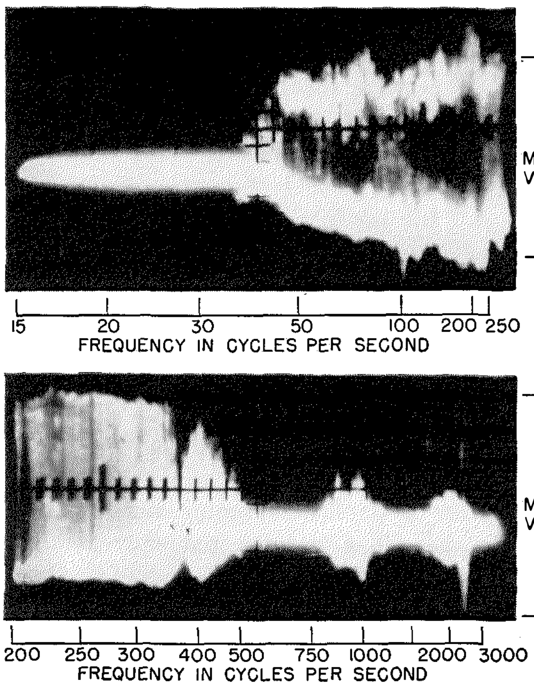

Figure 7—Noise spectrum of a miniature radio-frequency pentode.

Figure 7 shows the noise output from a typical pentode valve over the frequency range of 15 to 3000 cycles per second. The high noise output in the lower frequencies between 30 and 400 cycles per second is due to loose electrodes, which constitute a manufacturing variation.

The faults detailed above are adequately revealed by a 50-cycle-per-second vibration test with an acceleration of $4g$.

The fundamental vibration of the electrodes is determined by their physical constants—dimensions and properties of the constituent materials—and once the design has been established it is important to check that the production does not vary from the prototypes. This is done by sample testing conducted on an electromagnetic transducer under controlled conditions. Such a machine is described by E. G. Rowe.[12]

Whilst this machine will permit detailed examination of noise output at resonance it is easier to test every valve by an audio-frequency feedback method in which the valve is placed in the first stage of a high-gain amplifier having a linear response characteristic from 15 to 3000 cycles per second and which is terminated by a loudspeaker facing free space. The valve is placed in front of the speaker, care being taken to ensure that there is no rigid connection between it and the speaker. As a production test the gain is preset and valves that cause the circuit to break into regenerative feedback are rejected. Figure 8 is a photograph of such an equipment whilst Figure 9 gives the gain distribution in a batch of pentode valves. The degree of repeatability of measurement with untrained operators is to within 1 decibel in a range from 60 to 80 decibels.

2.3 Shock Testing

The basic shock requirement is that the valve shall operate satisfactorily during and after a high acceleration and therefore it is important that the definition of shock shall be concise so that correlation with users' equipment is possible.

The behaviour of the valve under shock is a design feature because failures are due to the movement and distortion of the electrodes, which

[12] References will be found in the bibliography, section 7.

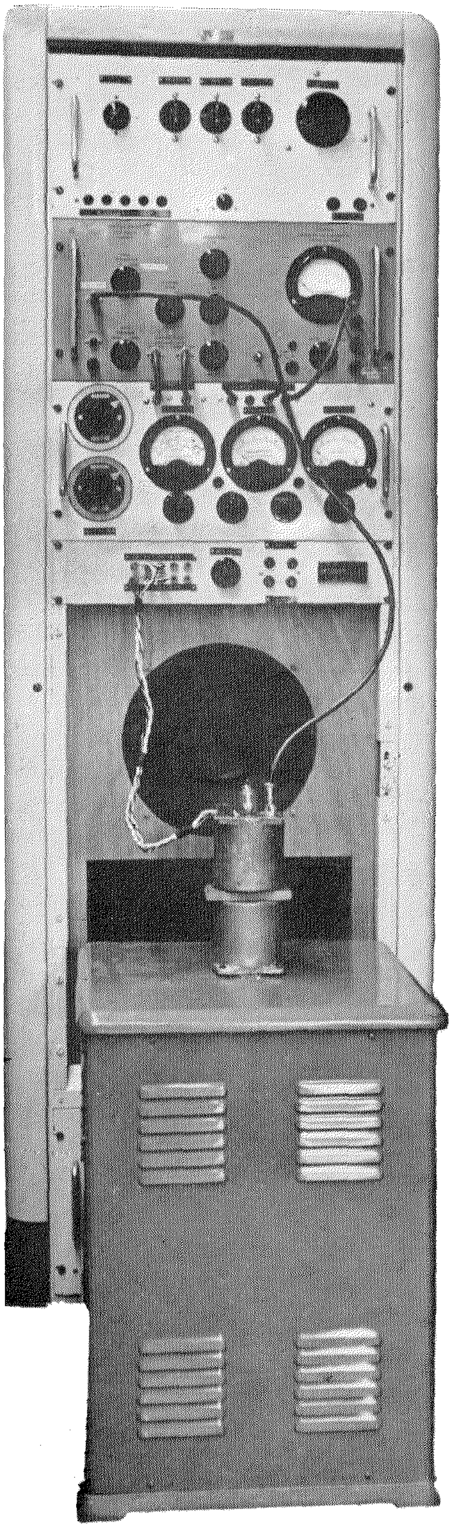

Figure 8—Audio-frequency-feedback test gear. This apparatus is simple to operate and provides a rapid production test for noise caused by electrode vibration.

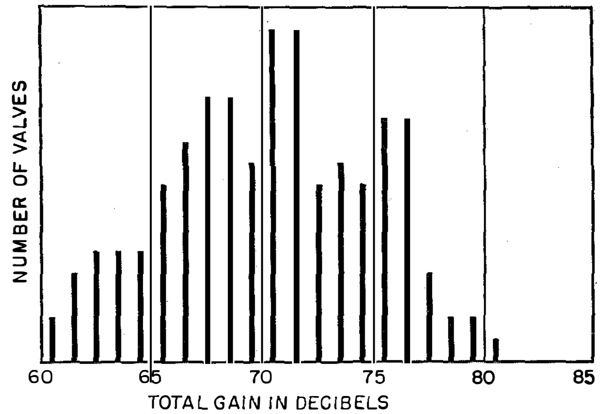

Figure 9—Gain in decibels required to start regenerative feedback with the valve 8 inches (20 centimetres) from the speaker and in a position giving a resonance for a batch of high-frequency pentodes. The mean value is 70·3 decibels.

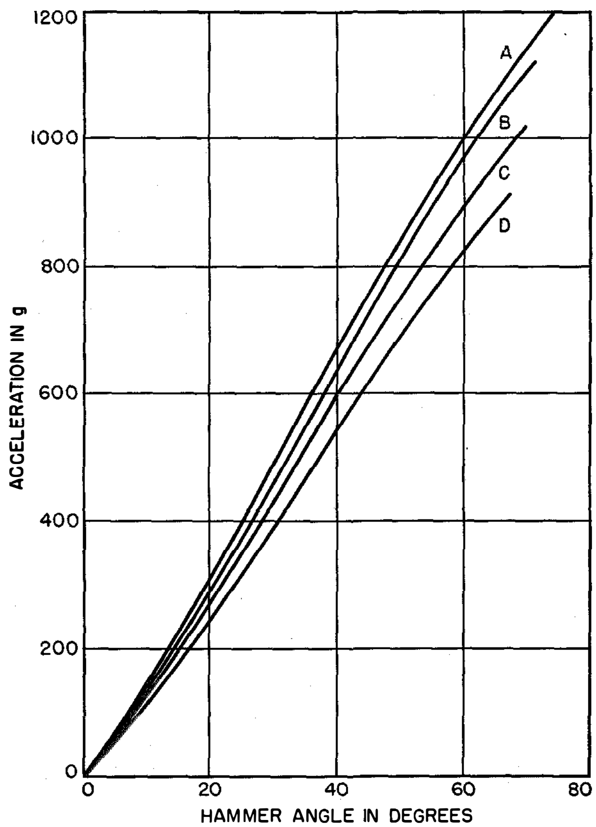

Figure 10—Calibration of a Taft–Pierce high-impact shock machine. The method of mounting is significant and *A* is for the table alone, *B* is with phosphor-bronze clamps, *C* includes a layer of felt, and *D* is with a thin rubber lining.

are dependent on the physical properties of the materials of which they are made. The apparatus used for performing the acceleration test is a modified form of the Taft–Pierce shock machine and has been described by R. J. E. Whittier[13] and others. Calibration of the machine is best done by using a parallel-plate capacitor with one plate connected to the moving table and the other to the frame, this being more accurate than the crystal methods.

Figure 10 shows an acceleration chart for such a machine and, as the method of holding the valve influences the acceleration it actually receives, correction factors are given for various mountings.

2.4 Fatigue Testing

Each individual user has his own conception of the critical frequency for fatigue testing. In addition to this complication is the fact that the actual frequency measured on any particular application is rarely sinusoidal and yet from an engineering standpoint it is desirable to correlate all vibrations to a sinusoidal movement.

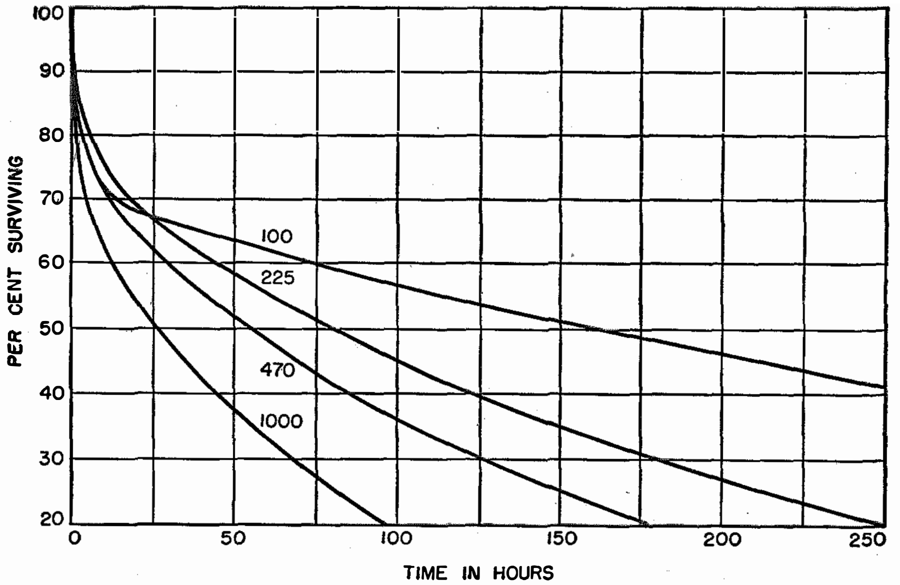

Figure 11—The survival rate for samples of 100 valves each from a batch of high-frequency pentodes measured at different frequencies as indicated on each curve. The acceleration in every case was 4*g*.

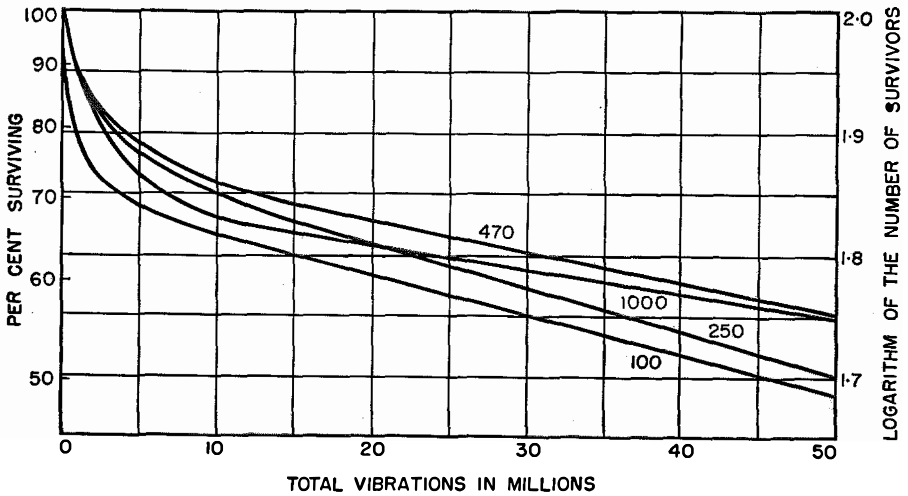

Figure 12—Showing Figure 11 replotted as the logarithm of the percentage survivors against the number of vibrations. The frequency of vibration is indicated and it is clear that the curves are quite similar.

Tests have been conducted on valves of commercial manufacture at frequencies of 1000, 470, 225, and 100 cycles per second whilst the valves were being operated and continuously monitored for noise and anode current. These tests show that the survival curves all have the same general shape as may be seen in Figure 11. By redrawing these diagrams as functions of the number of vibrations (Figure 12), it is clear that valve failure becomes independent of frequency, provided the acceleration is constant and that the excitation frequency does not

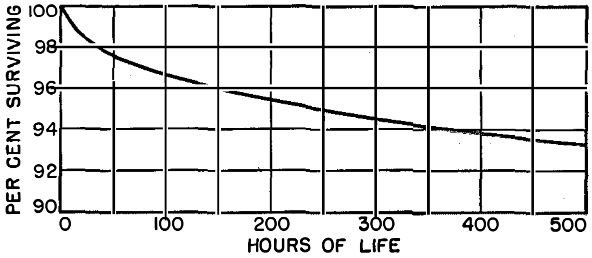

Figure 13—A typical survival curve for a batch of commercial-type valves shows an exponential rate of failure with time.

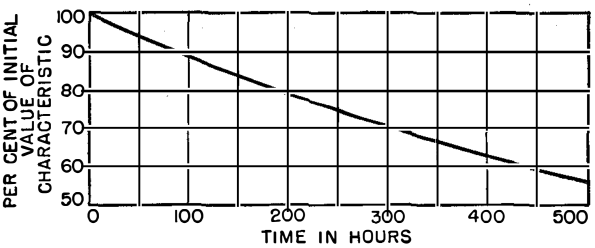

Figure 14—Typical variation of anode current of a commercial miniature pentode with time shown as a percentage of the initial value.

coincide with the resonant frequency of one of the components.

The reliable valve has a survival curve that does not include the high initial failures shown in Figures 11 and 12.

2.5 Life Testing

Life testing of commercial valves over many years has shown that the survival curves have a shape typical of that shown in Figure 13. The first part of the curve has a steep slope and is due to the high incidence of catastrophic failure; after this the failure rate is much slower and follows approximately an exponential law.

The controlled manufacture of the reliable valve and the quality level that is achieved by the testing sequence ensure that the number of catastrophic failures is very small but adequate control of this feature calls for a much larger sample for life testing. This sample consists of 20 valves from each batch and to increase the sensitivity of the scheme it is usual to consider the results of 5 batches as a continuous moving average.

It is difficult to ascertain the failure rate of the reliable valve because it normally involves very long periods of life testing. However, since the predominant failures are due to falling emission or heater failure a reasonable index of valve quality may be obtained by considering the percentage change of valve characteristics and by switching tests conducted on the heaters.

The percentage fall of characteristics also tends to follow an exponential curve (Figure 14). By examining the average fall on a small group of valves it is possible to estimate the average life in terms of the life-test conditions and arbitrary end-point. As a rule, anode current is selected as the variable and the arbitrary end-point as a 50-per-cent fall. Figure 15 indicates the application of this method to small samples of four types of commercial valves. This approach gives a very sensitive index of valve quality.

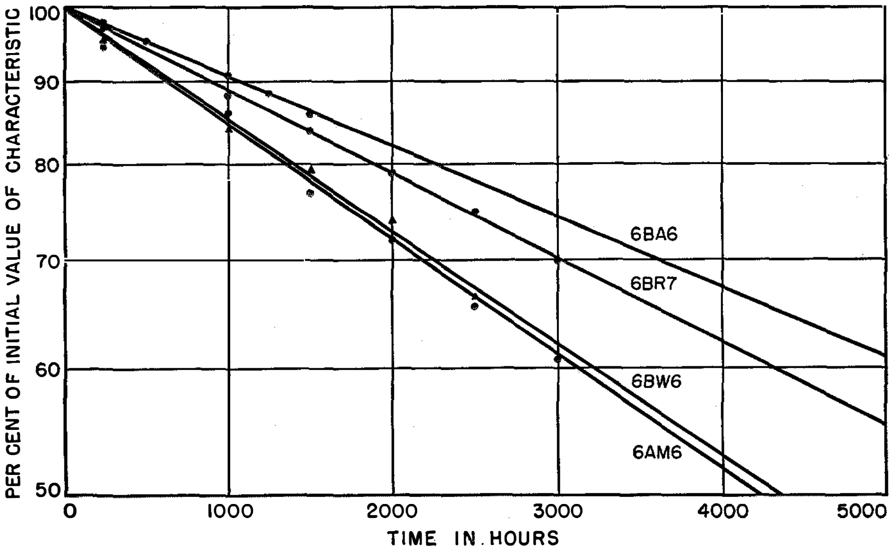

Figure 15—Extrapolated characteristics showing the use of the average fall of the characteristics of a batch, which may serve as an index of valve quality. In each case the sample size was 4 and the valves were of commercial manufacture.

The heater testing is conducted at the same time as fatigue testing.

2.6 Summary of Complete Testing Procedure

Tests designed to safeguard against the normal field rejects have been described and the reasons for choosing 100-per-cent or sample testing have been explained. In addition to the electrical tests a description has been given of special mechanical tests and of life tests. It remains to set out the order in which the tests are performed so that the maximum amount of information can be obtained about each batch with the minimum of testing time. The scheme shown in Table 4 is followed with valves received from the exhausting station.

TABLE 4

Comprehensive Testing Procedure

Test	Remarks
Thermal Shock for Glass	Extract a sample for inspection of pin position and return to batch. Extract a sample for thermal-shock test (section 1.3.3) and destroy after testing.
Short-Circuit at High Voltage	
Heater Flash	
Activation	
Short-Circuit and Continuity	
Electrical Characteristic	
Vibration	Extract a sample for check of characteristics before 3-hour life run and return to batch (quality control).
Short Life–3 Hours	Recheck the sample to assess drift of characteristics (quality control) and return to batch.
Underheating to Find Catastrophic Failures	
Store	Extract a sample for life test and destroy after testing. Extract a sample for resonance test and return to batch. Extract a sample for fatigue test and destroy after testing. Extract a sample for shock test and destroy after testing.
Feedback	
Electrical Retest After Shelf Life	

Failures in excess of 5 per cent for the full tests and failure to meet the sample tests cause batch rejection.

The testing scheme applies equally to continuous production although the illustrations are relative to a batch. When continuous production is used it is necessary to take samples at regular intervals and to maintain a moving average of the results of 100-per-cent tests. For the batch system, production must be sufficiently large for batches of 500 or more valves to be tested at a time. Below this figure, production processing tends to become inconsistent and the product is liable to go out of control.

3. *Design Considerations for Reliable Valves*

3.1 Reduction of Noise

Noise due to manufacturing errors such as short circuits, disconnections, and lint is minimized by manufacturing large quantities of valves under the most-efficient production-control methods.

The design engineer is not vitally concerned with such noise but must concentrate rather on noise produced by electrode rattle and by the fundamental vibration of the electrodes themselves.

Rattle noise is caused by the unsatisfactory locking of electrodes and the order of importance of such locking considerations is from the cathode outwards. The effect is aggravated by the fact that the top of the valve usually moves more than the base under conditions of vibration and because of the high compliance between insulator and bulb the movement is transferred to the electrodes. In addition, the electrode structure must remain relatively unrestricted at the top end because locking tapes, connections, et cetera, are best applied at the base end. Considerable reductions in rattle noise may be achieved by using two insulators instead of one at the top end of the valve and by ensuring that the holes in which the electrodes are held are a tight fit. However, this double insulator can adversely affect valve performance by excessive local cooling of the cathode sleeve. Because heater switching causes expansion and contraction of the cathode thereby enlarging the hole in which it fits it is essential to make the cathode-to-mica fit as tight as possible bearing in mind the above limitations and this is usually done by locking the cathode with a bead or bell shape or by pinching as shown in Figure 16. The second insulator is not in contact with the cathode.

A further improvement can be made by locking the grids in the insulator by means of tapes fixed

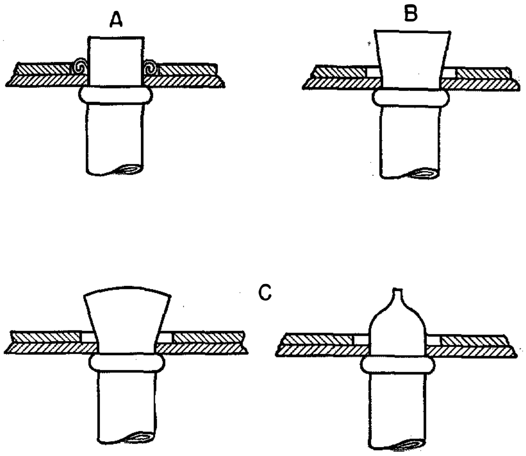

Figure 16—Methods of locking cathodes. At top left is the eyelet form, top right is the bell shape, and at the bottom are front and side views of the pinching technique.

to the insulator and welded to the grid leg. By taking these precautions, rattle noise has been eliminated almost completely in the reliable valve.

Resonance noise is produced by the fundamental vibration of the electrodes themselves. Investigation of this problem has shown that the resonant frequency of grid support wires, grid laterals, cathodes, and most other parts may be predicted accurately by empirical formulae.

For nickel cathodes, the resonant frequency for circular cross sections is given by

$$f = \frac{1{\cdot}42 \times 10^5 (r_1^2 + r_2^2)^{1/2}}{l^2}$$

and for rectangular cross sections by

$$f = \frac{1{\cdot}64 \times 10^5 (a^2 + aa' + a'^2)^{1/2}}{l^2},$$

where r_1 and r_2 are internal and external radii, a and a' are the internal and external dimensions across either of the principal axes through the centre of gravity of the cross section, and l is the length between insulators; all dimensions are in inches. For grid support wires of any material, the resonant frequency is given by

$$f = \frac{1}{2\pi l^2}\left[\frac{19\,Yr^2}{\rho\{1 + (\bar{w}/w)\}}\right]^{1/2},$$

where r is the radius of the wire, l is the length between the insulators in inches, w is the weight per unit length, $\bar{w}$ is the weight per unit length of half the lateral wires attached to the support, Y is Young's modulus in dynes per square centimetre, and ρ is the density of the material in grammes per cubic centimetre.

For the commonly used materials, the formulae become:—

for nickel,

$$f_{\mathrm{Ni}} = \frac{1{\cdot}3 \times 10^5 \times r}{l^2\{1 + (\bar{w}/w)\}^{1/2}},$$

for copper,

$$f_{\mathrm{Cu}} = \frac{1{\cdot}088 \times 10^5 \times r}{l^2\{1 + (\bar{w}/w)\}^{1/2}},$$

for 5-per-cent chrome copper,

$$f_{\mathrm{CrCu}} = \frac{1{\cdot}09 \times 10^5 \times r}{l^2\{1 + (\bar{w}/w)\}^{1/2}},$$

and for mild steel,

$$f_{\mathrm{Fe}} = \frac{1{\cdot}42 \times 10^5 \times r}{l^2\{1 + (\bar{w}/w)\}^{1/2}}.$$

A simplified calculation for grid lateral wires is obtained by approximating the profile either to the arc of a circle or to a rectangle as shown in Figure 17 and the formulae become:—

for the arc of a circle,

$$f = \frac{0{\cdot}17r}{(2{\cdot}78d^2 + 0{\cdot}558R^2)}\left(\frac{Y}{\rho}\right)^{1/2}$$

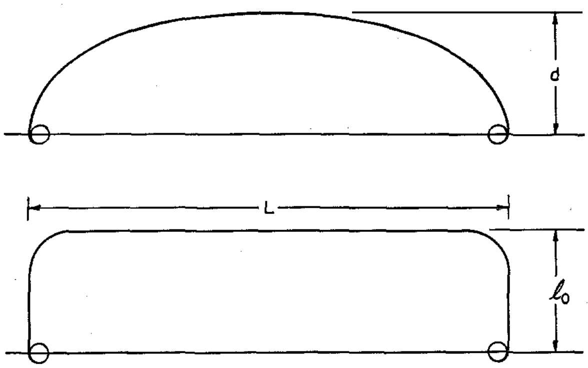

Figure 17—Grid profiles used for computing vibration frequencies.

and for a rectangular section,

$$f = \frac{0{\cdot}17r}{(2{\cdot}9l_0^2 + 0{\cdot}325L^2)}\left(\frac{Y}{\rho}\right)^{1/2},$$

where r is the radius of the wire, d is the depth of the arc, and R is the radius of the arc; l_0 and L are the dimensions of the rectangle (all measurements being in inches), Y is Young's modulus, and ρ is the density.

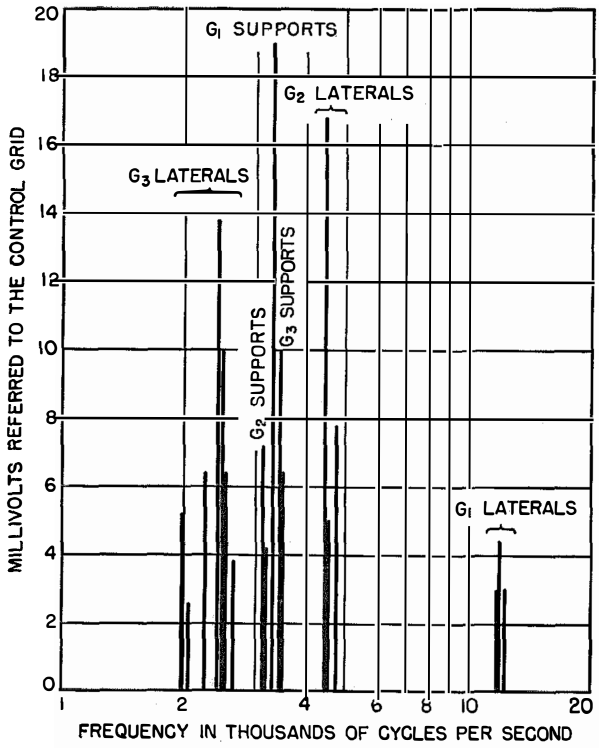

Figure 18—Resonance diagram for a vari-μ radio-frequency pentode.

Figure 18 shows a typical resonance diagram marked with the frequencies due to various grids, et cetera. In general, the noise output produced at resonance appears to vary with the square root of the applied acceleration and there are few resonances below 1000 cycles per second. Most cathodes are well up in the 3-kilocycle-per-second region and most resonance noise is created by the individual grid lateral wires and tends to spread in a band about the mean calculated figure. Suppressor grids usually have the lowest resonant frequency and typical cases show a band width of 300 to 400 cycles per second.

Little can be done to reduce the resonance noise produced by the grid laterals except by the choice of material and size to ensure that the frequency is as high as possible. The noise produced by grid supports resonating may be improved by about 1·67 times by clamping the support at both ends and this practice is used in special cases where exceptionally low values of noise are required. This is shown diagrammatically in Figure 19.

It is unfortunate that the general improvements that are incorporated in the reliable valve to guard against low-frequency rattle and fatigue usually result in a more-rigid structure that then offers less compliance between the individual electrodes and the exciting forces. For example, the double insulators are a better fit in the glass bulb and therefore transmit energy more easily to the electrodes. In cases where trouble has resulted, it has been found necessary to change the materials of the grid in order to increase the resonant frequency.

Comparison of experimental batches of valves and production samples to assess the results of changes can only be made by measuring a quantity of valves, preferably by the audio-frequency feedback method.

3.2 Effects of Fatigue Vibrations

The examination of valves that have failed under fatigue testing shows that they divide into three classes consisting of those which in a relatively short time show high grid currents and/or falling emission due to gas evolution because of breaking up of the insulator pips,

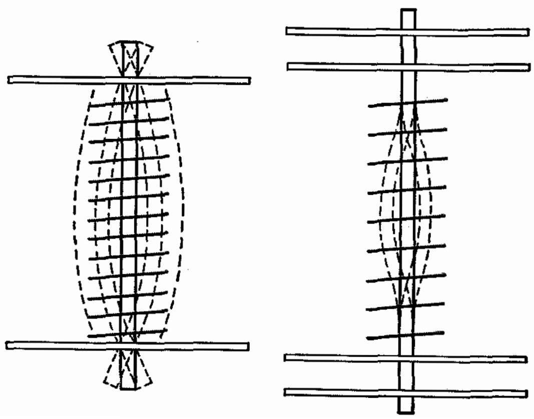

Figure 19—The freely vibrating grid structure has a resonant frequency of approximately 1100 cycles per second. With the ends locked, the frequency is increased to about 1700 cycles per second.

those that give rattle noise over a longer time interval because of the wearing of slots and holes holding the electrodes; and finally those with fractured connecting links and stem wires due to the ultimate fatiguing of the piece-parts.

The mounting position of the valve under vibration has a considerable effect on the resultant type of failure. Vibration parallel to the main axis is the most important as it is the usual position and this produces wear of the insulator pips or snubbers. Vibration across major and minor axes produces wear of the holes holding the electrodes, the major-axis position being the more severe.

The ordinary commercial valve is often prone to the first type of failure because it has a relatively loose structure designed to permit rapid assembly and this allows a considerable differential movement of mount and glass bulb under vibration with consequent production of mica dust and gas poisoning of the emission. To reduce this effect, it is necessary to stop the differential movement from occurring, and this may be done by ensuring that the bottom insulator is rigidly attached to the glass stem either by the method used to assemble the valve or directly by using eyelets or metallic tapes clinched in the insulator and welded directly to the stem wire. The top insulator is then rigidly clamped to the assembly. To achieve the maximum rigidity, it is better to weld tapes across the electrode lugs projecting through the top insulator than to bend the lugs over, unless the bending is done mechanically. In general, structures in which the insulators are supported around the periphery are to be preferred and therefore where there is not adequate support, extra supporting members are necessary. Both insulators are designed with protruding pips around the periphery to take up the variations in bulb size and are controlled to give a good tight fit. When these precautions have been taken the wear of insulators gives the same order of rejection as the general fatigue of the rest of the valve.

The wear of electrode holes and slots may be considered as a second-order effect and can be reduced by attention to design. Round holes should be used where possible and if shaped electrodes are to be held it is necessary that the securing lugs be positioned so that vibration is prevented in all directions. Improvement that can be obtained in the method of supporting an anode by ensuring that the two lugs are at right angles is shown in Figure 20. In all cases double insulators at the top of the valve are to be preferred and, where possible, additional aids such as grid straps should be provided in order that movement of the electrodes be damped adequately.

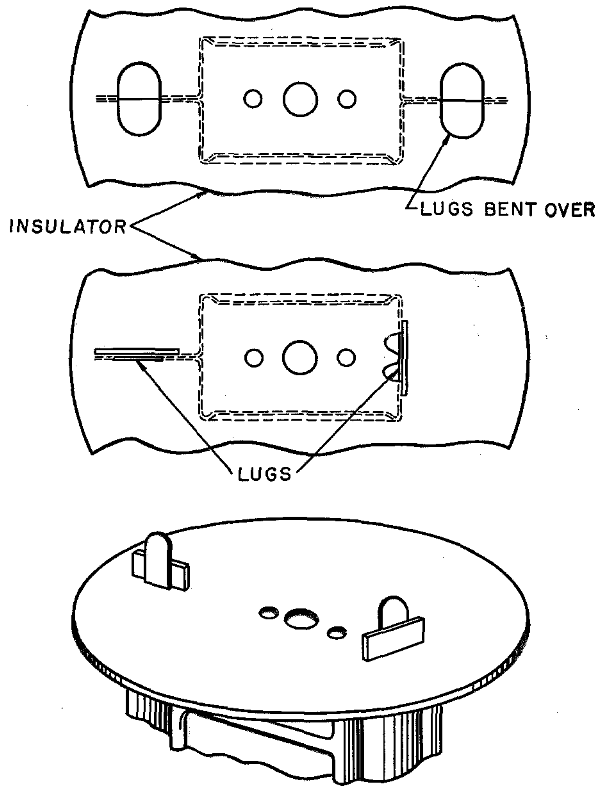

Figure 20—The upper drawing shows the old form of inserting two lugs through the insulator and bending them over to secure the anode. The lower two figures show the new method of putting the lugs at right angles and welding the locking strap to the lug.

The third-order effects of fatigue, due to the actual fatigue of the metallic parts especially of connecting links and stem wires, are avoided only by complete changes of technique from the modern method of the soft-glass base.

3.3 Effects of Shock

Two effects of shock have been noted, the first being an emission phenomenon and the second a distortion of the electrodes.

Figure 21 shows the difference in grid voltage required to give a reference anode current of 10 milliamperes in a typical high-slope pentode valve before and after shock testing. It has been noted in general that the initial shock appears to cause a general reduction of the anode current in the valve and that further shocks do not cause such serious changes. The reason for this is not clear because apart from this slight shift of characteristic there does not appear to be any other change.

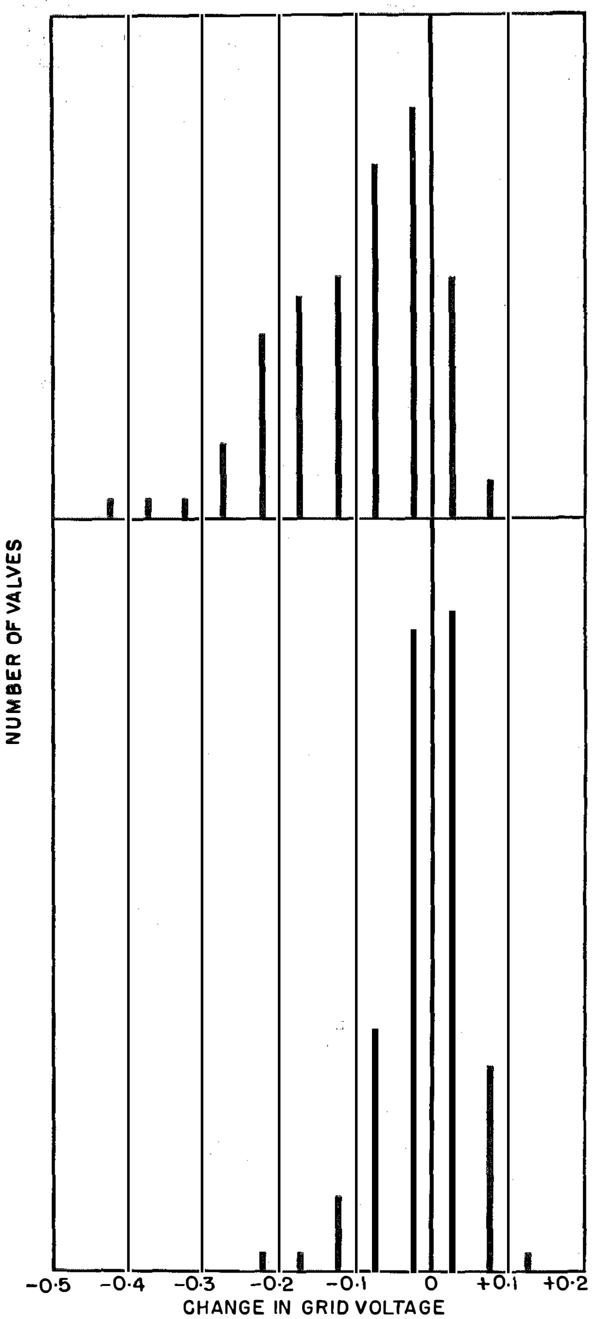

Figure 21—These two sets of histograms are for a single batch of high-slope pentode valves. The change in grid voltage required to produce an anode current of 10 milliamperes after one impact is shown at top. The lower histogram shows the relatively small effect of five successive blows after the initial shock.

The second effect of shock is electrode distortion and, generally, valves will withstand a higher acceleration when the direction of force is parallel to the principal axis. The characteristic effects of shock in this direction are discrete changes of anode current, cut-off, and capacitance that increase as the shock becomes greater up to the limiting point where the assembly is completely distorted. In the two other axes the amount of distortion of grids, et cetera, is proportional to the degree of shock and only comparably small values of acceleration can be tolerated. The time of impact is important for very-short-duration shocks, but where the acceleration remains constant over a period the amount of damage does not appear to be a function of time. This point has been proved by centrifuge tests.

Improvements to the shock performance when the acceleration is parallel to the principal axis may be made by rigidly attaching the bottom insulator to the stems of the valve in at least three equidistant places around its periphery, and then ensuring that all electrodes, especially the grids and cathode, are locked securely in one or other of the insulators. The distortion caused by shocks across the other axes may be reduced by making the assembly as short as possible and by using the thickest and strongest materials.

4. General

Production techniques including process control, raw-material quality checks, and methods of inspection and assembly, et cetera, have not been discussed although they have an important bearing on the final result. The engineering approach to the subject, including the detailed analysis of causes of rejection will give a very precise indication of production efficiency when instituted in the form of the tests described. In this respect it must be emphasized that the essence of good reliable-valve manufacture is the controlled uniformity of the product and such a

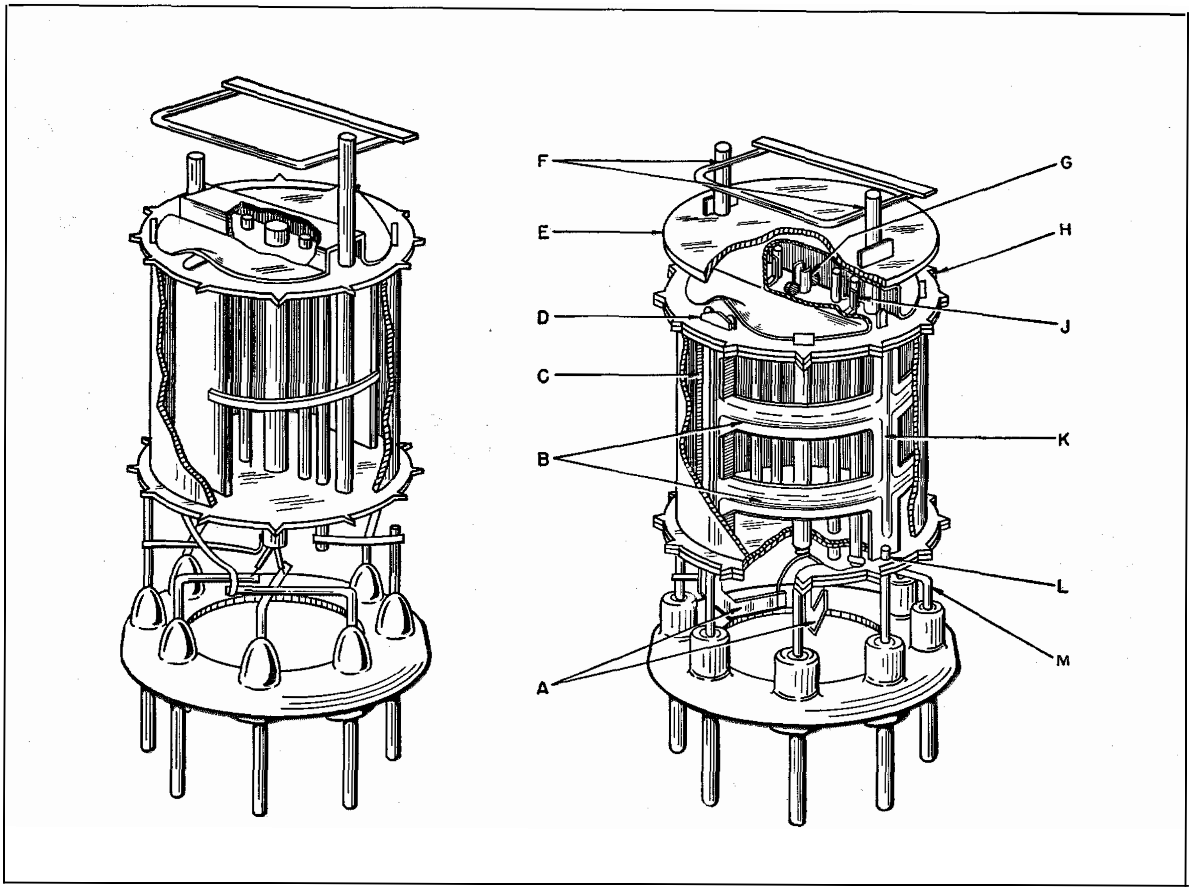

Figure 22—The drawing at the right shows an ideal reliable valve. The features that are stressed as contributing to trustworthy performance include: *A*—heater bars fixed to mica insulators and welded to the valve leads, *B*—one-piece ribbed anode structure with two bars, *C*—edges of anode bent out for strength, *D*—two lugs on anode locked by strap to mica insulator, *E*—insulator protects valve structure from getter splash, *F*—getter assembly welded in two places, *G*—cathode locked in top mica insulator, *H*—double mica insulators, *J*—grid locking clips in mica insulator, *K*—extra anode support, *L*—extra support, and *M*—valve leads welded directly to half supports.

state of affairs can only exist when sufficient quantities of valves are being made that the individual operator becomes familiar with the job.

5. Conclusions

The engineering approach inevitably culminates in certain general design methods, which are best illustrated by a hypothetical case of a reliable-valve design, shown in Figure 22. Valves of this type in controlled manufacture will pass all of the tests designed to prove the mechanical performance and it remains only for the full field results to be correlated to find out if the present performance level is satisfactory. Results to date indicate that the general standard of associated circuit equipment will now become the limiting factor to most electronic apparatus.

6. Acknowledgments

Much of the work described has been done under contract between the Admiralty and the Directors of Standard Telephones and Cables Limited, and the authors express their thanks for permission to publish this information.

7. Bibliography

1. I. L. Cherrick, "Rugged Electron Tubes," *Electronics*, volume 21, pages 111–113; April, 1948.

2. E. B. Callick, "Notes on the Design and Manufacture of Reliable Valves," February, 1950; unpublished.
3. E. K. Morse, "Reliable Electron Tubes for Use in Airborne Electronic Equipment," May, 1950; unpublished.
4. E. K. Morse, "Long-Life Tubes for Industry," *Electronics*, volume 23, pages 68–69; September, 1950.
5. D. D. Knowles, "Reliability in Electronics," *Westinghouse Engineer*, volume 10, pages 242–244; November, 1950.
6. Papers presented at the Joint American Institute of Electrical Engineers—Institute of Radio Engineers Conference on Electron Tubes for Computers; December 11–13, 1950. Summaries of the papers appear in *Electrical Engineering*, volume 70, pages 163–165; February, 1951.
7. M. A. Acheson and M. McElwee, "Concerning the Reliability of Electron Tubes," *Sylvania Technologist*, volume 4, pages 38–40; April, 1951.
8. G. H. Metson, Discussion on, "How Reliable is a Radio Valve," *Proceedings of the Institution of Electrical Engineers*, Part 3, volume 98, pages 207–208; May, 1951.
9. J. R. Steen, "The JETEC Approach to the Tube-Reliability Problem," *Proceedings of the IRE*, volume 39, pages 998–1000; September, 1951.
10. F. H. Cusack, "Vacuum-Tube Reliability," *Western Union Technical Review*, volume 5, pages 154–159; October, 1951.
11. R. Bird, "Measurement of Microphony in Valves," *Electronic Engineering*, volume 23, pages 429–431; November, 1951.
12. E. G. Rowe, "Technique of Trustworthy Valves," *Electrical Communication*, volume 28, pages 257–275; December, 1951: also, *Journal of the British Institution of Radio Engineers*, volume 11, pages 525–543; November, 1951: also, *Wireless World*, volume 58, pages 105–108; March, 1952: also, *Proceedings of the IRE*, volume 40, pages 1166–1177; October, 1952.
13. R. J. E. Whittier, "Mechanical Considerations Affecting Vacuum Tube Reliability," *Tele-Tech*, volume 11, pages 42–44 and 62; and pages 54–56, 102, 104, and 106; February and March, 1952.
14. D. O. Holland, I. E. Levy, and W. J. Davis, "Loss of Thermionic Emission in Oxide-Coated-Cathode Tubes due to Mechanical Shock," *Proceedings of the IRE*, volume 40, pages 587–590; May, 1952.
15. D. G. Koch, "Increasing Tube Reliability in Industrial Circuits," *Product Engineering*, volume 23, pages 175–181; June, 1952.
16. H. A. Hammel, "Life Testing Reliable Tubes," *Electronics*, volume 25, pages 169, 172, and 176; July, 1952.

New Chart for the Solution of Transmission-Line and Polarization Problems

By G. A. DESCHAMPS

Addendum to Volume 30, pages 247–254; September, 1953

In an article[1] published in 1946, Dr. Steiner, using the stereographic projection of the complex-numbers plane, obtained the representation of impedances by points on a sphere. He then considered the orthogonal projection of this sphere on an equatorial plane that gives, in effect, the projective chart. An application of that chart to the determination of impedance by the 3-probes method, anticipating part of the results in the section "Problems on Power" in the title paper, is also described.

[1] F. Steiner, "Die Anwendung der Riemannschen Zahlenkugel und ihrer Projektionen in der Wechselstromtechnik," *Radiowelt*, volume 1, pages 23–26; October, 1946.

Fixed-Beam Aircraft Approach System *

By R. A. HAMPSHIRE

Federal Telecommunication Laboratories, a division of International Telephone and Telegraph Corporation; Nutley, New Jersey

A FIXED-BEAM approach system for aircraft was designed for the United States Air Force. The equipment is compatible with existing instrument-approach-system installations and consists of a localizer operating between 108 and 112 megacycles per second and a glide slope operating between 329 and 335 megacycles. The localizer incorporates the dual-beam system of operation.

• • •

A new design of instrument low-approach equipment has been undertaken by Federal Telecommunication Laboratories for the United States Air Force. This equipment works interchangeably with existing instrument-approach-system equipment; the localizer being in the 108-to-112-megacycle band, the glide slope in the 329-to-335-megacycle band, and each utilizing 90- and 150-cycle-per-second modulations. There have been added certain new features of interest. This is particularly true of the localizer, which is of the dual-beam type. Investigations of this type of localizer were started at Wright Field, Dayton, Ohio, several years ago. Similar investigations were conducted under the auspices of the Air Navigation Development Board at the technical development and evaluation center of the Civil Aeronautics Administration at Indianapolis, Indiana.

The principle of this dual-beam localizer is based on the proposition that very-narrow lobes of energy radiated from the localizer antenna system will eliminate siting problems and that a superimposed localizer, operating on another frequency, will provide proper off-course indications outside of the region served by the narrow main lobes. Paraboloidal reflectors, half-cheese antennas, broadside arrays, and waveguide antennas have been utilized for the generation of the narrow lobes. At the time this new design was started, about three years ago, the choice of a best means to generate narrow lobes was difficult. Parabolic cylinders and broadside antennas were investigated, and it was found that broadside antennas as developed by Andrew Alford Associates showed the most promise; the next step was to proceed with the specific design of a broadside array.

The basic design requirements may be explained by reference to Figure 1. The normal localizer provides left and right guidance to the airplane by modulating a signal with 90 cycles and 150 cycles in such a way that the 180-degree sector to one side of the runway centerline shows a predominance of 90-cycle modulation over 150-cycle modulation and the sector on the other side of the runway centerline more 150-cycle modulation than 90-cycle modulation. The tone modulations are equal only on the runway centerline and the front and back extensions thereof. Now when an aircraft at position *A* receives a signal not only from the localizer but also by reflection from some object such as the building shown, this reflected signal is characterized by a preponderance of one tone and according to the radio-frequency phase, it adds to the direct signal and will upset the equality of tone modulations one way or the other. This causes the aircraft's indicator to deflect to the left or right even though the aircraft is situated accurately on the runway centerline.

As the airplane proceeds inbound toward its landing, the relative phase of the direct signal and the reflecting signal varies because the direct ray is being shortened more rapidly than the reflected ray. This causes the reflected signal alternately to add and subtract and causes the aircraft's indicator to swing back and forth—a phenomenon called course bending. It may be seen that if the building were situated far to the side, this phase variation would be quite rapid. On the other hand, if the building were very close

* Reprinted from *Convention Record of the IRE 1954 National Convention*, volume 2, part 5—Aeronautical Electronics and Telemetry, pages 77–83. Presented at the National Convention of the Institute of Radio Engineers in New York, New York, on March 23, 1954.

to the runway at position *B2*, for example, the phase variation would be very slow. We can see in addition to this that the rapidity of phase variation is also a function of the distance out to the point *A* where the aircraft receives the signal. As the aircraft flies in from a great distance, the bends become more rapid. This is a way of saying that the phase variation is more rapid as the angle between the reflected ray and the direct ray becomes greater.

Now a reflecting object at position *B2*, very close to the runway, will produce such a slow phase variation that the effect is a very minor shift of the course, free of abrupt bends and kinks. Since the type of a reflecting object this close to the runway is small, the effect is not harmful. The building, however, being some 400 or 500 feet off the runway can produce damaging effects. A restriction of radiant energy to the

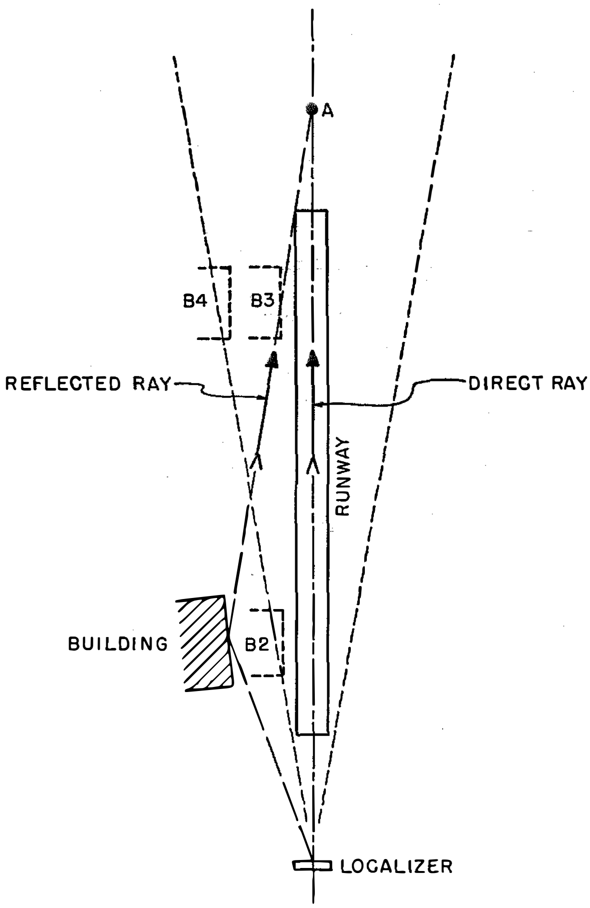

Figure 1—Buildings may reflect radio waves to the aircraft at *A* in such a manner as to distort the localizer fields on which a safe approach depends.

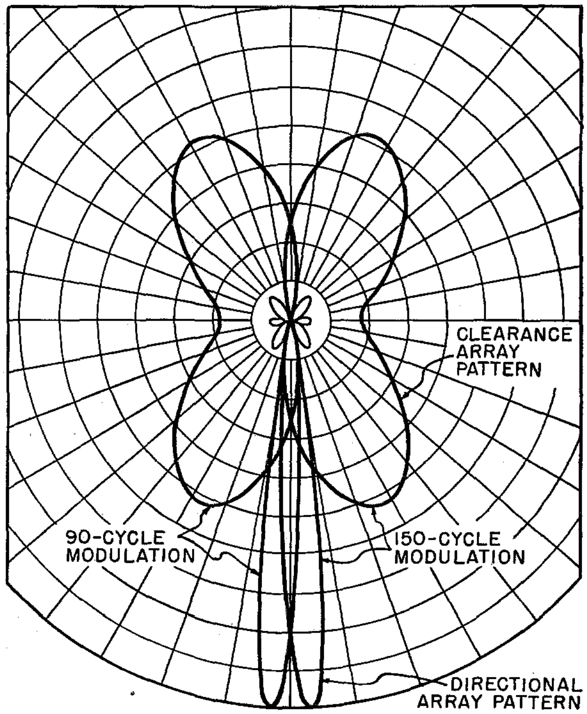

Figure 2—Calculated directivity patterns of both the broad and narrow localizer radiations. The broad pattern permits the aircraft to find the narrow pattern that is used for the actual approach.

sector between the dotted lines keeps the signal from striking the building and is an effective means of reducing course bends. As for reflecting objects at positions *B3* and *B4*, which may still lie within the localizer sector, these are too small and too remote and thus too little illuminated to cause trouble. Experience has shown that almost all objects large enough and close enough to the runway to cause trouble fall outside a sector some 12 or 15 degrees each side of the runway center-line.

Figure 2 shows the kind of radiation patterns utilized in the new localizer. The two narrow lobes define the localizer course. Note that the peaks of radiation are about 3 degrees off the course and the strength is reduced to zero at 12 degrees off course. The necessary course sharpness is produced with a crossover between the two lobes at values of about 80 percent of the lobe peaks. The ratios of on-course to off-course signal are such that reflecting objects more than 8 or 10 degrees off course are not sufficiently illuminated to cause trouble even though they are quite close to the localizer.

These radiation patterns naturally have many minor lobes, which in this case are more than 20 decibels below the peaks of the main lobes. These minor lobes would cause false courses if only the narrow-lobe radiation were utilized. There is therefore superimposed on this basic localizer a second localizer having the broad radiation patterns shown. The on-course signal strength from the broad localizer is approximately one-third of the signal strength from the main localizer. The signal strengths become equal at 8 degrees off course and elsewhere throughout the azimuth the broad localizer, which is called a clearance localizer, predominates by a factor of at least 3 to 1.

Now since these two localizer signals are radiated on carriers only 9 kilocycles per second apart, and since the aircraft receiver has a much broader bandwidth than this, both signals are picked up. It is a well-known phenomenon that the modulation on the weaker signal is suppressed. This suppression is used to advantage here because any reflection of the clearance-localizer signal that may be picked up by the aircraft while it is flying the course is suppressed and does not produce course bends or oscillations of the aircraft's indicator.

Figure 3 is a diagram showing what happens in the receiver. On the left, is depicted a situation where one signal is stronger than the other by a factor of 3 to 1. Note that in this case the beat note is nearly a sine wave modulated by the tone of the weaker signal. Detection and averaging through the beat note yields the modulation envelope of the stronger signal. The phenomenon is described in Terman's textbook[1] and in a paper[2] by Butterworth. In the right half of Figure 3 is shown a situation in which the two signals are equal. The beat note in this case is not a sinusoid. Sharp cusps are generated when the radio-frequency vectors pass through the condition of phase opposition. Under these conditions, the result of detection and discarding the beat note does not restore the modulation due to the stronger signal alone. It is obvious from this that to achieve a smooth transition from a preponderance of one signal to a preponderance of the other—that is to maintain

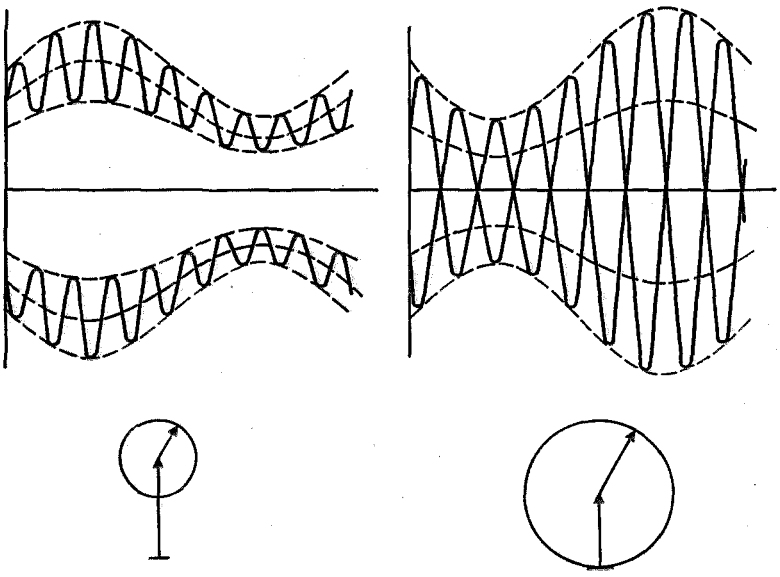

Figure 3—At the left, one received signal is 3 times the intensity of the other while at the right both signals are equal in amplitude.

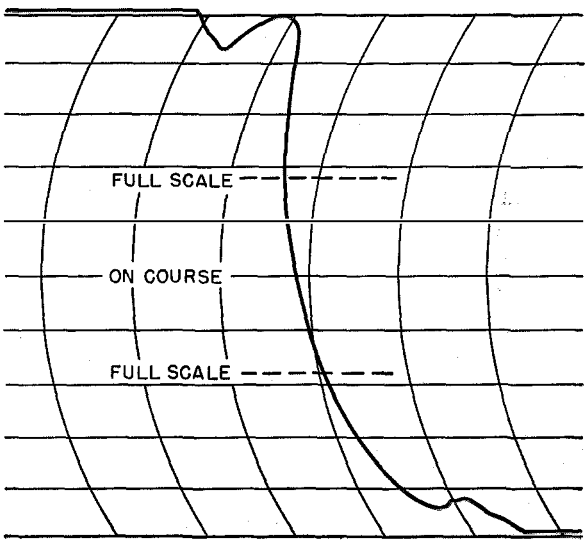

Figure 4—Recording taken in a flight across the localizer course.

[1] F. E. Terman, "Radio Engineering," second edition, McGraw-Hill Book Company, New York, New York; 1937: see pages 459–461.

[2] S. Butterworth, "Note on the Apparent Demodulation of a Weak Station by a Strong One," *Wireless Engineer*, volume 6, page 619; November, 1929.

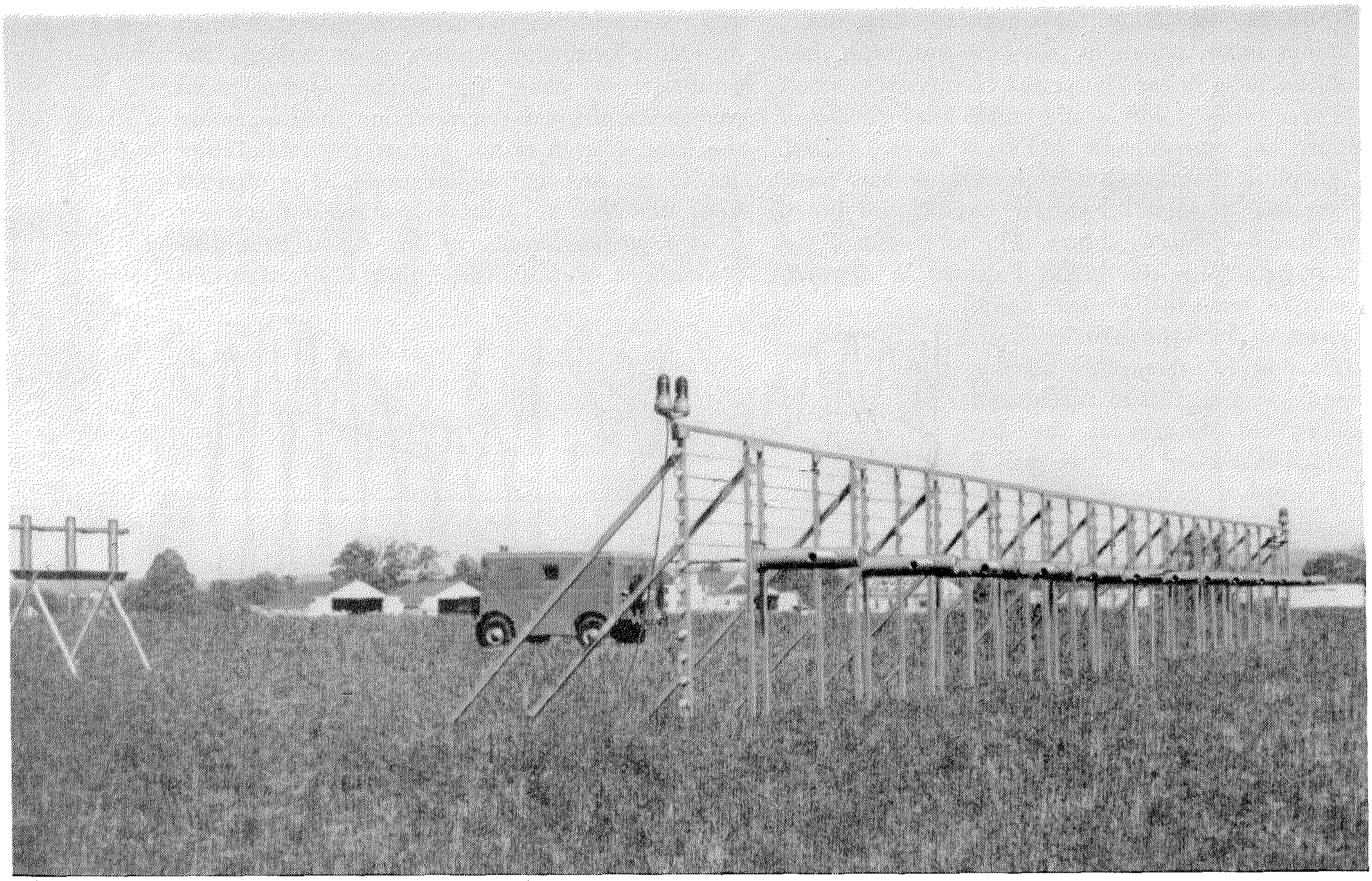

Figure 5—The *AN/MRN-7* equipment that produces both the broad and narrow localizer patterns.

proper tone modulation—the modulation tones on both signals must be in the same audio phase and must modulate the carriers to the same depths. This is the condition shown in Figure 3.

Figure 4 shows a tracing that was made of an actual flight recording across the localizer course. It has been traced accurately from the original Esterline–Angus paper. The smoothness of the crossover is apparent. The slight dips in crosspointer current are the effects of the transition that occurs approximately 8 degrees off course. The receiver output dips slightly here because the average value of the signal—that is, the value that effects the automatic gain control—has been raised slightly by virtue of the beat note between the two signals not being sinusoidal. The effect is quite minor since the clearance is still well beyond the full-scale indication of the aircraft meter and because the effect occurs about 8 degrees off course where monotonic indication is no longer required.

Figure 5 shows the equipment that generates these localizer signals. It is called Radio Set *AN/MRN-7*. The narrow radiation patterns are generated by broadside arrays of 12 dipoles mounted in front of a screen reflector. Horizontal wires on the stanchions eliminate backward radiation. The array is 85 feet (26 meters) long and 7 feet (2 meters) high. The clearance signal is generated by an array of three ramshorn antennas that is set up about 30 or 50 feet (9 or 15 meters) behind the main array. These antennas are a few inches higher than the upper edge of the main-array reflector, and provide for complete azimuth coverage without distortion by reflection or refraction from the screen. All of the transmitting equipment is located in the small van-type trailer shown in the background. For transport, the antennas and cables are stowed in the trailer and the antenna structure is collapsed and carried on the roof.

Figure 6 is a diagram of the main array showing at the top the 12 dipoles arranged in a broadside array. Each of these dipoles is identical and interchangeable. To generate the crossed lobes, the current supplied to the antennas is divided into two parts: one, the familiar dumbell, or reference, signal and the other, the sideband, or clover-leaf, signal. Ten of the 12 elements are excited with carrier signal. The distribution of currents is plotted immediately below the antennas. The sideband signals supplied to the array are distributed according to the curve superimposed. The sideband currents in half the array are, of course, in phase opposition to the other half and are each in quadrature with the carrier currents. Below is shown schematically the antenna distribution unit. Six regular hybrid bridge circuits are used. These prevent coupling between the carrier and sideband inputs and provide the proper phasing of antenna currents. The bridge on the right is not needed to prevent coupling, but is utilized to maintain phasing over the frequency band of 108 to 112 megacycles. The distribution of powers is arranged by taps on quarter-wave transmission-line sections of adjustable characteristic impedance.

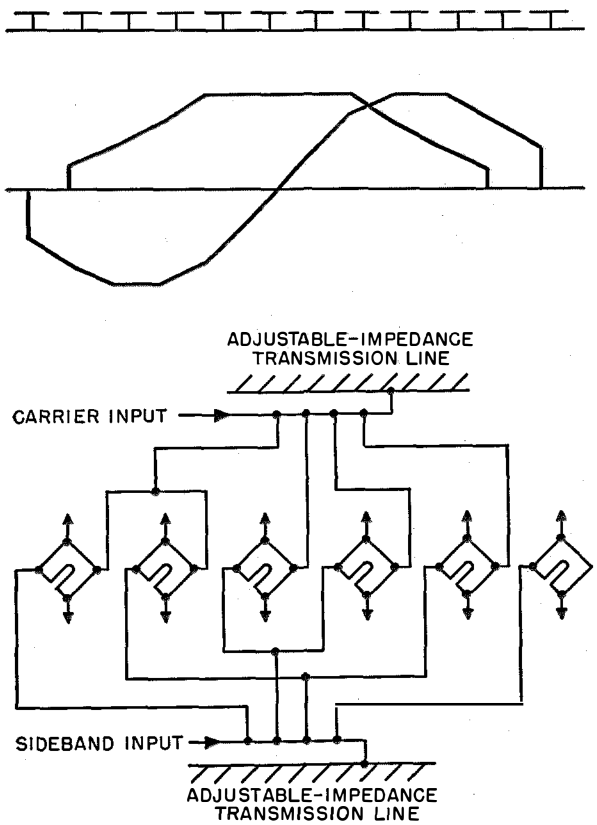

Figure 6—Main array of dipoles with current distributions at top. Below is the method of supplying power to the antennas, which are connected to the vertical corners of the 6 radio-frequency bridges.

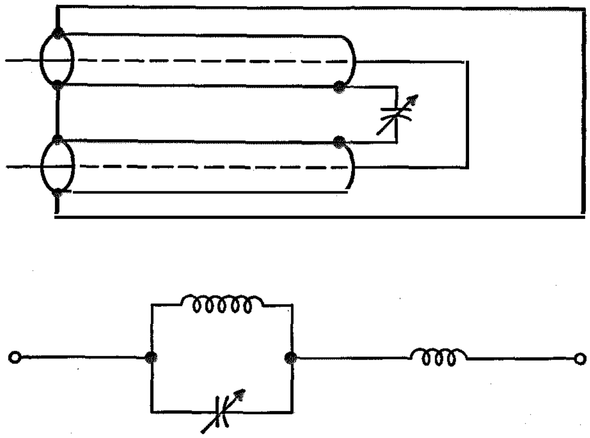

Figure 7—Schematic diagram of modulation trough.

These are so arranged that the standing-wave ratio on the lines is better than 1.1 over the band. All adjustments are made according to calculations of dimensions. No field adjustment is necessary. The 12 cables that connect the antenna tuning unit to the antennas are equal in length and are interchangeable.

The modulation at 90 and 150 cycles is generated by a mechanical modulator operating in principle like those now in use. The output of a simple transmitter is divided into two branches and passes through two modulation troughs. Figure 7 is a schematic diagram of one of these troughs. It is connected in a coaxial-transmission-line circuit and operates on the principle of inserting a tunable wave trap in the outer conductor. The input and output lines project into the shielded box. The outer conductors terminate in a capacitor that is tuned and detuned by a motor-driven plate. The inner conductor is continuous. Since the device is symmetrical, the rotor plate is placed in the neutral plane to prevent leakage of radio-frequency energy along the rotor shaft. The equivalent circuit of the modulator trough is shown at the bottom of the figure. The untuned inductance is the section of bare inner conductor. The tuned inductor is the stub formed by the outside of these two outer conductors. The parameters are arranged so that the wave trap may be tuned toward resonance to achieve the modulation troughs and detuned in the capacitive direction for the modulation peaks. At the modulation peaks, the fixed inductor nearly resonates the capacitive reactance of the variable section and provides for a low standing-wave ratio at the modulation peaks.

Figure 8 is a photograph of the transmitter–modulator combination. All of the equipment is mounted on one front panel that hinges downward out of the cabinet. One side of the panel is occupied by the transmitter and modulator for the main array and on the other side by the transmitter and modulator for the clearance array. At the top of the panel are the two 4-tube transmitters that generate the radio-frequency signals; one for the main array and the other for the clearance array. Immediately below it are the 4 modulation troughs situated side-by-side. One trough on each side is tuned by a 5-bladed rotor and the other by a 3-bladed rotor to achieve the 90- and 150-cycle modulations. A motor in the middle is directly coupled to the two shafts, thus providing accurate audio phasing. The hybrid bridge circuits that are used to separate the sidebands from the carrier are located between the two modulators.

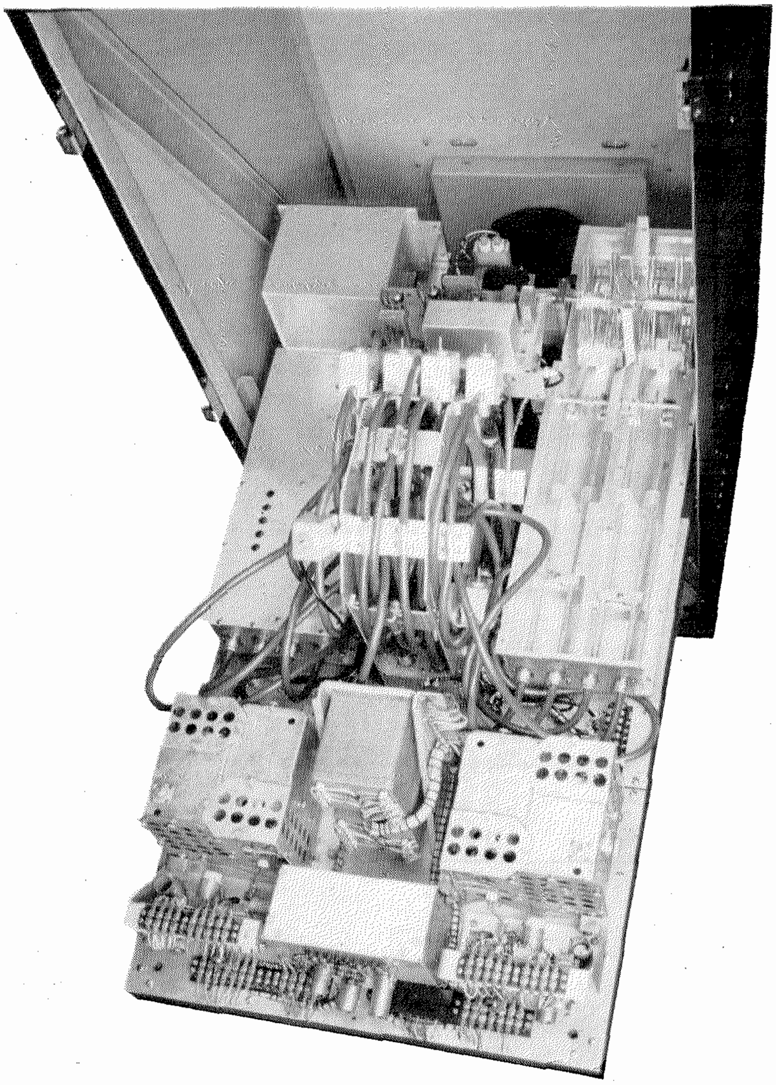

Figure 8—Transmitters and modulators.

Figure 9 is a photograph of this cabinet in operating position. The tuning controls for the two transmitters are shown at the top. The slide immediately beneath is an amplitude-control unit that adjusts the amount of sideband power output so that the course width may be varied. It dumps unwanted sideband power into a dummy antenna. The adjustment is made without phase shift.

Figure 10 is a block diagram of the complete system. In one cabinet are located all of the power supplies and in another are the transmitter and modulator. The outputs of the modulator go to a transfer unit and thence to the antennas. Note that a voltage regulator and frequency converter are with the power supplies. These permit operation on any line voltage between 95 and 135 or between 190 and 270 and on any line frequency between 45 and 75 cycles.

This transfer unit together with an alarm box and remote-control unit are situated in another cabinet. The alarm box is the device that monitors the performance of the equipment. It is connected to 3 simple monitors set up in the field in front of the equipment at the proper locations to check course position, course width, and clearance. Complete standby equipment consisting of another transmitter–modulator, another power supply, and a duplicate alarm box is provided. The equipment is turned on and off by remote control; it is self-monitoring and equipped for automatic changeover from main to standby.

The glide-slope equipment that provides for vertical guidance of the aircraft in the standard 329-to-335-megacycle band operates on the familiar null-reference principle. This equipment is shown in Figure 11. The upper of the 3 antennas is the null antenna that radiates a signal similar to the sideband, or clover-leaf, signal of the localizer. The null in the vertical radiation pattern is, of course, produced by ground reflection. The antenna below this is the carrier, or reference, antenna situated at one-half the height above ground. Next is a 3-element antenna radiating the same kind of signal as the upper antenna—that is, sideband only—this is the modifier antenna, and is used to straighten the glide slope at its lowermost extremity.

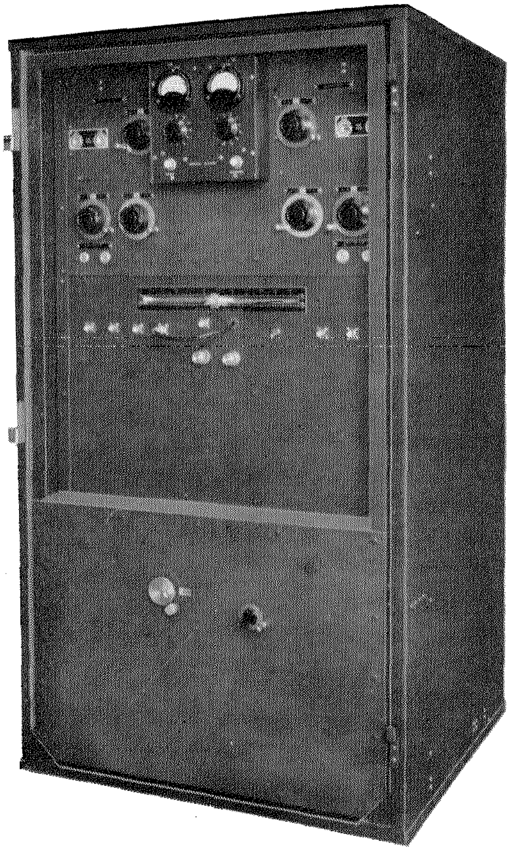

Figure 9—Complete transmitter in its cabinet.

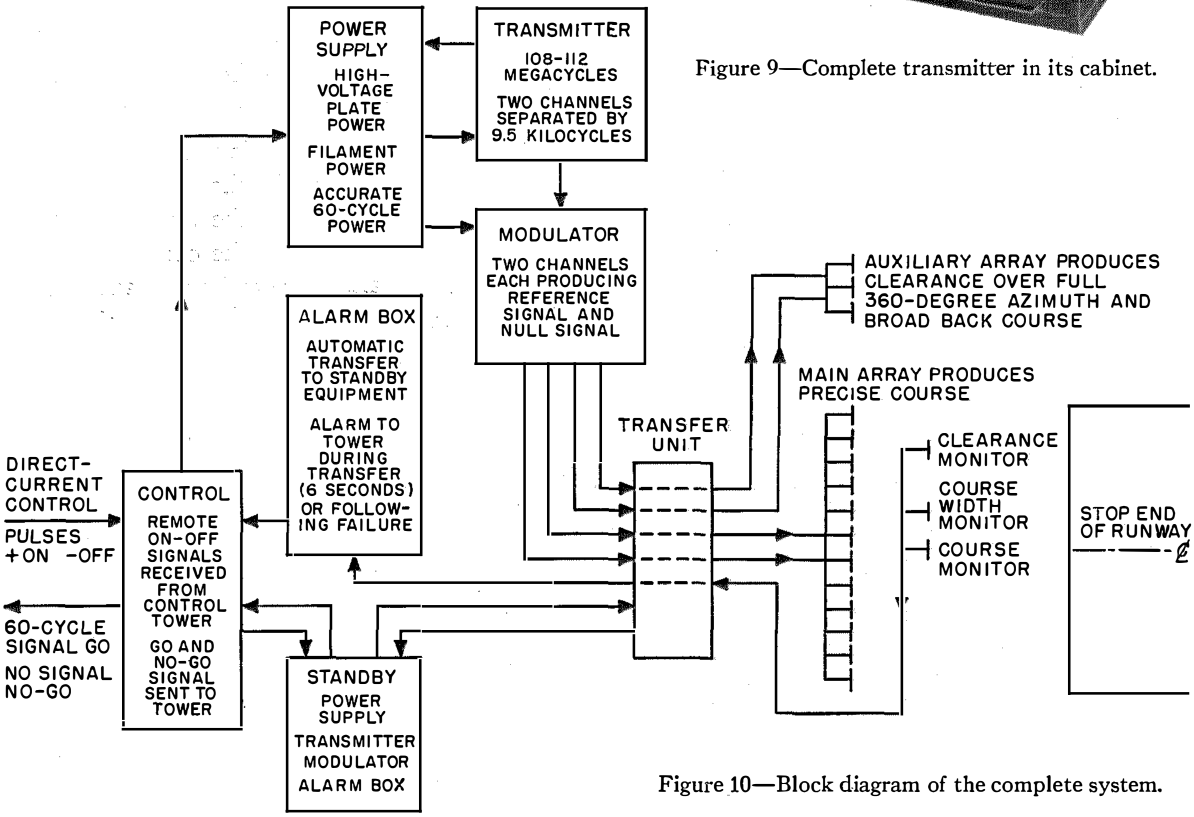

Figure 10—Block diagram of the complete system.

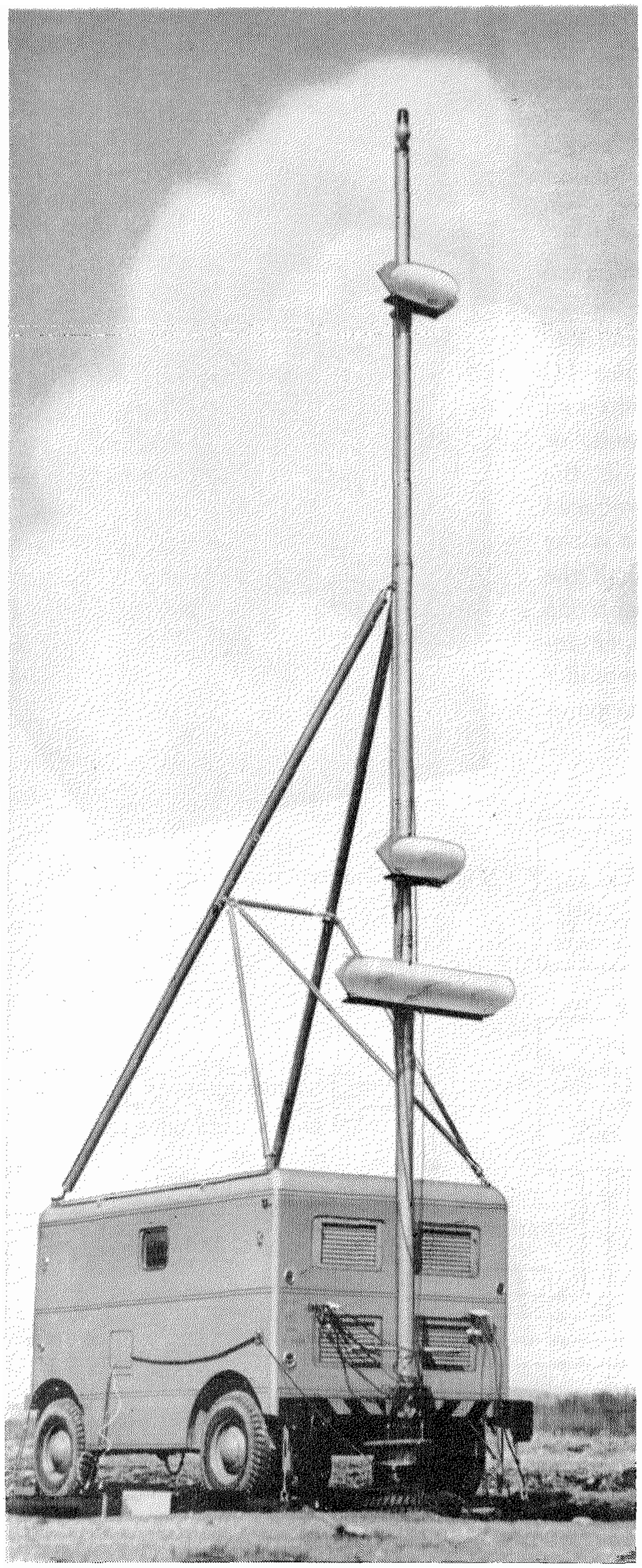
Figure 11—Glide-slope equipment.

Figure 12 is a photograph of the glide-slope-transmitter modulator. It, like the localizer, is mounted on a single panel that hinges downward and outward from the cabinet for maintenance. The glide slope, of course, has only one carrier frequency; thus, the cabinet contains only one transmitter and one modulator. The transmitter, at the top, utilizes 5 tubes. The modulator has two troughs that in this case are situated one on each side of a single motor. Immediately above the modulator is a small chassis containing tubes and crystals that are a portion of the built-in test equipment. Twenty-kilocycle-per-second signals are generated here and go to crystal detectors inserted in the transmission lines at the output of the modulator trough and in the carrier and sideband transmission lines to the antenna system. These permit transfer of the modulation to a 20-kilocycle tone that is presented on a cathode-ray oscilloscope in the equipment and provides for complete field-maintenance adjustment of the modulators.

Figure 13 is a photograph taken inside the trailer of the glide-slope equipment. On the left is one transmitter-modulator cabinet and on the right is the standby transmitter-modulator. In the center there are, from top to bottom, the test oscilloscope, the main alarm box, the control unit, the standby alarm box, and the transfer unit. Dummy antennas are located in the transfer unit so that the standby- or the main-equipment output may be applied to dummy loads for maintenance purposes while the main equipment is performing its normal functions. Two more cabinets, not shown, are situated in the other end of the trailer and house the power supplies.

Although not specifically referred to previously, the localizer cabinet arrangement and test-equipment facility are the same.

Figure 14 is a photograph of one of the 3 glide-slope monitors. The pickup antenna is adjustable to provide for different glide-slope angles. As in the case of the localizer, 3 monitors are used: one for slope position, one for slope width, and one for slope shape (modifier-antenna radiation).

Both the *AN/MRN-7* and *AN/MRN-8* equipments use standard construction and components wherever practicable. Every effort has been made to provide easy setup and maintenance. The equipments are self-contained, except for primary power, which must be provided at either 115 or 230 volts; 4 kilowatts is required. For transport, both antenna structures are carried on the trailer roofs and the cables, field monitors, and antenna radiators are stowed inside the trailers. The number of vacuum tubes utilized in the power supplies and transmitters has been kept to a minimum. Reliable types of tubes have been used in the monitor, control, and test circuits.

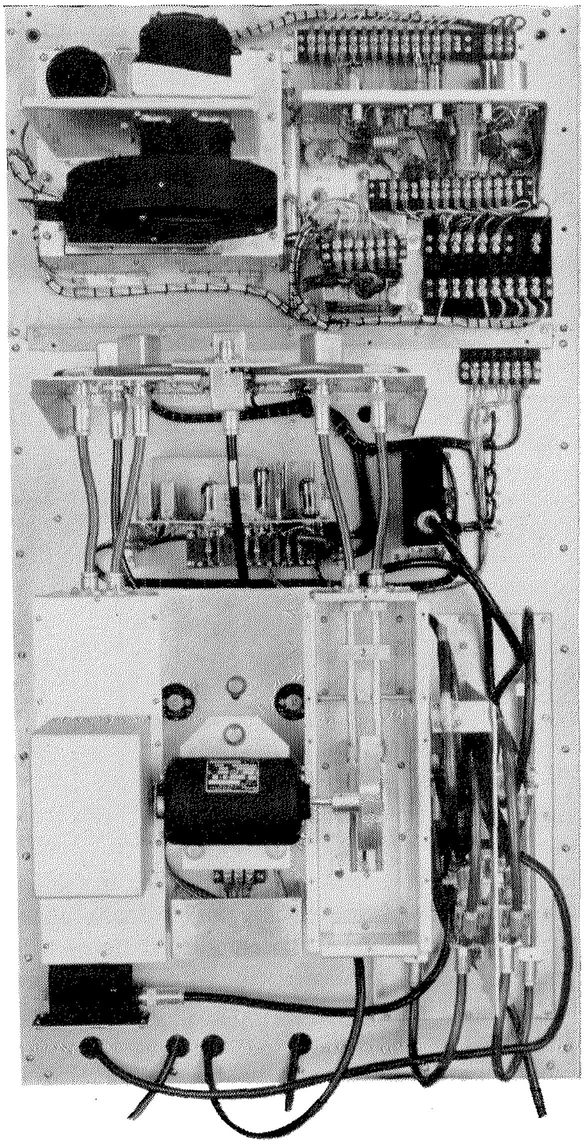

Figure 12—Modulator for the glide-slope transmitter.

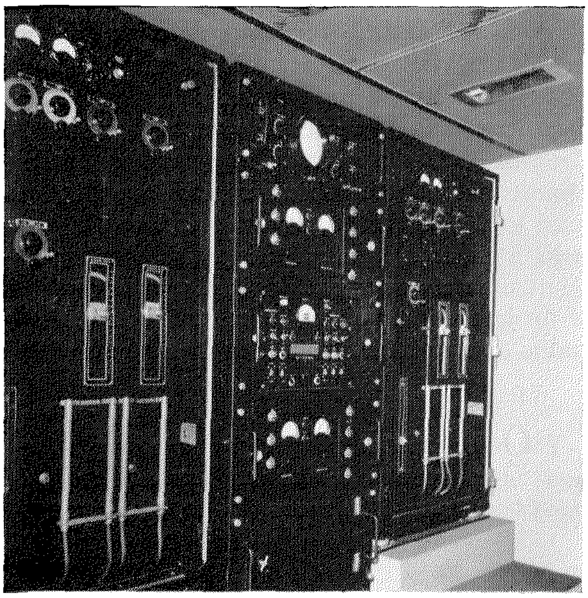

Figure 13—Interior of the glide-slope trailer

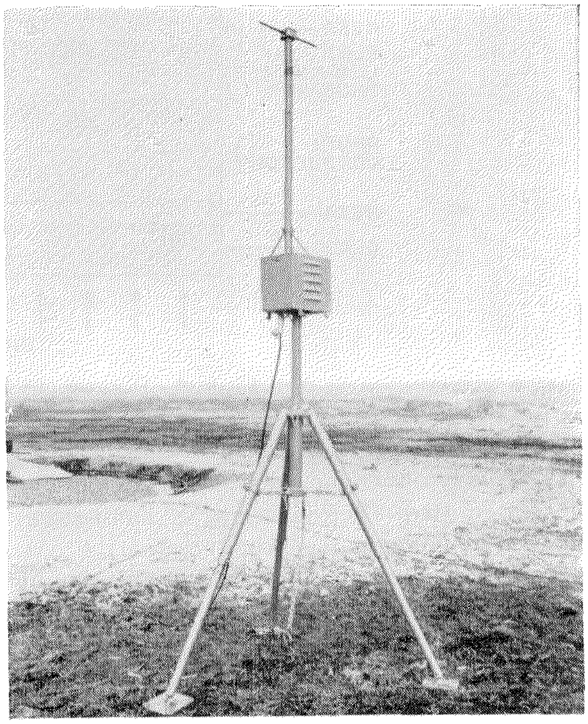

Figure 14—One of the glide-slope monitors.

Solid-State Image Intensifier*

By R. K. ORTHUBER AND L. R. ULLERY

Capehart–Farnsworth Company, a division of International Telephone and Telegraph Corporation; Fort Wayne, Indiana

A METHOD for image intensification that avoids evacuated envelopes and utilizes a sandwiched layer of photoconductor and electroluminescent phosphor is described. The behavior of those components is approximated by empirical expressions that are used to derive the brightness gain feasible with such a device. This gain expression has been approximately substantiated. A working model of an image-intensifying panel was constructed and is able to intensify images by a factor of 2.

• • •

The conventional method of image intensification or conversion of images between spectral ranges consists of the successive steps of converting optical images into electron images by a photoemissive layer and electron-optical focusing of the emitted electrons onto a luminescent screen. To increase the brightness of the converted image, methods such as intensification by secondary emission or by repetition of the conversion have been proposed.[1]

Recent advances in the development of electroluminescent phosphors have suggested a new solution to the problem of image intensification. Characteristic of this proposal is the exclusive application of solid-state components that do not require evacuated envelopes as do methods mentioned heretofore.[1] Such an intensifier has the appearance of a flat screen and is therefore especially adaptable to the intensification of large images such as projected television pictures or fluoroscopic images.

The basic operation of the proposed image intensifier screen is outlined as follows.

In Figure 1, a cross-section of the screen is shown. A glass plate is coated with a transparent electroconductive layer consisting, for instance, of Nesa. On top of this coating, an electroluminescent layer is applied; it is characteristic of this type of layer to luminesce if a strong alternating electric field is applied between its two surfaces. The brightness of this luminescence increases with the amplitude and the frequency of the

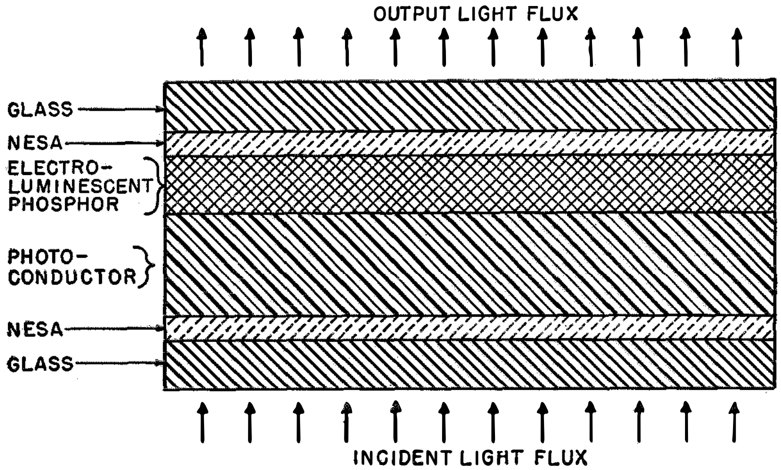

Figure 1—Diagram of a solid-state image intensifier.

* Reprinted from *Journal of the Optical Society of America*, volume 44, pages 297–299; April, 1954.

[1] V. K. Zworykin, G. A. Morton, E. G. Ramberg, J. Hiller, and A. W. Vance, "Electron Optics and the Electron Microscope," John Wiley and Sons, Incorporated, New York, New York; 1945.

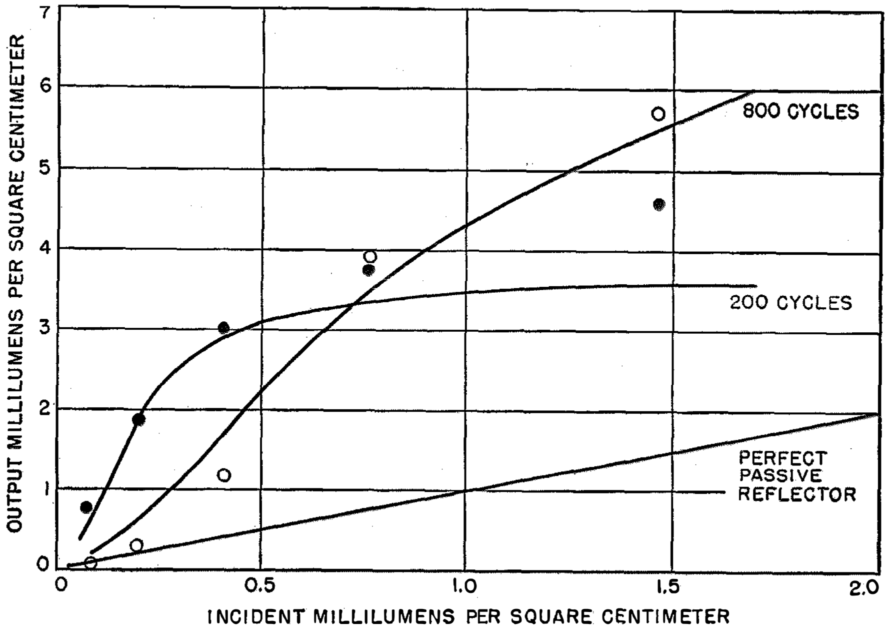

Figure 2—Brightness-illumination diagram for the series combination of a cadmium-sulphide radiation detector and an electroluminescent phosphor. The sensitivity varies with the frequency of the voltage source as shown. The curves indicate calculated performance and the points show the results of measurements.

applied electric field. Detailed descriptions[2–6] of this effect have been given. The next lamina consists of a photoconductor of high dark resistance followed by another Nesa coating applied to a second glass plate.

It should be mentioned that unless light feedback is desired, an opaque insulating film should be sandwiched between the phosphor and the photoconductor.

For operation of this screen, an alternating voltage in the audio-frequency range (60 to 3000 cycles per second at 600 to 800 volts) is applied between the Nesa layers. If the dark resistance of the photoconducting layer is high enough, and if the admittance per square unit is considerably lower for the photoconductive layer than for the electroluminescent layer, the voltage applied between the Nesa layers will be divided so that only a small fraction of this voltage will appear across the electroluminescent layer, which will therefore stay dark as long as the photoconductive layer is kept dark.

If the photoconductor is illuminated to a level at which its conductivity considerably exceeds its capacitive admittance (which is the case at very low illumination levels for sensitive photoconductors), the image-intensifier screen or an element thereof may be represented as a series combination of an ohmic resistor and a capacitor; the power factor is of the order of 0.1.

A straightforward derivation leads to (1), relating the brightness B of the phosphor to the applied voltage V, the illumination I, the capacitance C per square centimeter of the phosphor, and the driving frequency $\omega/2\pi$.

$$B=\frac{\beta V^m \gamma^m I^{mn}}{(\gamma^2 I^{2n}+\omega^2 C^2)^{m/2}}. \quad (1)$$

The following assumptions have been made.

A. The conductivity K of the photoconductor is related to illumination I by a power law

$$K=\gamma I^n. \quad (2)$$

B. The phosphor brightness B is related to the voltage drop V_p across the phosphor by a relation

$$B=\beta V_p{}^m. \quad (3)$$

From (1) the brightness gain may be written

$$G=\frac{\beta V^m \gamma^m I^{(mn-1)}}{(\gamma^2 I^{2n}+\omega^2 C^2)^{m/2}}. \quad (4)$$

[2] G. Destriau, "On the Phenomena of Electrophoto Luminescence," *Philosophical Magazine*, volume 38, pages 700–888; 1947.

[3] E. C. Payne, E. L. Mager, and C. W. Jerome, "Electroluminescence—A New Light Source," *Sylvania Technologist*, volume 4, pages 2–5; January, 1951.

[4] J. F. Waymouth, C. W. Jerome, and W. C. Gungle, "Electroluminescence—Electrical and Optical Properties," *Sylvania Technologist*, volume 5, pages 54–59; July, 1952.

[5] K. Lehovec, C. A. Accardo, and E. Jamgochian, 'Injected Light Emission of Silicon Carbide Crystals," *Physical Review*, volume 83, pages 603–607; August 1, 1951.

[6] S. Roberts, "Field Strength and Temperature Studies of Electroluminescent Powders in Dielectric Media, "*Journal of the Optical Society of America*, volume 42, pages 850–854; November, 1952.

To check the validity of the assumptions and to determine values for m, n, β, γ, and C, a series of measurements were made using cadmium-sulphide radiation detectors[7] as the photoconductive elements and small electroluminescent

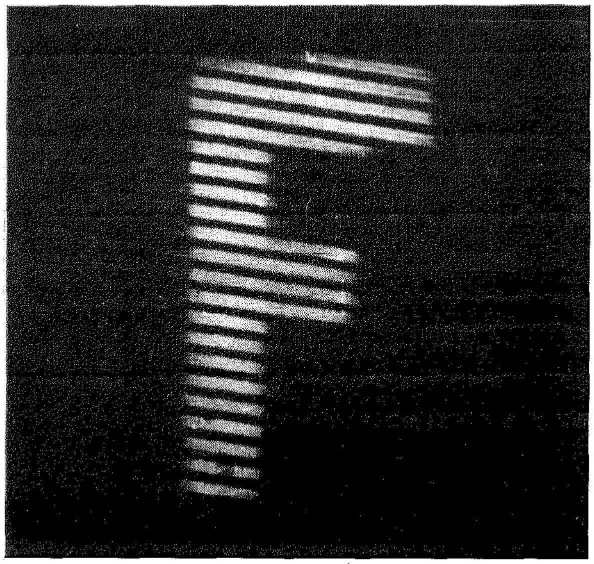

Figure 3—A photograph in approximately actual size of the viewing surface of a solid-state image intensifier displaying an intensified image.

panels.[8] The experiments lead to the following numerical values for these parameters.

$$n = 0.9,$$
$$m = 1.9,$$
$$\gamma = 101 \times 10^{-6},$$
$$\beta = 1.4 \times 10^{-8},$$

if I and B are in lumens per square centimeter, V in volts, and K in mhos, and

$$C = 75 \times 10^{-12} \text{ farad per square centimeter.}$$

It was found that (2) and (3) could be used for an approximate description of the photoconductor and electroluminescent-screen performance.

Equation (1) was then numerically evaluated for 700 volts applied to the series combination of the electroluminescent phosphor and photoconductor. The results of these computations (full line) and experimentally determined values obtained by measuring the illumination of the crystal and the corresponding brightness of the electroluminescent phosphor (circles) are shown in Figure 2. Considering the approximate nature of the assumptions made, the coincidence of computed and measured gain values is satisfactory.

The best value of intensification, measured with 200 cycles per second applied and an illumination of 0.08 millilumen per square centimeter was approximately 24. It must be mentioned, however, that the results of Figure 2 are based on a phosphor element of 40-square-millimeter area and having a capacitance of 35×10^{-12} farad. The controlling crystal had a light-intercepting cross section of only 2 square millimeters. Therefore, if the gain is expressed as the ratio of the resulting to the controlling light flux, its value in this example would become 480. If the size of the associated phosphor and photoconductive element is equal (as in the sandwich panel in Figure 1), brightness and flux gains will become equal.

A 3-by-3-inch (8-by-8-centimeter) panel basically similar to Figure 1 was constructed. The sandwich panel was composed of an electroluminescent phosphor such as suggested by Waymouth[4] and a layer of cadmium sulphide on a glass substrate. A photograph of the output face of this intensifier, displaying an image with a brightness gain of 2, is reproduced in Figure 3. The image shown in this figure has a height of approximately 2 inches (5 centimeters). In the intensifier panel used in this experiment, the input-side Nesa electrode of Figure 1 was replaced by a series of opaque parallel platinum strips. Their position is indicated by the black bars in Figure 3. The intensification is achieved with a primary image in the visible region. The low gain factor of 2 is attributed to the behavior of the particular photoconductor used in the visible region of illumination.

It should be mentioned that with gain values above 1, it was necessary to prevent light emitted by the phosphor from reaching the controlling photoconductive element. If this is not done, optical feedback will occur, driving the phosphor to saturation brightness independ-

[7] Purchased from General Electric Company, X-Ray Division; Milwaukee, Wisconsin.

[8] Purchased from Sylvania Electric Company, Lamp Division; Salem, Massachusetts.

ently of the applied illumination. This behavior of a series combination of an electroluminescent phosphor and a photoconductor has been utilized[9] by Bramley and Rosenthal to achieve a holding action for a light flash produced by a short voltage pulse applied to the electroluminescent phosphor.

[9] A. Bramley and J. F. Rosenthal, "Transient Voltage Indicator and Information Display Panel," *Reviews of Scientific Instruments*, volume 24, pages 471–472; June, 1953.

After completion of this work it was called to the attention of the authors that a similar idea for intensification of x-ray images has been proposed[10] by White.

[10] W. White, United States Patent 2,650,310; August 25, 1953.

Recent Telecommunication Development

Etching of H. A. Lorentz

Hendrik Antoon Lorentz (1853–1928), Dutch physicist, is the subject of the latest etching in the series published by the International Telecommunications Union. Lorentz was born at Arnheim, Holland; he attended school at Leyden, where he became professor of mathematical physics in 1878 and remained an honorary professor at the university after his appointment in 1923 as director of research at Teyler Institute in Haarlem.

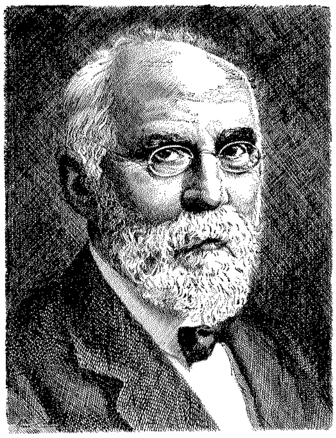

The major part of Lorentz's work dealt with various aspects of relativity. He attempted to arrive at a universally applicable theory of electricity, magnetism, and light, based on the concept of an omnipresent stationary ether. When certain applications of this theory failed, he added a factor relating to time. Extensions of this work led to the Lorentz transformation, which formed the basis of the restricted theory of relativity. He was honored with a Nobel prize for his work.

The etching of Lorentz is the nineteenth in the series that was started in 1935. On a good grade of paper measuring 9 by $6\frac{5}{8}$ inches (23 by 17 centimeters) including margins, these etchings are available at 3 Swiss francs each from Secrétariat général de l'Union internationale des Télécommunications, Palais Wilson, 52, rue des Pâquis, Genève, Suisse. The entire series is comprised of etchings of Ampère, Baudot, Bell, Erlang, Faraday, Ferrié, Gauss and Weber, Heaviside, Hertz, Hughes, Kelvin, Lorentz, Marconi, Maxwell, Morse, Popov, Pupin, Siemens, and Tesla.

Ultra-High-Frequency Omnidirectional Antenna Systems for Large Aircraft*

By WILLIAM SICHAK and J. J. NAIL†

Federal Telecommunication Laboratories, a division of International Telephone and Telegraph Corporation; Nutley, New Jersey

THIS PAPER discusses the problem of obtaining omnidirectional coverage from antennas operating between 1000 and 3000 megacycles per second on large aircraft. Electromagnetic modeling was used to determine the limitations of several single antenna sites on typical commercial aircraft. Considering all azimuth angles and ± 30 degrees in elevation to be equally important, the best coverage obtainable from a single radiator is equivalent to the radiation from a free-space dipole for 50 percent of the time. To improve this, dual antenna systems must be used. Dual antenna requirements depend on whether or not the airborne equipments know when they should be receiving a signal. The distance-measuring equipment (DME) is a typical system that knows when it should be receiving a signal while the radar safety beacon equipment does not know when or from what direction it is being interrogated. Direct parallel feed, the least complicated method of operating dual antennas, allows simple hybrid multiplexing to be used. With this type of operation, interference occurs where the individual patterns overlap. Performance in this region is investigated on a probability basis for beacon operation and found favorable; for distance measuring, this region is uncertain. In addition, performance is predicted when the radio-frequency voltage in one of the dual antennas is: *A*, shifted periodically in phase; *B*, delayed; and *C*, interrupted periodically. Considerations involved in an antenna system common to distance-measuring and beacon systems are discussed.

• • •

1. Introduction

Above 1000 megacycles per second, the airborne-antenna problem becomes easier in some respects, but obtaining omnidirectional coverage (the usual requirement) becomes considerably more complicated than at lower frequencies. It does not appear possible to obtain omnidirectional coverage with a single antenna on large aircraft so that systems requiring this coverage must use two or more antennas.

It is reasonable to assume that individual equipment requirements will vary considerably so that this problem had to be approached from the viewpoint of supplying information that allows a choice to be made between performance and complexity, weight, and expense. The aim of this paper is to present information on single antennas as well as dual antenna systems so that a reasonable choice can be made to fit a specific system.

2. Method of Measurement

Modeling appeared to be the most practicable method if the Fraunhofer condition (phase error across the largest dimension less than about 1/16th wavelength) could be violated. It appeared that this could be done since the radiator and its immediate surroundings could be properly illuminated while reflections from the extremities of the model would cause, primarily, errors in locating the true position of the minima or maxima.

* Reprinted from *Transactions of the IRE Professional Group on Antennas and Propagation*, volume AP-2, pages 6–15; January, 1954. This paper covers a portion of the work being done under Bureau of Aeronautics contract NOa(s)-12212 for the Air Navigation Development Board. This project is one of a group initiated to provide basic information for the development of a common military–civil system of aids to air navigation.

The Air Navigation Development Board (ANDB) was established by the Departments of Defense and Commerce in 1948 to carry out a unified development program aimed at meeting the stated operational requirements of the common military–civil air-navigation and traffic-control system. This project, sponsored and financed by the Board, is a part of that program. The Board is located within the administrative framework of the Civil Aeronautics Administration for housekeeping purposes only. Persons desiring to communicate with the Board should address the Executive Secretary, Air Navigation Development Board, Civil Aeronautics Administration, W-9, Washington 25, District of Columbia.

† Now with Bell Telephone Laboratories; Whippany, New Jersey.

Figure 1A shows a pattern (θ polarization) of a quarter-wave monopole on a 1/24th-scale model of a *DC-3* (94-wavelength wingspan) with a transmitter–model separation of 2.1×10^4 wavelengths while Figure 1B shows the patterns minimized by tilting the transmitting antenna. The field in the area to be occupied by the model was probed before measurements were made. The model mount shown in Figure 3 was designed to handle models with wingspans up to 6 feet

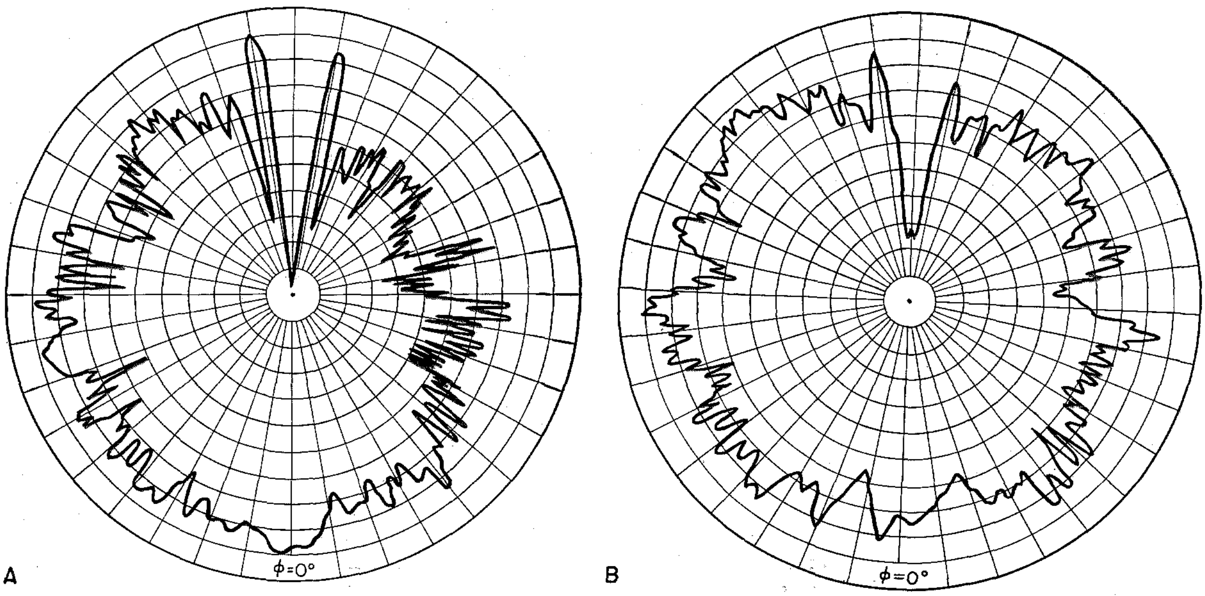

Figure 1—Effect of separation between transmitter and aircraft model on measured field-strength patterns. *A* is for a separation of 2.1×10^4 wavelengths and a 0.056-wavelength maximum phase error across the wingspan. *B* is for 1.2×10^3 wavelengths separation and a 1.0-wavelength maximum phase error across the wingspan.

with 1.2×10^3 wavelengths separation. The calculated maximum phase errors across the wingspan are 0.056 (20 degrees) and 1.0 (360 degrees), respectively. The differences in the patterns are minor. (Note that these two patterns are plotted in power; all other patterns in this paper are plotted in voltage.) Small transmitter–model separations can introduce serious errors in measuring the characteristics of certain types of direction-finding antennas and broadside and end-fire arrays of large aperture so that small transmitter–model separation should be used with caution.

Except for the distance between antennas and the height and strength of the model mount, the modeling system is the conventional one. A block diagram is shown in Figure 2. A photograph of the range showing the rotating mount is shown in Figure 3.

The model frequency was 24,000 megacycles, the highest frequency for which components were readily available. Ground reflections were (1.83 meters). Another mount was built to rotate models with spans up to 14 feet (4.27 meters). The speed of rotation was variable from $\frac{1}{5}$ to 1 revolution per minute, the speed being determined by the size of the model taking into account the dynamic writing speed of the recorder and the size of the patterns. For fine-lobe structure, the dynamic recording speed of the Airborne Instrument Laboratories (AIL) type-*116* polar recorder was about half the free-running speed of 15 inches (38 centimeters) per second. To insure that the allowable recording speed was not exceeded, initial patterns were monitored with a high-speed rectangular recorder.

3. Data Compilation and Analysis

3.1 Compilation of Data

Although it is desirable to know the relative amplitude of the field at all points at a constant distance about the model, such a quantity of data requires a prohibitive number of measurements.

In the practical case, a limited amount of data must be taken. The path in space about the model to be investigated will depend on many factors. For larger models, the restrictions placed on rotating the model are severe. In general, due to excessive stresses produced in the rotating mount or the model, it is impracticable to take patterns other than constant θ (see Figure 4). The limitations on the manner of compiling data, as well as the amount of data required, are both directly proportional to plane size and frequency. However, there is some compensation in the fact that the larger planes do not require coverage at all values of θ.

Obviously, errors may be encountered in interpolating between data taken along constant-θ paths if the increment in θ is not made much smaller than the minimum lobe width in the interference pattern. Before deciding what increment of θ to use, the model may be nodded and the vertical pattern noted at strategic values of ϕ.

The region investigated about the model was 60 degrees $\leqslant \theta \leqslant$ 120 degrees and included all values of ϕ. In most cases, 13 patterns (5-degree increments of θ) were taken to investigate one antenna location.

3.2 Analysis of Data

The primary data consist of 13 patterns for each aircraft type, antenna location, and full-scale frequency. A typical set is shown in Figure 4. These patterns are very useful but contain too much information. Contour plots with 4-decibel intervals are used as summaries; it was found

Figure 2—Block diagram of model range. The 24,000-megacycle transmitter was mounted in a truck and the 2-foot (61-centimeter) paraboloidal antenna was placed outside of the truck. The distance to the model was varied up to 900 feet (274 meters). The crystal detector from which the receiver obtained its signal was inside the aircraft model. The output from the audio-frequency amplifier at the base of the model mount passed through a shielded cable for about 150 feet (46 meters) to the test house.

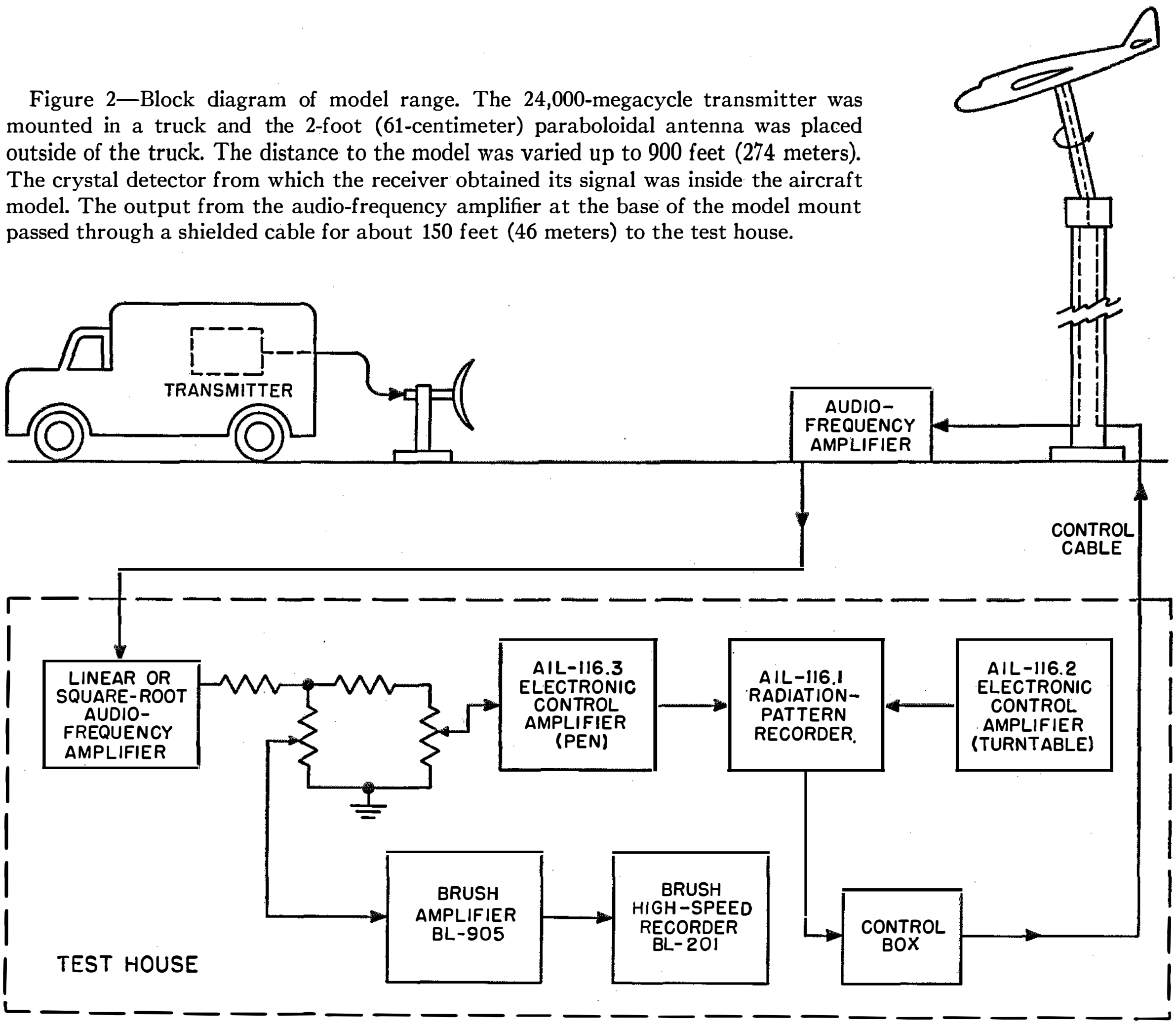

that plots with 2-decibel intervals were too detailed.

Another method of summarizing the data is to show the probability that the range (proportional to field strength) is greater than some specified value, assuming that all angles in the region $0 \leqslant \phi \leqslant 360$ degrees and 60 degrees $\leqslant \theta \leqslant 120$ degrees are equally possible. The maximum range is normalized to unity since no attempts were made to measure the gain directly.

The gain of each antenna was determined[1] by mechanical integration after approximating the shape of the elevation pattern outside the region where 60 degrees $\leqslant \theta \leqslant 120$ degrees. The gain was approximately 6 decibels, so that a normalized range of 0.5 corresponds to the range obtainable with a half-wave dipole in free space.

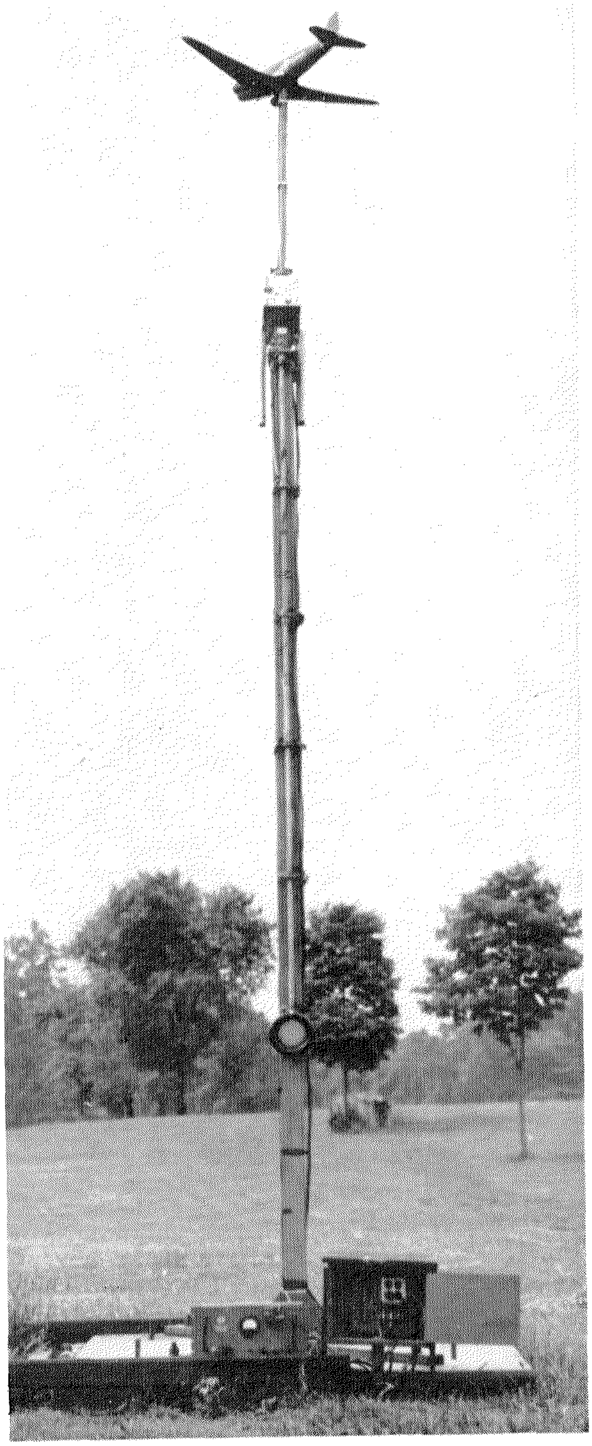

Figure 3—Photograph of model mount.

4. *Single Antennas*

The radiation patterns of single antennas at various locations on several representative models were studied. Contour maps showing typical results appear in Figures 5 through 11 and a probability curve is shown in Figure 12. Dots on some contour maps indicate sharp lobes (less than 5 degrees wide) at least 2 decibels above the background. Table 1 summarizes the results obtained.

TABLE 1

PROBABILITY OF OBTAINING FREE-SPACE-DIPOLE RANGE

Figures are in percent. All Points in Azimuth and ±30 Degrees in Elevation of Equal Importance

Aircraft Type	Top of Fuselage	Bottom of Fuselage	Top of Vertical Stabilizer	Frequency in Megacycles
DC-3	50	27	21	1000
XB-51	14	22	22	1200
DC-6	32	46	13	1500
DC-3	47	42	—	3000

The site atop the vertical stabilizer was uniformly poor as a result of the finer lobe structure in the vertical interference pattern. The coverage on the *XB-51* could be improved by selecting a site to minimize the azimuth angle over which strong wing interference is encountered. All top and bottom fuselage sites were chosen opposite

[1] See, for example, E. C. Jordon, "Electromagnetic Waves and Radiating Systems," Prentice-Hall Incorporated, New York, New York; 1951: page 420.

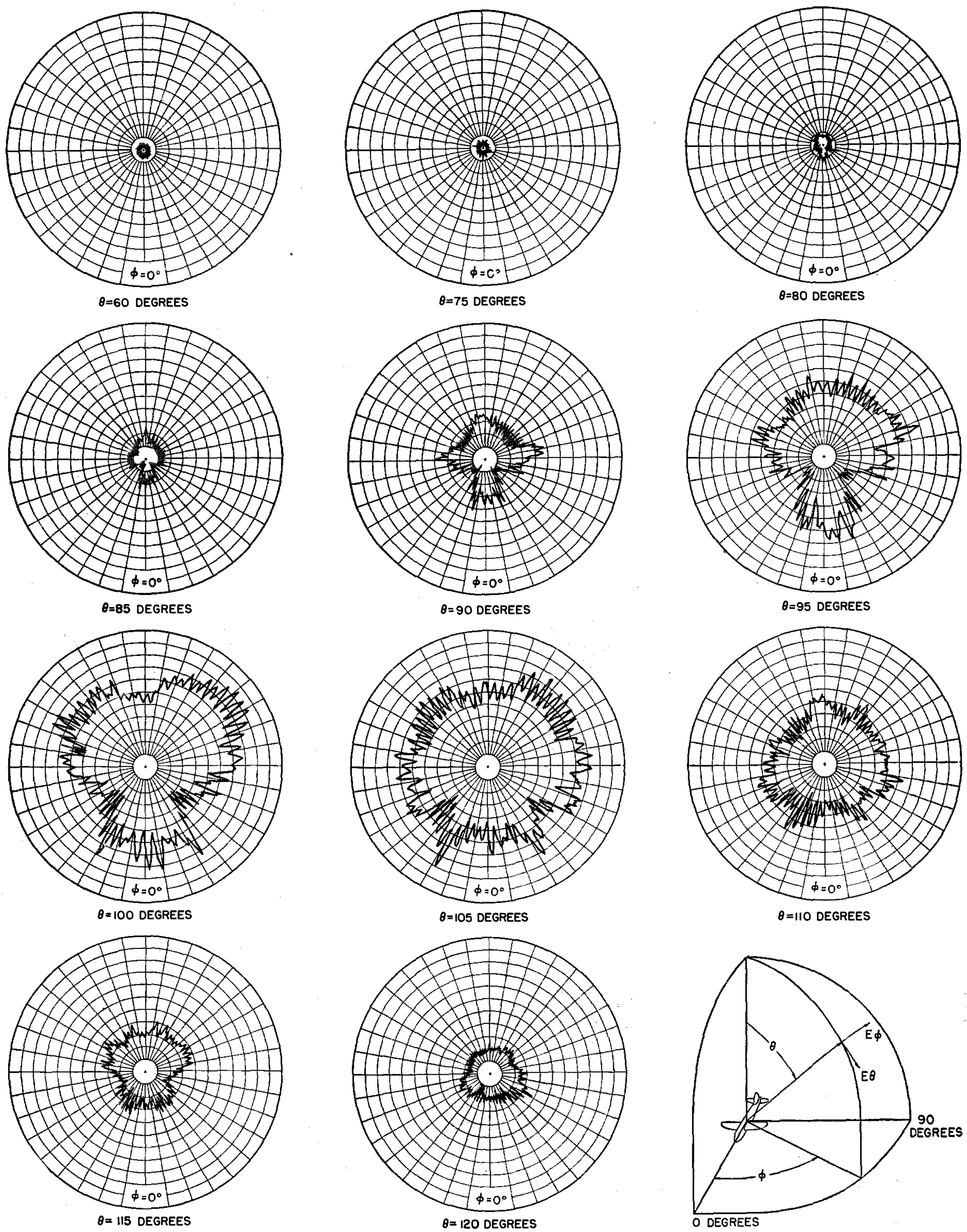

Figure 4—Typical set of field-intensity patterns for a quarter-wavelength stub antenna mounted on the bottom of the fuselage at the center of the wing root of a 1/24th-scale model of a *DC-3* aircraft. Vertically polarized signals transmitted over a 900-foot (274-meter) path are plotted in voltage for all values of ϕ, with zero corresponding to the nose of the aircraft. Diagrams for $\theta = 65$ and 70 degrees have been omitted here as not differing significantly from the adjacent plots.

the wing-root, the optimum position for aircraft with straight wings. For aircraft with swept-back wings, the optimum site for fuselage antennas is probably forward of the wing root. The coverage from the bottom fuselage site on the *DC-3* at 1000 megacycles suffers from shadowing and reflections from the engine nacelles. This same site gave better coverage at 3000 megacycles. The reason for this is not clearly understood. However, this particular site places the antenna over the equivalent of an irregularly shaped ground screen so that the effect of varying frequency is difficult to predict. The top fuselage site on the *DC-6* produced a coverage figure somewhat below that obtained from the *DC-3*. This is caused by the flat-top characteristic of the *DC-6* fuselage, which caused the resultant vertical pattern to tilt up about 20 degrees.

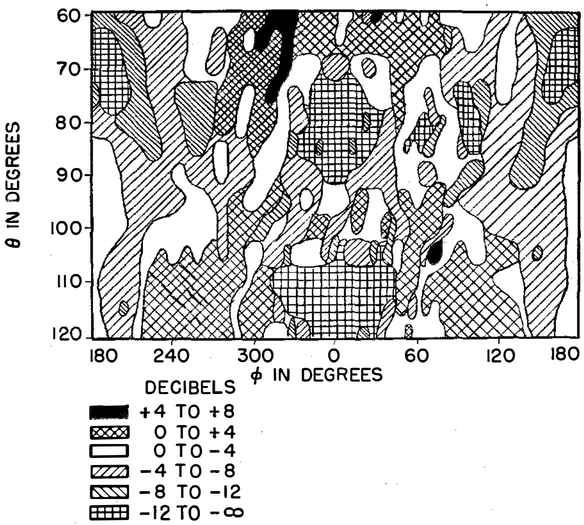

Figure 5—Contour map for a discone antenna mounted on the vertical stabilizer of a *DC-3* at 1000 megacycles.

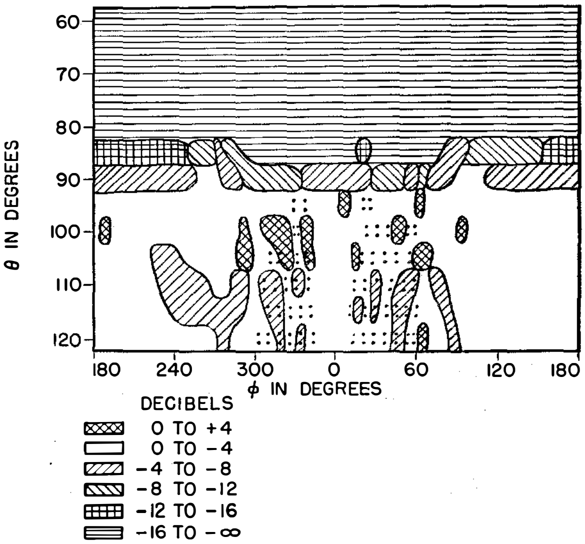

Figure 7—Contour map for a quarter-wavelength stub antenna mounted on the bottom of the fuselage on the center line of the wings of a *DC-6* at 1500 megacycles.

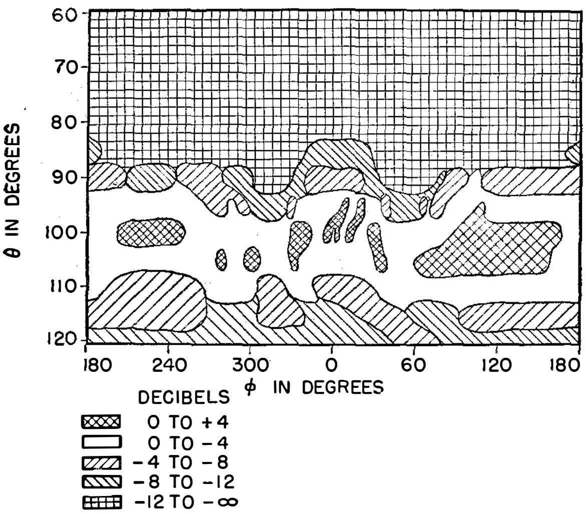

Figure 6—Contour map for a quarter-wavelength stub antenna mounted on the bottom of the fuselage on the center line of the wings of a *DC-3* at 1000 megacycles.

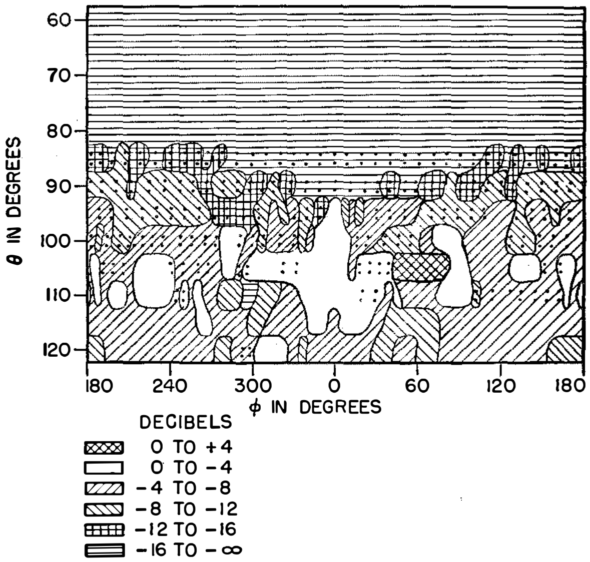

Figure 8—Contour map for a quarter-wavelength stub antenna mounted on the bottom of the fuselage on the center line of the wings of an *XB-51* at 1200 megacycles.

In general, the performance of aircraft antennas on large aircraft is more easily predicted[2] at ultra-high than at very-high frequencies and below. As might be expected, specular reflection was encountered and, within practical limits, scattering could be predicted from scalar field theory.[3] Although in some locations improvement in coverage may be obtained by shaping the free-space pattern of the radiator so as to minimize reflections, there is nothing that can be done in the way of antenna design to reduce shadowing.

[2] R. H. J. Carey, "A Survey of External and Suppressed Aircraft Aerials for Use in the High Frequency Band," *Proceedings of the Institution of Electrical Engineers*, Part 3, volume 99, pages 197–209; July, 1952.

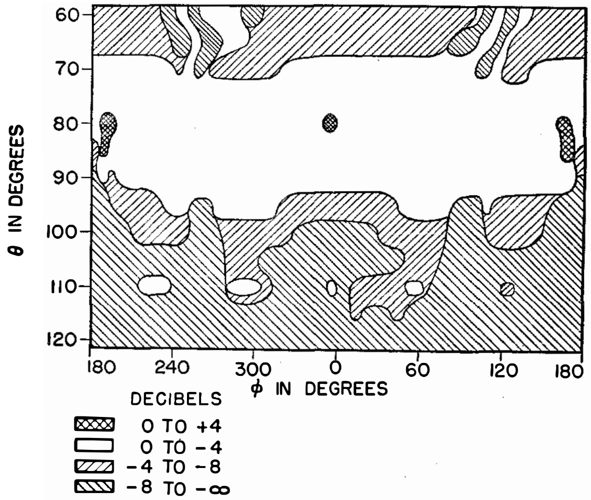

Figure 9—Contour map for a quarter-wavelength stub antenna mounted on the top of the fuselage on the center line of the wings of a *DC-3* at 1000 megacycles.

5. Dual Antenna Systems

Air-navigation and traffic-control equipments can be divided into two classes: *A*, that class that knows when it should be receiving a signal, such as the distance-measuring equipment[4] and *B*, that class that does not know when it should be receiving a signal, such as the radar safety beacon.[5] For systems of the former class, the space about the aircraft may be divided into sectors with only one sector covered at any instant of time, while systems of the latter class require coverage that is equally receptive over some finite time interval to signals from any point in azimuth and approximately ± 30 degrees in elevation.

[3] H. J. Riblet and C. B. Barker, "A General Divergence Formula," *Journal of Applied Physics*, volume 19, pages 63–70; January, 1948.

[4] R. C. Borden, C. C. Trout, and E. C. Williams, "Description and Evaluation of 100-Channel Distance-Measuring Equipment," *Proceedings of the IRE*, volume 39, pages 612–618; June, 1951.

[5] G. Heath, "Air Traffic Control Systems," *Electronics*, volume 25, pages 152–154; June, 1952.

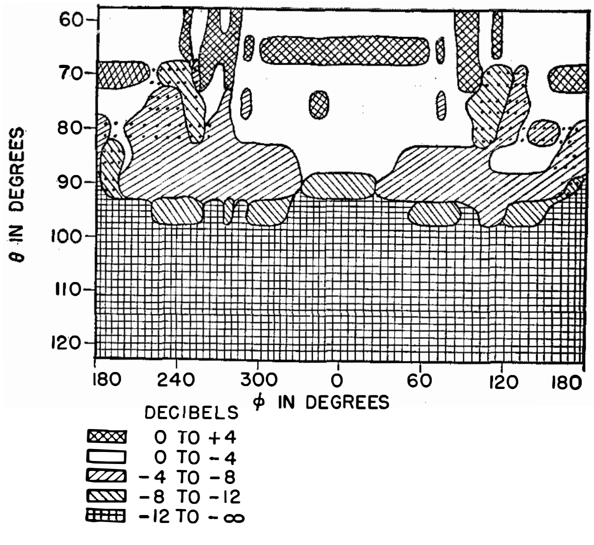

Figure 10—Contour map for a quarter-wavelength stub antenna mounted on top of the fuselage near the center line of the wings of a *DC-6* at 1500 megacycles.

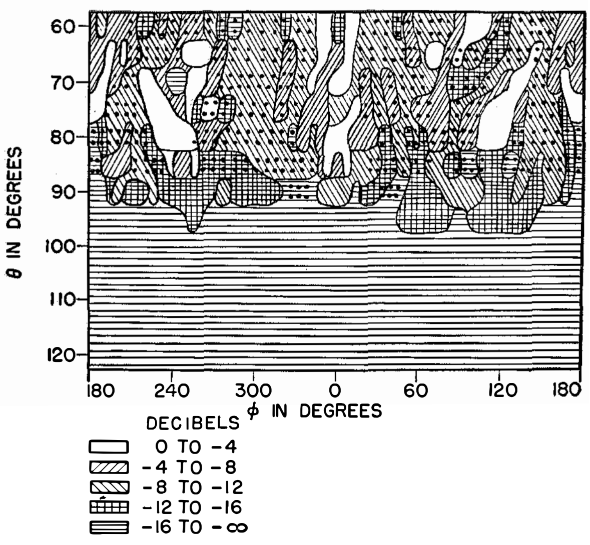

Figure 11—Contour map for a quarter-wavelength stub antenna mounted on top of the fuselage on the center line of the wings of an *XB-51* at 1200 megacycles.

In considering means of utilizing dual antennas, the following outline will be used.

Passive systems employing dual antennas in parallel (section 5.1), and dual antennas with a delay line (section 5.2).

Systems using moving parts and having dual antennas with a radio-frequency switch (section 5.3), employing dual antennas with a phase shifter (section 5.4), and using a common antenna system (section 5.5).

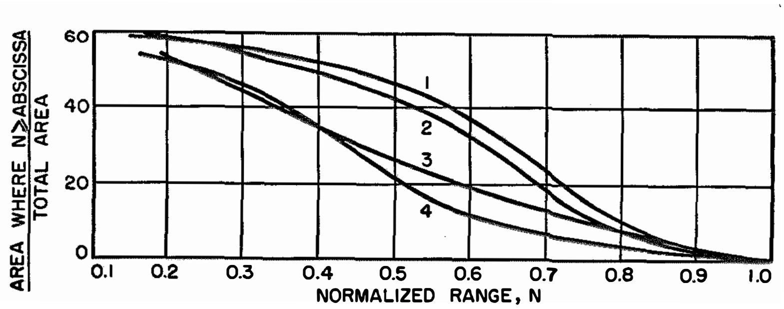

Figure 12—Probability that the range exceeds a specified value for a quarter-wavelength stub antenna mounted on the bottom of the fuselage of the airplane.

Curve	Airplane	Scale	Frequency in Megacycles
1	*DC-6*	1/16	1500
2	*DC-3*	1/8	1000
3	*DC-3*	1/24	3000
4	*XB-51*	1/20	1200

5.1 Dual Antennas in Parallel

The least-complicated system is to operate in parallel dual antennas with complementary patterns. Interference is encountered where individual patterns overlap (see Figure 13). Fundamental disadvantages are A, long cables are sometimes required and B, in all cases a 3-decibel junction loss must be considered.

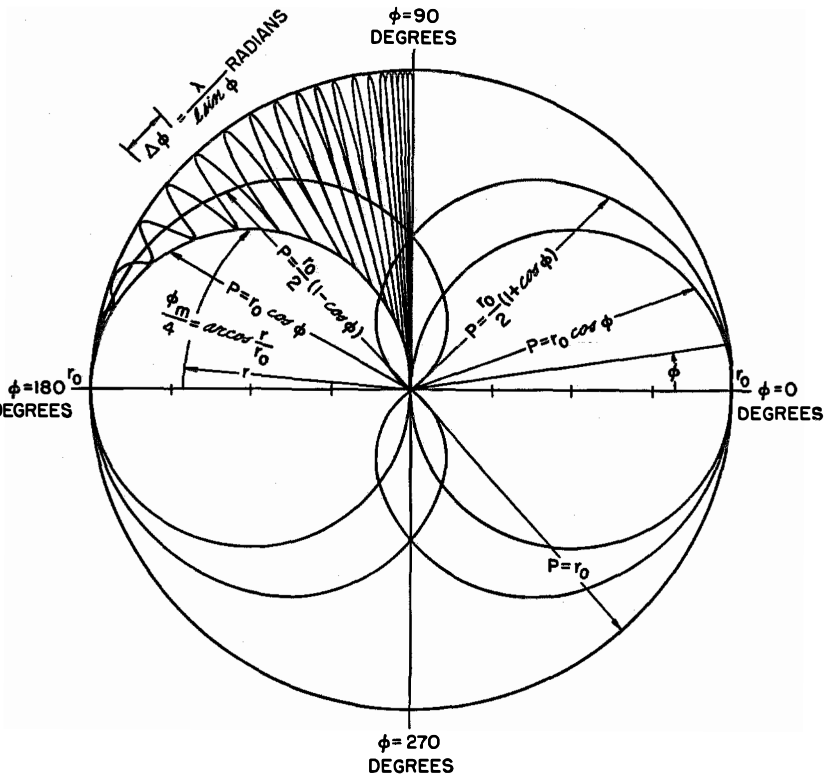

Figure 13—Resultant of two cardioid patterns connected in parallel. r_0 = maximum range, l = spacing between antennas, ϕ_m = total angle for which the range $\geqslant r$.

It will be shown that the radar safety beacon can operate satisfactorily in certain types of interference regions. The performance of the present distance-measuring equipment in an interference region is uncertain. It appears that some portions of the interference regions may be usable but for a conservative analysis the interference regions will be considered unusable for distance measuring.

5.1.1 Distance-Measuring Equipment

Wingtip antennas, each antenna having essentially a cardioid pattern, is one possible system; nose and tail antennas of similar type is another system. Both systems have interference only at certain values of ϕ but require long transmission lines. Antennas located top and bottom of the fuselage produce vertical interference making distance-measuring operation uncertain at all values of ϕ and hence will not be considered.

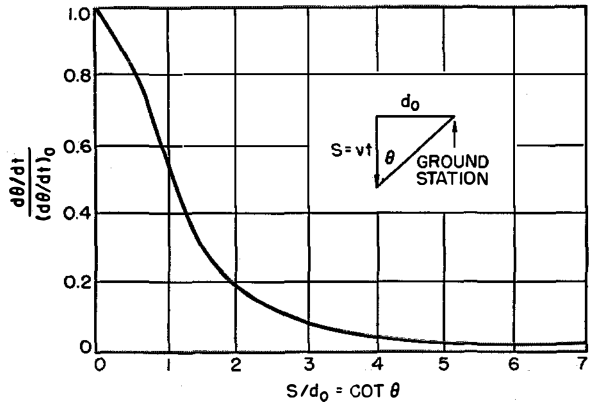

Figure 14—Normalized rate of change of an angle $d\phi$ versus distance.

$S/d_0 = \cot\theta$. $(d\theta/dt)/(d\theta/dt)_0 = 1/[1 + (S/d_0)^2]$.

An antenna with a cardioid pattern in the horizontal (ϕ) plane and enough vertical (θ) directivity to give a maximum average gain of 5 decibels over a dipole is about the highest-gain antenna that can be used if vertical coverage between $\theta = 60$ degrees and 120 degrees is required. Taking transmission-line loss and junction loss into account, the maximum range that can be expected is free-space-dipole range. If a range of 70 percent of free-space-dipole range is usable, acceptable performance can be obtained 45 percent of the time. In the event a smaller sector, say ± 15 degrees in elevation, can be used, free-space-dipole range can be obtained 45 percent of the time.

5.1.2 Beacon

For simplicity, assume that cardioid antennas are mounted on the nose and tail. The coverage is good in two symmetrical sectors fore and aft but toward the sides there will be narrow lobes and the coverage there may or may not be good, depending on many factors. If the interrogating radar is never more than a few degrees off the course of the airplane, the coverage will be very good. If, on the other hand, the interrogating radar is in the interference region off the wing, the coverage may become uncertain.

The geometry is shown in Figure 13. Near $\phi = 90$ degrees, the minima approach zero making this region the most-critical one. As the aircraft flies at a constant velocity V, the rate of change of angle with respect to a ground radar (located at $\phi = 90$ degrees and a minimum distance d_0 between line of flight and ground station) is $d\phi/dt_0 = V/d_0$. Plotted in Figure 14 is the normalized rate of change of ϕ as a function of distance along the line of flight. The time required for one lobe to move past the ground radar is

$$T = \frac{3600}{V_m}\frac{\lambda}{l}\frac{d_0}{\sin^3\phi},$$

where

V_m = velocity in miles per hour
d_0 = minimum distance between line of flight and ground station in miles
l = separation between antennas
λ = wavelength.

Thus the time required for one lobe to move past the ground radar varies from 6.3 to 18 seconds as ϕ varies from 90 to 45 degrees when velocity = 200 miles (322 kilometers) per hour, $l = 100$

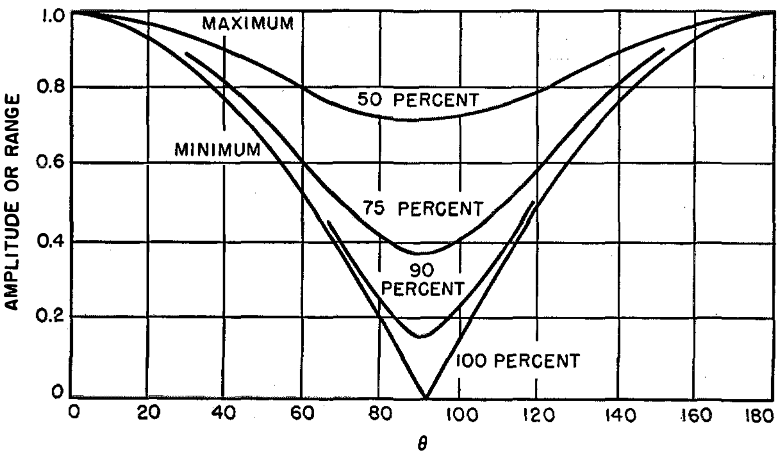

Figure 15—Percentage of each lobe in the interference region exceeding a certain amplitude plotted against the angle θ.

feet (30 meters), frequency = 2700 megacycles, and d_0 = 100 miles (161 kilometers).

Figure 15 shows how much of each lobe in the interference region exceeds a certain amplitude. This figure gives the probability of receiving a single interrogation. This probability is correct only for the case where the aircraft is in the beam of the interrogating radar for a time that is considerably less than the time required for one lobe to move past the interrogating radar. This assumption is not valid when the ground antenna is searchlighting the airplane.

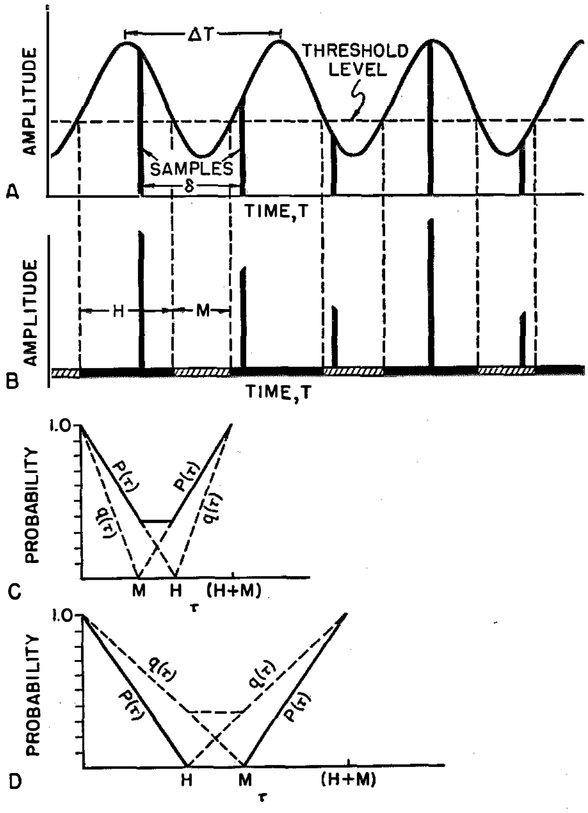

Figure 16—Periodic signal being sampled at time intervals δ is shown at A, the sampling is at B. The solid base line in B indicates the signal to be above the threshold level and the shaded line indicates it to be below threshold value. C is a probability diagram for $M<H$ and D a similar diagram for $M>H$.

To a first approximation, the motion of the airplane is essentially smooth and the ground-radar antenna rotates at a regular rate so that the problem becomes one of periodic sampling of a periodic wave. If the airplane transmitted continuously, the field strength at the ground radar would be periodic in time, as shown in Figure 16A. (The period is not constant, but for small time intervals it is approximately so.) As the radar antenna scans, it samples the periodic wave. If the period of the wave and sampling interval are known, a diagram similar to Figure 16B can be drawn in which the length of a segment represents the time during which the signal is above the threshold and the gap represents the time during which the signal is below the threshold. The probability of one hit in one try is the same as that given above. The probability of two hits out of two tries is equal to $P_1P(\tau)$, where P_1 is the probability of one hit in one try at time T and $P(\tau)$ is the probability of getting a hit on the second try at time $T+\tau$ if the first try were a hit. $P(\tau)$ has the form shown on Figure 16C. Diagrams are shown in Figure 17. To construct these curves: draw a straight line from $P = 1$, $\tau = 0$ to $P = 0$, $\tau = H$, draw a straight line from $P = 0$, $\tau = H$ to $P = 1$, $\tau = H + M$. If these lines overlap, add the P's in the overlap region.

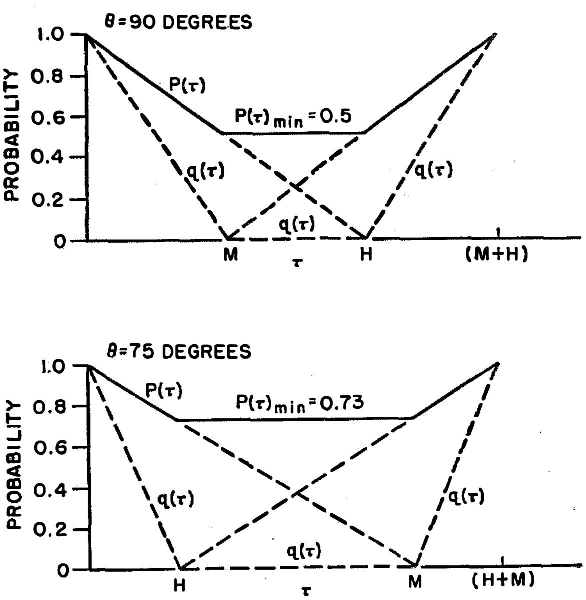

Figure 17—Probability diagram applicable to a *DC-6* at 2700 megacycles when V_m = 200 miles (322 kilometers) per hour, l = 100 feet (30 meters), and d_0 = 100 miles (161 kilometers).

The probabilities for various combinations are as follows:

1	2	Probability
Hit	Hit	$P_1 P(\tau)$
Miss	Miss	$(1 - P_1)q(\tau)$
At least one hit		$1 - (1 - P_1)q(\tau)$.

If the first try at time T were a miss, $q(\tau)$ is the the probability of getting a miss at time $T + \tau$.

The minimum value of P_1 and P_T for any set of conditions will be taken since no assumptions will be made concerning the sampling rate; conversely the maximum values of q_1 and $q(\tau)$ will be taken. This means that the expression for at least one hit in two tries reduces to P_1 when $q(\tau) = 1$.

The probabilities considered here are independent of the rate at which the lobes in the interference region move past the ground station provided the time required for one lobe to move past the radar is less than the time per scan of the ground antenna. For nose and tail or wingtip antennas on large aircraft, there is no advantage in high-speed switching or phase shifting.

Following this procedure and with the same constants used in the previous example, the probability plots shown in Figures 17 and 18 were made.

5.2 Dual Antennas Connected Through a Delay Line (for Beacon)

Locate two antennas with complementary coverage on the aircraft (Figure 19A). Now connect the two antennas together but place in one antenna lead a delay line with a time delay of the order of one pulse length and connect the combination to the transmitter–receiver (Figure 19B). When an interrogating pulse is received, the output of antenna A cannot interfere with the output of antenna B because output B is delayed by a whole pulse length. The receiver input, therefore, will be one of the forms shown in Figure 19C. When the transmitter replies, the input to the ground receiver is also, by reciprocity, one of the forms shown in Figure 19C.

The delay line can be placed in the ground equipment if orthogonal polarizations are used. Two ground antennas are needed, with the delay line connected to one antenna only. To prevent interference, all of the antennas must be relatively free of cross polarization at angles at which both receive.

A rotary phase shifter can be used instead of the delay line. Its advantages are smaller size and less loss. Its disadvantages are that some pulses may be lost and that it is a rotating device that needs power and maintenance. For ground use, the delay line may be preferable. The major disadvantage is loss in the delay line. The advantage is that all circuits are passive. If phase shifters are used, the major disadvantages are complexity, size, and weight; the advantage is less insertion loss.

5.3 Dual Antennas Connected Through a Radio-Frequency Switch (for Distance Measuring)

This is an obvious solution for distance measuring since it knows when it should be getting a signal. For the case of single $\lambda/4$ stub antennas located on the top and bottom of the fuselage, the average coverage figure obtained for all the models was 70 percent. It is reasonable to assume that in most cases a coverage figure of 70 to 90 percent can be obtained for top and bottom antennas by using some vertical directivity.

For nose and tail antennas with cardioid patterns having 5 decibels of gain and 3 decibels of cable loss, the best coverage figure obtainable theoretically is 60 percent. This is based on ± 30-

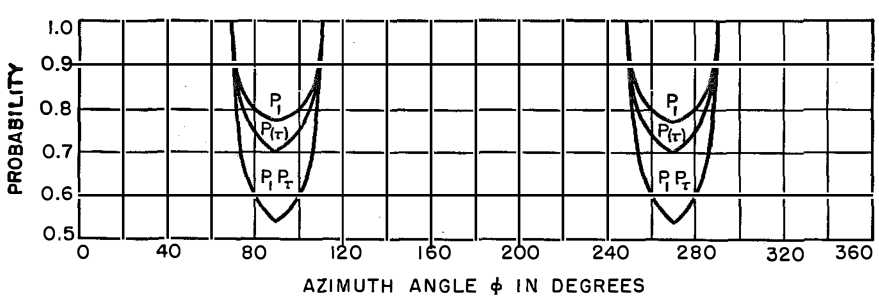

Figure 18—Probability versus azimuth angle for the same parameters of Figure 17. The usable range is 0.35 of the maximum range.

degree coverage, which limits the gain to 5 decibels. This figure can be improved somewhat by using antennas with sharper cutoff characteristics in the overlap region.

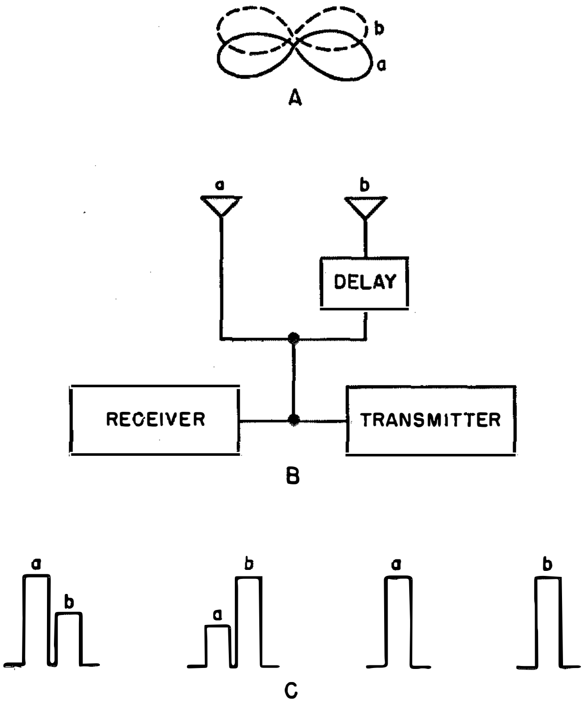

Figure 19—Dual antenna with delay line. *A* is the pattern overlap, *B* is the arrangement of the equipment, and *C* is the input waveforms to the receiver.

If automatic switching is employed, the circuitry for nose and tail or top and bottom antennas may have to be different.

5.4 Dual Antennas Connected Through a Phase Shifter

A feasible system using top and bottom antennas is to use one low-speed phase shifter to sweep the lobes past the ground radar at a rate that exceeds the rotational rate of the ground radar antenna. Unfortunately, the coverage is uncertain at all values of ϕ and the uncertainty is greatest at $\theta = 90$ degrees, which is the region of maximum interest.

5.5 Common Antenna Systems for Distance Measuring and Beacon

Probably the best multiple-antenna solution to the beacon problem is one consisting of radiators on the nose and tail, producing interference off the wings; while the best multiple-antenna solution for the distance-measuring problem is a system consisting of top and bottom antennas with an automatic switch. Unfortunately the distance-measuring equipment does not respond favorably to the type of interference pattern favorable to beacon systems, nor is switching of antennas favorable to beacon operation.

The simplest common-antenna system is the nose and tail antennas operated in parallel. Since relative phase is not significant, a simple hybrid bridge may be used as a multiplexer. This system is very desirable because of its simplicity. However, its performance suffers from cable and junction loss. Also, for distance measuring the interference region is doubtful. Otherwise, the requirements that a common-antenna system imposes on a multiplexer are severe and might result in a device whose complexity would make the system impractical. In the event a practical multiplexer can be built, there is no basic reason why separate additional filtering cannot be employed to enable the antennas in a multiple-antenna system to be tied together over one frequency band and operated separately over an adjacent band.

6. *Acknowledgements*

The writers express their appreciation to Mr. A. G. Kandoian for over-all supervision of this work, to Mr. W. Spanos for assistance in taking and analyzing the pattern data, and to Mr. A. J. Lombardi for mechanical design of the model mount. Also helpful were conferences with Messrs. Henry Senf and Walter Pike of the Air Navigation Development Board and with Professor L. J. Chu of Massachusetts Institute of Technology.

Microstrip Kit

RECENTLY, Federal Telephone and Radio Company has introduced the *FTR–101* Microstrip Kit. It contains an assortment of microstrip circuit components, connectors to join them together electrically, and an easel to which they may be mechanically fastened.

In a matter of minutes, a microwave receiver like the one illustrated can be assembled and its performance will compare favorably with a unit constructed of conventional waveguide- or coaxial-type components.

The kit, which is packaged in a sturdy wooden carrying case, contains a selection of components adequate for the assembly of a complete microwave receiver or a number of alternate circuit arrangements. Coaxial cables may be connected to fittings mounted on certain components. The broadband characteristics of microstrip allow circuit operation from 1000 to 8000 megacycles per second. Components such as hybrids and crystal holders that are frequency sensitive are provided in various sizes for the different frequency ranges.

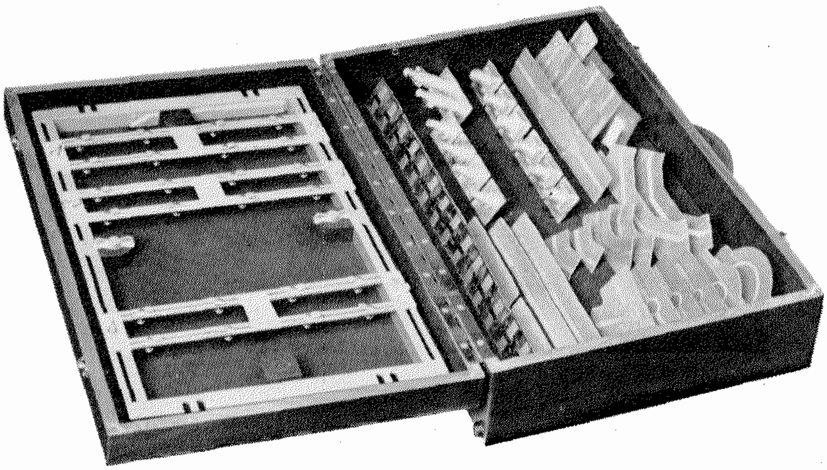

Designed primarily for experimentation, the kit provides an unusually simple and rapid means for building microwave assemblies and is particularly effective for instructional use in colleges.

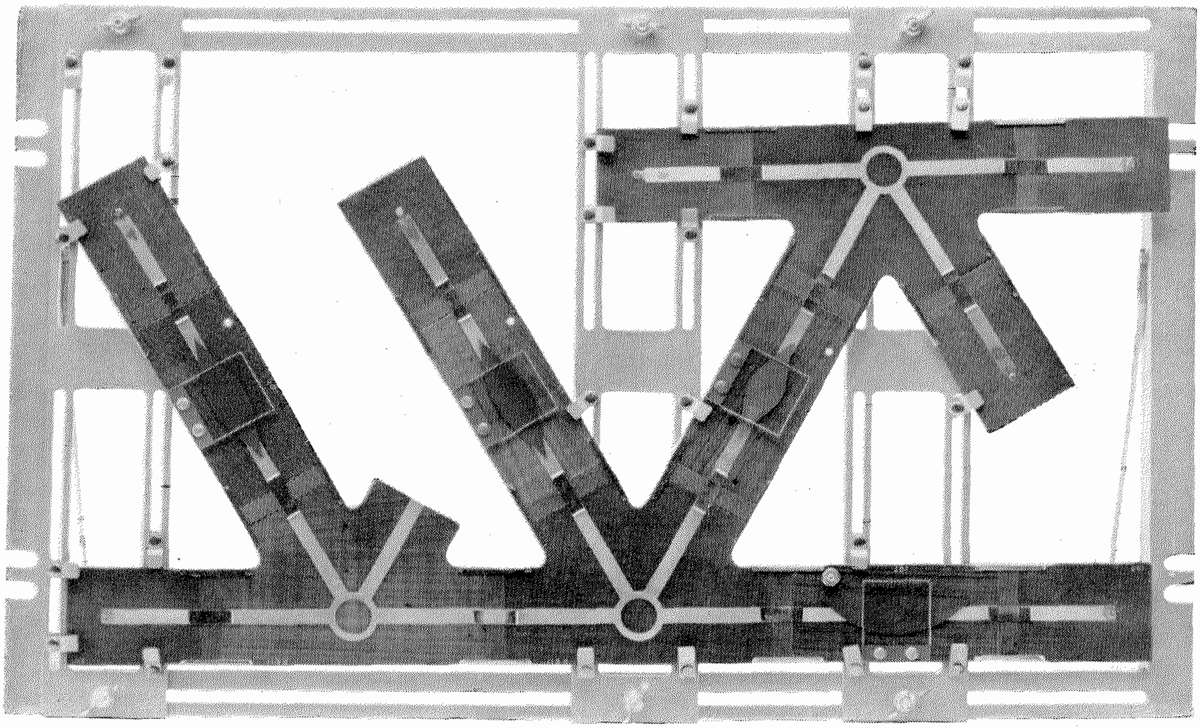

Mechanism of Rectification in Vacuum-Tube Diodes at Microwave Frequencies*

By GEORGE PAPP

Capehart–Farnsworth Company, a division of International Telephone and Telegraph Corporation; Fort Wayne, Indiana

NOTING that at microwave frequencies the space charge in the vicinity of the cathode of a diode acts as a dielectric with a dielectric constant of approximately unity and that the rectification takes place in essence in the space between the cathode and the potential minimum, the problem of high-frequency rectification is attacked by calculating the motion of the electrons in the resultant of the direct-current and high-frequency fields. The explicit form of the equation of motion permits the calculation of the currents through the diode showing that appreciable rectification is present in diodes at microwave frequencies. Measurements appear to verify the predictions advanced by the theory.

• • •

1. Introduction

The operating mechanism of vacuum-tube diodes at low frequencies is well understood. Since the rate of change of the plate voltage is relatively slow, the diode is always in equilibrium. The instantaneous values of plate voltage and electron current at every instant satisfy the Child-Langmuir space-charge equation. The plate current of the diode is simply the mean value of the instantaneous values.

In a low-impedance circuit at low frequencies, the plate current of the diode is greater than the direct current flowing through it in the absence of the alternating-current field. The diode operates as a rectifier. The current excess, which can be called the rectified current, may be computed easily.

In a high-impedance circuit, however, as in every detector circuit for example, the change in plate voltage rather than the current change is of importance. This voltage change will be equal to the amplitude of the alternating-current voltage, at least in circuits of very-high impedance; for example, in the case of diode alternating-current voltmeters. This follows from the fact that as long as the plate is positive with respect to the cathode, electrons will pass to the plate. If the impedance is infinitely large, these electrons will remain on the plate, imparting to it higher and higher negative voltages. This process continues as long as there are instants when the voltage of the plate is higher than that of the cathode and the plate can pull over additional electrons. The limit is reached when the plate voltage becomes equal to the (negative) peak voltage V_1 of the alternating current.

In actual diodes, the limiting plate voltage will be $-(V_1 + V_{th})$, where eV_{th} is the thermal energy of the emitted electrons. However, since in the absence of an alternating current the plate voltage is $-V_{th}$, the change in plate voltage will be V_1.

It is not difficult to realize that the operating mechanism just described does not hold at high frequencies. This difference is due to the fact that the voltage changes before the electrons leaving the cathode in the proper phase have an opportunity to reach the plate. Thus, in contrast to the almost steady electron stream from cathode to plate at low frequencies, in the case of high frequencies an oscillating motion of the electrons will be typical. In a plane-electrode diode with a high-frequency field

$$E = E_1 \sin \omega t,$$

the amplitude of this oscillation will be

$$c = \frac{e/m}{\omega^2} E_1.$$

At moderately high frequencies, c is smaller than the cathode–anode distance. At 10^{10} cycles per second, $c = 0.5 \times 10^{-6}$ centimeter for a high-frequency field of amplitude $E_1 = 1$ volt per

* This work has been supported by the United States Army Bureau of Ordnance, Contract NOrd-9099, under the technical direction of the Applied Physics Laboratory, Johns Hopkins University; Baltimore, Maryland.

centimeter. The peak velocity will be $v = \omega c$, corresponding to an energy of

$$\tfrac{1}{2}mv^2 = \tfrac{1}{2}m\omega^2 \frac{e^2/m^2}{\omega^4} E_1^2 = \tfrac{1}{2}\frac{e^2/m}{\omega^2} E_1^2$$
$$= \tfrac{1}{2}ceE_1 = eV_{hf} \text{ electron-volts.}$$

This is the maximum energy collected by an electron in the high-frequency field. At the same time V_{hf} represents the maximum voltage to which the electrons can charge the plate.

The influence of the initial velocity of the electrons can easily be taken into account. The motion of the electrons will be the resultant of the translational and oscillating components. The plate will charge to a voltage equal to $V_{th} + V_{hf}$. In the presence of the high-frequency field, the voltage change will be V_{hf}, a voltage proportional to the square of the high-frequency voltage.

While for this type of operation the diodes may be of practical use at high power levels,[1] the results are quite hopeless at lower levels. For example, at the comparatively strong high-frequency field of 1 volt per centimeter, the rectified voltage will amount to only 0.25×10^{-6} volt and it will decrease rapidly with diminishing fields.

Detection is as utterly hopeless as this only in the high-impedance case. As will be shown, tube diodes are still practical in the detection of small microwave signals[2] in low-impedance circuits with positively biased plate. It may seem a paradox, but there will be significant rectification in a diode of large cathode–anode spacing with electron transit times equal to several hundred high-frequency periods. This is due to the fact that for the rectification of high-frequency voltages, only the immediate vicinity of the cathode (that is, the space between the cathode and the potential minimum) is of importance. In other words, all the electrons that have once passed the plane of the potential minimum will continue on to the plate, no matter how far away it may be located. The extension in space between the cathode and the potential minimum, hereinafter called simply the cathode space, is very small. As a result, the true electron transit angle is comparatively small, even in diodes of large physical dimensions.

From the preceding discussion it is possible to draw several important conclusions, of which two will be cited.

A. A theory developed for plane diodes may be applied to cylindrical diodes as well, since the cathode radius is large compared to the thickness of the cathode space, even in diodes with a directly heated cathode of the smallest practical diameter.

B. Since rectification is a quadratic function of the intensity of the electric field in the cathode space, detection may be achieved in cylindrical diodes that are by orders of magnitude larger than in corresponding plane diodes owing to the higher concentration of the high-frequency field around the cathode in cylindrical diodes.

These two important conclusions may be drawn in consequence of the very-high frequency, as will be explained in the following paragraphs.

In the low-frequency case, the alternating-current field cannot reach the surface of the cathode. In changing the plate voltage, the electron current is changed to some extent but the field at the cathode is changed only imperceptibly.

In a high-frequency field, all the electrons of the space charge are set into oscillating motion. Each electron contributes to the resultant value of the high-frequency field at every point. This field is the same as the field in a dielectric having a dielectric constant

$$\epsilon = 1 - 4N\frac{e^2/m}{\omega^2},$$

where N is the number of electrons per cubic centimeter and e and m are the electronic charge and mass, respectively.

In a diode with space-charge density of 10^{10} to 10^{11} electrons per cubic centimeter, ϵ is a negative number at low frequencies. For frequencies in the neighborhood of $\omega = 2\pi \times 10^{10}$, ϵ is positive and only slightly less than unity; consequently, the high-frequency field will reach the cathode and its intensity in first approximation will be the same as if the space charge were not present.

[1] P. O. Hawkins, H. J. Curnow, and R. Redstone, "A Diode Rectifier of Microwaves," *Services Electronics Research Laboratory* (*SERL*) *Technical Journal*, volume 3, pages 38–42; July, 1953.

[2] The work described here was finished in the first half of 1952. From an abstract appearing in *Proceedings of the IRE*, volume 41, page 426; March, 1953, we were made aware of similar work done independently by A. B. Bronwell, T. C. Wang, I. C. Nitz, J. May, and H. Wachowski. Recently, a paper by those authors, "Vacuum-Tube Detector and Converter for Microwaves Using Large Electron Transit Angles," appeared in *Proceedings of the IRE*, volume 42, pages 1117–1123; July, 1954.

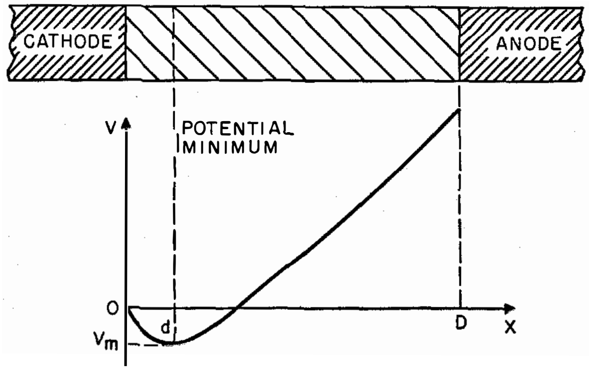

Figure 1—Static potential distribution in plane diodes.

Keeping this in mind, we may now develop a simple but adequate theory of the mechanism of rectification at microwave frequencies. In a second-order approximation, we may derive the equations of the motion of the electrons. By using the Maxwell-Boltzmann velocity distribution of the emitted electrons, we may calculate the current of the diode in the presence of a high-frequency field.

2. *Calculation of Diode Current*

As described in the preceding section, for small high-frequency signals the motion of the electrons is defined by

$$m\ddot{x} = -eE^{(0)} - eE^{(1)}, \tag{1}$$

where e and m are the electronic charge and mass, respectively, $E^{(0)}$ is the field intensity belonging to the direct-current potential distribution $V^{(0)}$ within the diode, and $E^{(1)}$ is the high-frequency field intensity; $E^{(1)} = E_1 \sin \omega t$.

Using parabolic approximation

$$V^{(0)}(x) = \tfrac{1}{2}ax^2 + bx + c$$

for $V^{(0)}$ in the cathode space and introducing a new variable $y = x - d$, where d is the distance of the potential minimum V_m from the cathode, Figure 1, (1) may be written in the form

$$m\ddot{y} - eay = -eE_1 \sin \omega t, \tag{2}$$

where $a = 2V_m/d^2$. For a diode with cathode temperature $T = 1000$ degrees Kelvin and saturation current $I = 0.4$ ampere per square centimeter, $V_m = 0.104$ volt and $d = 0.42 \times 10^{-3}$ centimeter.[3]

In the absence of a high-frequency signal, the motion of the electrons is

$$y(t) = A \exp[\alpha t] + B \exp[-\alpha t], \tag{3}$$

where

$$\alpha = \left(\frac{ea}{m}\right)^{1/2} = \left(\frac{2eV_m}{md^2}\right)^{1/2} = \frac{(2eV_m/m)^{1/2}}{d} = \frac{v_m}{d}$$

(having a value of 0.6×10^{10} per second in the diode described above) and

$$v_m = (2eV_m/m)^{1/2}.$$

A and B are to be chosen so that (3) will satisfy the initial conditions.

For an electron leaving the cathode at time $t = t_0$ with initial velocity v_i, the initial conditions are

$$\left.\begin{aligned} y(t_0) &= -d, \\ \dot{y}(t_0) &= v_i, \end{aligned}\right\} \tag{3A}$$

and therefore the values A and B are

$$\left.\begin{aligned} A &= \frac{v_i - \alpha d}{2\alpha \exp[\alpha t_0]} = \frac{v_i - v_m}{2\alpha \exp[\alpha t_0]} \\ \text{and} \quad B &= -\frac{v_i + v_m}{2\alpha \exp[-\alpha t_0]}. \end{aligned}\right\} \tag{3B}$$

From (3) we may conclude that for an electron to leave the cathode space, the requirement will be

$$A \geqslant 0, \tag{3C}$$

or,

$$v_i \geqslant v_m. \tag{3D}$$

All the electrons satisfying (3D) contribute to the current I of the diode. By applying the Maxwellian velocity distribution of emitted electrons, this current may be evaluated as

$$\begin{aligned} I &= -eN^* \exp\left[-\frac{\frac{1}{2}mv_m^2}{kT}\right] \\ &= I^* \exp[-v_m^2/v_T^2] = I^* \exp[-V_m/V_T] \end{aligned} \tag{4}$$

in a diode with saturation current $I^* = -eN^*$ at a cathode temperature T degrees Kelvin, where $(m/2)v_T^2 = eV_T = kT$; k is the Boltzmann constant.

In the presence of a high-frequency field, the motion will be

[3] K. R. Spangenberg, "Vacuum Tubes," First Edition, McGraw-Hill Book Company, Incorporated, New York, New York; 1948: page 193, equations (8.64) and (8.65)

$$y^{(t)} = A \exp[\alpha t] + B \exp[-\alpha t] + \Gamma \sin \omega t, \quad (5)$$

with

$$\Gamma = \frac{e/m}{\omega^2 + \alpha^2} E_1,$$

or at around 10^{10} cycles per second for the diode described above, approximately

$$\frac{e/m}{\omega^2} E_1$$

For an electron leaving the cathode at time $t = t_0$ with initial velocity $y = v_i$, the initial conditions are

$$\left.\begin{aligned} y(t_0) &= -d \\ \dot{y}(t_0) &= v_i \end{aligned}\right\} \quad (5A)$$

from which

$$\left.\begin{aligned} A &= \frac{v_i - \alpha d - \alpha\Gamma \sin \omega t_0 + \omega\Gamma \cos \omega t_0}{2\alpha \exp[\alpha t_0]} \\ &= \frac{v_i - v_m - w \sin(\omega t_0 + \psi)}{2\alpha \exp[\alpha t_0]}, \\ B &= \frac{-v_i - \alpha d - \alpha\Gamma \sin \omega t_0 + \omega\Gamma \cos \omega t_0}{2\alpha \exp[-\alpha t_0]} \\ &= -\frac{v_i + v_m + w \sin(\omega t_0 - \psi)}{2\alpha \exp[-\alpha t_0]}, \end{aligned}\right\} \quad (5B)$$

with

$$w = (\omega^2 + \alpha^2)^{1/2}\Gamma = \frac{e/m}{(\omega^2 + \alpha^2)^{1/2}} E_1 \quad (5C)$$

and $\tan \psi = \omega/\alpha$.

In the direct-current case, B is always negative. Consequently (3C) is the condition under which an electron will cross the potential minimum, $y = 0$.

In the present case, B is not necessarily negative and the expression for $y(t)$ is complicated by the presence of the $\Gamma \sin \omega t$ term. However, $B \exp[-\alpha t]$ is a rapidly decreasing function. Therefore, the condition for which y could have large positive values, and consequently for which the electron could go over to the anode, will apply here also;

$$A \geqslant 0, \quad (6)$$

or,

$$v_i \geqslant v_m + w \sin(\omega t_0 + \psi). \quad (6A)$$

Electrons satisfying (6A), and only those, leave the cathode space and go over to the plate. They add up to a current

$$\left.\begin{aligned} I_c(t_0) &= I^* \exp\left\{-\left[\frac{v_m + w \sin(\omega t_0 + \psi)}{v_T}\right]^2\right\} = I \exp\left[-\frac{2v_m w \sin(\omega t_0+\psi) + w^2 \sin^2(\omega t_0+\psi)}{v_T^2}\right] \\ &\approx I\left[1 - 2\frac{v_m w}{v_T^2} \sin(\omega t_0+\psi) + \left(2\frac{v_m^2}{v_T^2} - 1\right)\frac{w^2}{v_T^2} \sin^2(\omega t_0+\psi) + \cdots\right]. \end{aligned}\right\} \quad (7)$$

$I_c(t_0)$ does not necessarily give the electron current at the cathode at time t_0, since the current is always the difference of the current i_1 *leaving* the cathode and the current i_2 returning to it at time t_0.

The first term is always the saturation current, $i_1 = I^*$. We can state also that the electrons summing up to a current $I^* - I_c(t_0)$ will return to the cathode at later instants, but we cannot say anything of the time distribution of these events and consequently of the value of $i_2(t_0)$ without further investigations. However, we can state that *the mean value* of the current at any place is given by the mean value of $I_c(t_0)$, which will be

$$\overline{I_c(t_0)} \approx I\left[1 + \left(\frac{v_m^2}{v_T^2} - \frac{1}{2}\right)\frac{w^2}{v_T^2}\right]. \quad (7A)$$

This value is usually larger than the current I of the undisturbed case, the excess being the *rectified current*

$$\Delta I = I\left(\frac{v_m^2}{v_T^2} - \frac{1}{2}\right)\frac{w^2}{v_T^2}. \quad (8)$$

By using (4) and the value of w given in (5C), we can write (8) in the form

$$I = \tfrac{1}{2} I^* A E_1^2, \quad (8A)$$

where

$$A = \frac{I}{I^*}\left(\log \frac{I^*}{I} - \frac{1}{2}\right)\frac{e/m}{V_T}\frac{1}{\omega^2 + \alpha^2}. \quad (8B)$$

Equation (8A) shows that the rectified current increases proportionally to E_1^2, that is, the power of the high-frequency signal.

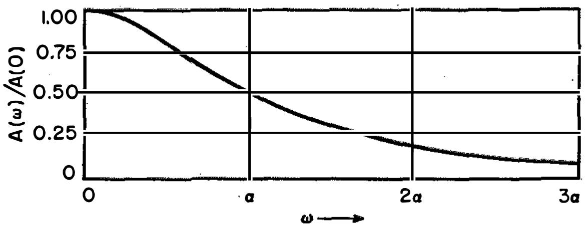

Figure 2—Frequency response of rectification.

The proportionality factor A of (8B) indicates that with increasing frequency the rectified current decreases as

$$1/(\omega^2 + \alpha^2).$$

(See Figure 2.) The decrease is slow at first but if ω exceeds α, it approaches $1/\omega^2$. This is already the case at a frequency of 10^{10} cycles per second in the diode described previously.

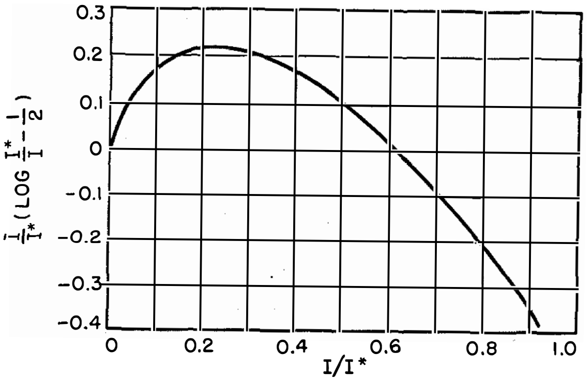

Figure 3—Rectification plotted against direct current.

According to (8A), the rectified current is apparently proportional to the saturation current I^* but it is also influenced by the value of I/I^* appearing in the factor A.

$$A \sim \frac{I}{I^*}\left(\log\frac{I^*}{I} - \frac{1}{2}\right).$$

This shows (see Figure 3) that ΔI is a *current increase* in the current range $0 < I < 0.606\, I^*$, having a maximum value at $I = 0.223\, I^*$; on the other hand, ΔI represents a *current decrease* if $I > 0.606\, I^*$.

Preliminary measurements have confirmed both the qualitative and quantitative predictions of the theory presented in this paper. Application of the theory to specific diodes as well as signal-to-noise considerations connected with it will be presented in a separate paper.

Recent Telecommunication Development

Thermionic Valves, Their Theory and Design

Mr. A. H. W. Beck, a member of the technical staff of Standard Telephones and Cables, Limited, is the author of a recently published book on "Thermionic Valves, Their Theory and Design" issued by Cambridge University Press, 200 Euston Road, N.W. 1, London, England, and 32 East 57th Street, New York 22, New York.

The book was written primarily for graduate engineers having degrees in physics or electrical engineering. It is divided into 3 major parts and 16 chapters.

Part 1—Physical Theory of Electronics
- Thermionic Emission
- Secondary, Field, and Photo-Electric Emission
- Fluorescence and Phosphorescence

Part 2—Mathematical Theory of Electronics
- Electrostatic Fields
- Electrostatic and Magnetic Electron Optics of Fields Without Space Charge
- Space Charge Flow and the Diode
- Transit Time Effects
- Fluctuation Noise in Valves

Part 3—Types of Valves
- Triodes for Low and Medium Frequencies
- Multigrid Receiving Valves
- Transmitter Valves
- Velocity-Modulated Valves
- Triodes at Ultra-High Frequencies
- Travelling-Wave Tubes and Beam Interaction Tubes
- Magnetrons
- Picture Convertors and Storage Tubes

The book is 6 by $8\frac{3}{4}$ inches (15 by 22 centimeters) and is bound in hard covers. It contains 565 pages of text, 4 pages of index, and 16 pages of preliminary material. The price of the book is 60 shillings or \$12.00 in London or New York, respectively.

United States Patents Issued to International Telephone and Telegraph System; February-April, 1954

United States patents numbering 20 were issued between February 1 and April 30, 1954 to companies in the International System. The inventors, titles, and numbers of these patents are given below; summaries of several that are of more-than-usual interest are included. In cases where corresponding Canadian patents have already issued, their numbers are given in parentheses.

J. I. Bellamy and T. L. Bowser, Primary–Secondary Spread Crossbar Telephone System, 2,674,657 (636,060).

R. A. L. Cole and A. V. Krause, Electron Gun for Cathode-Ray Tubes, 2,672,568.

P. W. Crapuchettes, Compensating Circuit for Cavity-Resonator Devices, 2,673,296.

L. A. de Rosa, Random-Impulse System, 2,671,896 (522,012).

M. den Hertog and G. X. Lens, Controlling of Selecting Mechanism for Individual Switches, 2,672,060.

H. Eggers, Tone Wheel to Produce Frequency-Modulated Low-Frequency Oscillations, 2,669,670 (627,065).

R. R. Fink, Freezer Cabinet, D. 171,392.

R. R. Fink, Freezer Cabinet, D. 171,393.

F. P. Gohorel, Double-Selection Electronic Switching System, 2,668,876.

M. A. Kreitchman, Pump, 2,671,408.

S. McLeod, Electric Frequency-Modulation System, 2,672,589.

D. S. Ridler, Printing-Telegraph Receiver, 2,668,870.

P. A. H. Roussel, Electric Pulse Regenerator, 2,672,554.

R. D. Salmon, Printing-Telegraph Apparatus, 2,675,425 (611,157).

R. D. Salmon, L. S. Munck, and F. J. L. Turner, Printing-Telegraph Apparatus, 2,669,602.

H. Stieltjes, Balancing of Carrier Cables, 2,673,895.

H. Stieltjes, Cable Balance, 2,675,428.

L. G. Stone, Removable Panel, 2,674,016.

S. Van Mierlo and P. R. Aigrain, Pulse Electrical Telecommunication System, 2,672,526 (613,015).

A. Violet and M. Cornilleau, Automatic Frequency Control for Reception of Carrier-Shift Signals, 2,668,871.

Double-Selection Electronic Switching System

F. P. Gohorel

2,668,876—February 9, 1954

A double-selection system comprising an assembly of primary selectors associated with a common control circuit that prepares the primary-selection operations as soon as the desired number has been received. The connection from the primary selector is delayed until the outgoing line of the secondary selector has been selected.

Printing-Telegraph Receiver

D. S. Ridler

2,668,870—February 9, 1954

This printing-telegraph receiver registers a received code combination and a type wheel is set in rotation from a known angular position. The number of character positions through which the type wheel is rotated is counted and the character corresponding to the received code combination is selected by stopping the type wheel in a position determined by a comparison between the number of character positions counted and the number representing the received code combination.

Pulse Electrical Telecommunication System

S. Van Mierlo and P. R. Aigrain

2,672,526—March 16, 1954

A bidirectional amplifier for amplifying impulses between two circuits periodically placed in communication. Means are provided for connecting the amplifier successively first in one direction and then in the other. Other circuits connected between each of the two circuits and the input and output of the amplifier prevent cross interference between the signals of the two channels.

Electron Gun for Cathode-Ray Tubes

R. A. L. Cole and A. V. Krause
2,672,568—March 16, 1954

An electron gun for a cathode-ray tube comprising a cathode, a first anode, and auxiliary electrodes together adapted to form a space-charge-limited electron beam converging to a crossover whose position and cross section are substantially independent of positive-potential variations occurring at the first anode. A focusing cylinder and a second accelerating anode together form the electrostatic lens for bringing the cathode beam to a second high-potential crossover at the aperture of the second anode.

Printing-Telegraph Apparatus

R. D. Salmon, L. S. Munck, and F. J. L. Turner
2,669,602—February 16, 1954

A page-printing-telegraph apparatus that in response to a distinctive signal will move the paper into a predetermined position and will, in response to a second kind of signal, release the answer-back transmitter. Release of the answer-back transmitter is delayed until the paper has been moved into position.

Primary–Secondary Spread Crossbar Telephone System

J. I. Bellamy and T. L. Bowser
2,674,657—April 6, 1954

A thousand-line crossbar exchange having up to forty trunks to other exchanges, each exchange being provided with an organization of relays and digit counters (block coupler) that records all digits for terminated calls and furnishes ringing and talking current to the called line. Common control apparatus on a selector (block-link) frame includes a block controller for all calls, a block translator for locally terminated calls, and an outgoing controller for outgoing calls.

Contributors to This Issue

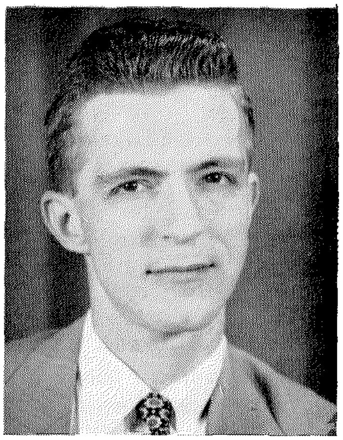

Coleman T. Clark

Coleman T. Clark was born in Plainfield, New Jersey, on October 27, 1924. In 1948, he received the B.S. degree in electrical engineering from Lehigh University.

In 1943 Mr. Clark joined the United States Navy. He served as a radio-radar officer for the United States Navy Bureau of Aeronautics and was released to inactive duty in 1946. During the next two years, he was with the Roller-Smith Corporation.

Mr. Clark joined the staff of Federal Telecommunication Laboratories in 1948 and is now a project engineer working on Navaglobe computing and indicating equipment.

In this issue, Mr. Clark is a coauthor of the Navaglobe paper.

• • •

Robert I. Colin was born in Brooklyn, New York on February 16, 1907.

Robert I. Colin

He studied engineering and physics at Cornell University and received a B.A. degree in 1928. The next year, under an exchange fellowship, he attended the University of Frankfurt (Germany). From 1929 to 1933, he served as a graduate assistant in physics at New York University and received an M.S. degree.

From 1934 to 1939, he was a member of the teaching staff of Hebrew Technical Institute. From 1941 to 1944, he was an instructor, then head, of the aircraft electrical systems branch of the Army Air Forces Technical School.

Entering Federal Telecommunication Laboratories in 1944 as an engineer and technical writer, he is now administrative assistant to the vice president in charge of the electronic special-projects laboratory.

Mr. Colin is the author of several published papers and is a coauthor of one on Navaglobe developments in this issue. He is a member of Phi Kappa Phi.

• • •

Milton Dishal was born on March 20, 1918, at Philadelphia, Pennsylvania. Temple University conferred on him the B.S. degree in 1939 and the M.A. degree in physics in 1941. He served as a teaching fellow in physics during the postgraduate years.

In 1941, he entered the employ of Federal Telecommunication Laboratories, where he is now a department head in charge of a group engaged in the development of radio receivers having special characteristics. Some of his work on Navaglobe is presented in this issue.

Mr. Dishal is a Senior Member of the Institute of Radio Engineers. He has been active in the work of the Radio Technical Committee on Aeronautics. He is also serving as a part-time instructor at Polytechnic Institute of Brooklyn.

• • •

Robert A. Hampshire was born on December 21, 1912 at Philadelphia, Pennsylvania. He graduated from Polytechnic Institute of Brooklyn in 1934 with a bachelor's degree in electrical engineering.

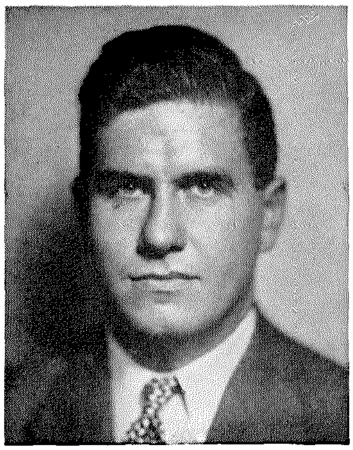

Milton Dishal

He was employed in 1934 and 1935 by the Ford Instrument Company of Long Island City, New York, and from 1935 to 1938 at the Radio Corporation of America research laboratories at Harrison, New Jersey.

From 1938 to date, Mr. Hampshire has been with Federal Telephone and Radio Corporation and lately with Federal Telecommunication Laboratories. Since 1941, he has been engaged in the development of instrument approach systems, on which he reports in this issue.

Mr. Hampshire is an Associate Member of the Institute of Radio Engineers and of the American Institute of Electrical Engineers and is a member of Tau Beta Pi.

• • •

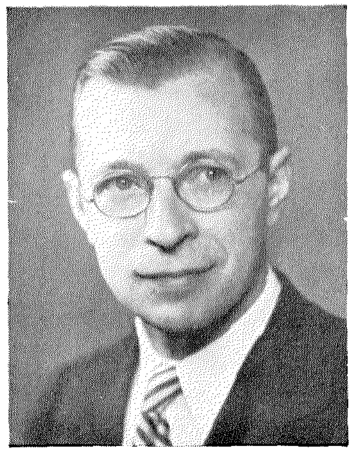

Robert A. Hampshire

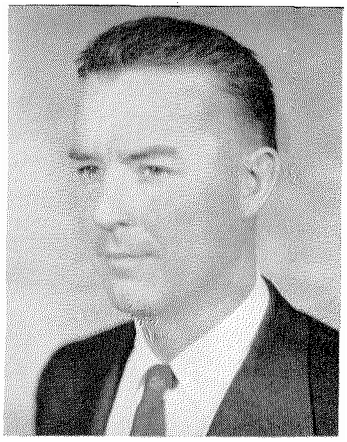

J. J. NAIL

J. J. NAIL was born in Belton, Texas, on August 2, 1920. He received the B.S. degree in electrical engineering from the University of Texas in 1943.

From 1943 to 1945, he was employed by the Sperry Gyroscope Company.

In 1945, he joined Federal Telephone and Radio Corporation, transferring to Federal Telecommunication Laboratories in 1947, where he worked on the development of antennas and associated components until 1953.

In this issue he is coauthor of a paper on aircraft antennas. Mr. Nail is presently employed by Bell Telephone Laboratories, where he is engaged in the development of military electronic equipment.

• • •

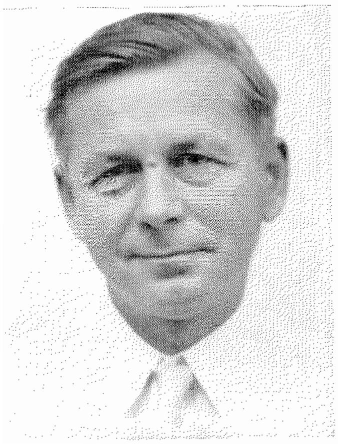

R. K. ORTHUBER

R. K. ORTHUBER received a masters degree from the Technical University of Stuttgart and a Ph.D. degree from the Technical University of Berlin.

From 1935 to 1947, he did physical research in Berlin and from 1948 to 1951 he was a consultant to the Office of Air Research at Wright Field in Dayton, Ohio.

Dr. Orthuber joined the Capehart–Farnsworth research staff in 1951. A number of patents have been issued to him on semiconductor photocells, electron multipliers, image converters, and phosphorescent screens. He is a coauthor in this issue of a report on a solid-state image intensifier.

• • •

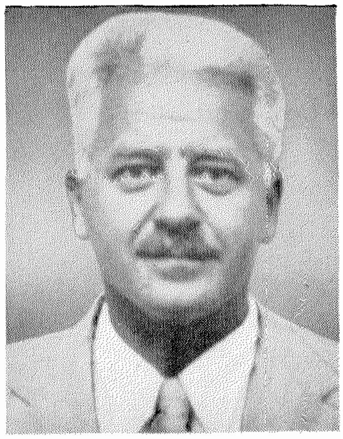

GEORGE PAPP

GEORGE PAPP was born in Szamosujvar, Hungary, on September 27, 1912. He studied at the universities of Budapest and Szeged in Hungary and received his Ph.D. degree from the University of Budapest in 1937.

He worked first at the Biochemical Institute of the University of Szeged. From 1938, he was assistant and later assistant professor in atomic physics at the Technical University of Budapest. Dr. Papp was a consultant of the research laboratory of Tungsram, Budapest, working especially with electron-multiplier tubes and very-fast-coincidence measuring techniques.

Dr. Papp came to the United States in 1949 and worked as a research associate at George Washington University in Washington, District of Columbia. He joined Capehart–Farnsworth Company in 1952 and has worked on electron tubes for microwave detection and for image conversion, amplification, and storage. Some of his work on microwave-detection tubes is reported in this issue.

• • •

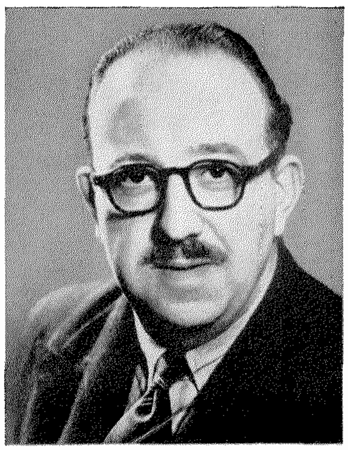

ERNEST G. ROWE

ERNEST G. ROWE was born in 1909 at Plymouth, England. He received from London University an honours degree in engineering in 1932 and a M.Sc. degree a year later.

He joined the development staff of the M. O. Valve Company in 1933, becoming later chief of valve development.

At the end of 1948, he was named chief receiving-valve engineer of the Brimar Valve Division of Standard Telephones and Cables, Limited. He is coauthor of the paper on reliable valves.

Mr. Rowe is a Member of the Institution of Electrical Engineers, an Associate of the City and Guilds of London Institute, and holds the diploma of the Imperial College of Science and Technology.

• • •

WILLIAM SICHAK was born on January 7, 1916, in Lyndora, Pennsylvania. He received the B.A. degree in physics from Allegheny College in 1942.

From 1942 to 1945, he was engaged in developing microwave radar antennas at the Radiation Laboratory

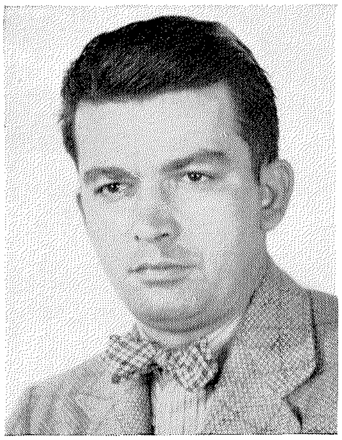

William Sichak

of Massachusetts Institute of Technology. Since then, he has been with Federal Telecommunication Laboratories, working on microwave antennas and allied equipment. In this issue, he is coauthor of a paper on omnidirectional aircraft antennas.

Mr. Sichak is a department head in the radio and radar components division of the laboratories. He is a Member of the Institute of Radio Engineers and of the American Physical Society.

• • •

T. DeWitt Talmage was born in Lincoln, Illinois, on July 21, 1903. He studied electrical engineering at Milwaukee School of Engineering and the University of Cincinnati.

In 1949, he joined the sales division of Kellogg Switchboard and Supply Company and in 1953 became manager of the customers' training program that is described in part in this issue.

Previously, Mr. Talmage served with the Tennessee Valley Authority for 15 years on the design of communication systems. He also was associated with the Illinois Telephone Association as a transmission engineer and editor-in-chief of the Illinois Telephone Handbook.

He is the author of many published articles on telephone practices. He is a Member of the American Institute of Electrical Engineers and is serving on its carrier-current committee. He holds membership in the Independent Telephone Pioneer Association and is on the plant committee of the United States Independent Telephone Association. He is a registered professional engineer in the state of Tennessee.

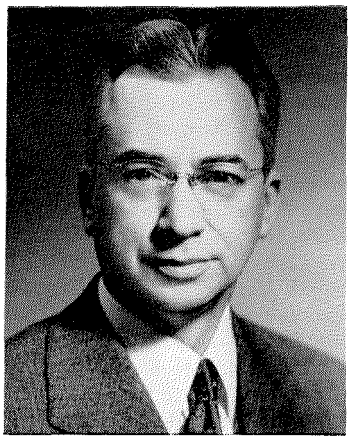

T. DeWitt Talmage

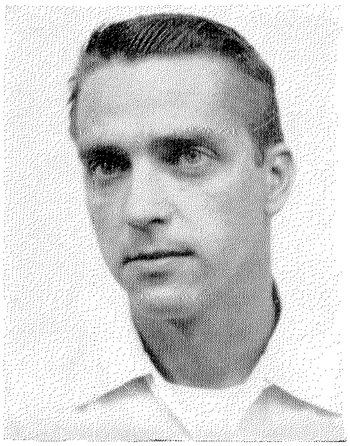

L. R. Ullery

• • •

L. R. Ullery received a B.S. degree in physics and an M.S. degree in physical electronics from the University of Notre Dame.

He has been a research physicist at Capehart–Farnsworth Company since 1952, and is a coauthor of a paper on a solid-state image intensifier in this issue.

• • •

Peter Welch. A photograph and biography of Mr. Welch, coauthor of the paper on trustworthy valves, will be found on page 72 of the March, 1954 issue.

INTERNATIONAL TELEPHONE AND TELEGRAPH CORPORATION

MANUFACTURE AND SALES

North America

UNITED STATES OF AMERICA —

Divisions of International Telephone and Telegraph Corporation

Capehart-Farnsworth Company; Fort Wayne, Indiana

Coolerator Company; Duluth, Minnesota

Federal Telephone and Radio Company; Clifton, New Jersey

Kellogg Switchboard and Supply Company; Chicago, Illinois

Federal Electric Corporation; Clifton, New Jersey

International Standard Electric Corporation; New York, N w York

International Standard Trading Corpo ation; New York, New York

Kellogg Credit Corporation; Chicago, Illinois

Thomasville Furniture Corporation; Thomasville, North Carolina

CANADA — (*See British Commonwealth of Nations*)

British Commonwealth of Nations

ENGLAND —

Standard Telephones and Cables, Limited, London

Creed and Company, Limited, Croydon

International Marine Radio Company Limited, Croydon

Kolster-Brandes Limited, Sidcup

CANADA — Federal Electric Manufacturing Company, Ltd., Montreal

AUSTRALIA —

Standard Telephones and Cables Pty. Limited, Sydney

Silovac Electrical Products Pty. Limited, Sydney

Austral Standard Cables Pty. Limited, Melbourne

NEW ZEALAND — New Zealand Electric Totalisators Limited, Wellington

Latin America and West Indies

ARGENTINA — Compañía Standard Electric Argentina, S.A.I.C., Buenos Aires

BRAZIL — Standard Electrica, S.A., Rio de Janeiro

CHILE — Compañía Standard Electric, S.A.C., Santiago

CUBA — Compañía Distribuidora de Productos Standard S. A., Havana

MEXICO — Standard Electrica de Mexico, S.A., Mexico City

PUERTO RICO — Standard Electrica de Puerto Rico, Inc., San Juan

Europe

AUSTRIA — Vereinigte Telephon- und Telegraphenfabriks A. G., Czeija, Nissl & Co., Vienna

BELGIUM — Bell Telephone Manufacturing Company, Antwerp

DENMARK — Standard Electric Aktieselskab, Copenhagen

FRANCE —

Compagnie Générale de Constructions Téléphoniques, Paris

Le Matériel Téléphonique, Paris

Les Téléimprimeurs, Paris

GERMANY —

Standard Elektrizitäts-Gesellschaft A.G., Stuttgart

Divisions

Mix & Genest, Stuttgart

Süddeutsche Apparatefabrik, ürnberg

C. Lorenz, A.G., Stuttgart

G. Schaub Apparatebau G.m.b.H., Pforzheim

ITALY — Fabbrica Apparecchiature per Comunicazioni Elettriche, Milan

NETHERLANDS — Nederlandsche Standard Electric Maatschappij N.V., The Hague

NORWAY — Standard Telefon og Kabelfabrik A/S, Oslo

PORTUGAL — Standard Eléctrica, S.A.R.L., Lisbon

SPAIN —

Compañía Radio Aérea Marítima Española, Madrid

Standard Eléctrica, S.A., Madrid

SWEDEN — Aktiebolaget Standard Radiofabrik, Stockholm

SWITZERLAND — Standard Telephone et Radio S.A., Zurich

TELEPHONE OPERATIONS

BRAZIL — Companhia Telefônica Nacional, Rio de Janeiro

CHILE — Compañía de Teléfonos de Chile, Santiago

CUBA — Cuban American Telephone and Telegraph Company, Havana

CUBA — Cuban Telephone Co pany, Havana

PERU — Compañía Peruana de Teléfonos Limitada, Lima

PUERTO RICO — Porto Rico Telephone Company, San Juan

CABLE AND RADIO OPERATIONS

UNITED STATES OF AMERICA —

American Cable & Radio Corporation; New York, New York

All America Cables and Radio, Inc.; New York, New York

The Commercial Cable Company; New York, New York

Mackay Radio and Telegraph Company; New York, New York

ARGENTINA —

Compañía Internacional de Radio, Buenos Aires

Sociedad Anónima Radio Argentina, Buenos Aires (*Subsidiary of American Cable and Radio Corporation*)

BOLIVIA — Compañía Internacional de Radio Boliviana, La Paz

BRAZIL — Companhia Radio Internacional do Brasil, Rio de Janeiro

CHILE — Compañía Internacional de Radio, S.A., Santiago

CUBA — Radio Corporation of Cuba, Havana

PUERTO RICO — Radio Corporation of Porto Rico, San Juan

RESEARCH

UNITED STATES OF AMERICA —

Federal T ecommunication Laboratories; Nutley, New Jersey; *a division of International Telephone and Telegraph Corporation*

International Telecommunication Laboratories, Inc.; New York, New York

ENGLAND — Standard Teleco m nication Laboratories, Limited, London

FRANCE — Laboratoire Central de Télécommunications, Paris

ASSOCIATE LICENSEES FOR MANUFACTURE AND SALES IN JAPAN

Nippon Electric Company, Limited, Tokyo

Sumitomo Electric Industries, Limited, Osaka